

**THE TRANSPORT OF VOLATILE COMPOUNDS ACROSS THE
CAPILLARY FRINGE**

Kathleen Ann McCarthy

B.S., Civil Engineering, Portland State University, 1986

A dissertation submitted to the faculty of the
Oregon Graduate Institute of Science & Technology
in partial fulfillment of the
requirement for the degree
Doctor of Philosophy
in
Environmental Science and Engineering

October 1992

The dissertation "The Transport of Volatile Compounds Across the Capillary Fringe" by Kathleen Ann McCarthy has been examined and approved by the following examination committee:

Richard L. Johnson, Thesis Advisor

James F. Pankow

Carl D. Palmer

William Fish

Robert W. Gillham

DEDICATION

This work is dedicated to my mother and father whose unfailing love and belief in me provided the foundation to make this dream a reality.

ACKNOWLEDGEMENTS

There is, of course, no way to adequately thank all of the people who have helped me to accomplish this goal. The faculty, staff, and students of the Department of Environmental Science & Engineering and the entire OGI community are among the best folks to be found anywhere. They have made the past five years not only endurable, but a time I will always remember with happiness.

I would especially like to thank my advisor, Richard L. Johnson, for being the best of the best. Without his support (both moral and financial), expertise, enthusiasm, patience (not always deserved), and humor (all types), I would not have succeeded. I am also grateful to the other members of my thesis committee, James F. Pankow, Carl D. Palmer, William Fish, and Robert W. Gillham, for their support and advice throughout my research and especially during the preparation of my dissertation.

This work was supported in part by the University Consortium Solvents-in-Groundwater Program with corporate support from Dow Chemical Corp., Ciba-Geigy Corp., General Electric Corp., Eastman Kodak Corp., and Boeing Corp.; and in part by the U. S. Geological Survey under Grant Number 14-08-0001-G1917. I am very grateful for this support.

For her incredibly durable friendship, heartfelt thanks go to Leah Matheson. I am also grateful to my friends Liannha Sa (for not being an all-American bleeding-heart liberal), Judi Irvine (for not being under 35), Don Buchholz (for being able to think like a computer), Matt Perrott (for making me humble), Lorne Isabelle (for knowing everything--especially how to make me laugh), and Allan Ryall (for "vitreous humor").

The expertise, support, and patience provided by the library, glass shop, and machine shop personnel has been invaluable.

I am thankful, too, for the support of the U. S. Geological Survey and for the opportunity of continued employment throughout my graduate education. In particular, I am indebted to Marvin O. Fretwell, Edward L. Bolke, and William D. McFarland for their patience and for continually providing me with incentive. And, I am grateful to Ivan Barnes for his not-so-gentle shove in the right direction.

For introducing me to the self confidence necessary for pursuing higher education, I am grateful to my friend and first mentor, William S. Fletcher.

Finally, for nearly everything, I am thankful to my family.

TABLE OF CONTENTS

Dedication	iii
Acknowledgements	iv
List of Figures	ix
List of Tables	xiii
Abstract	xiv
1. INTRODUCTION	1
1.1 Problem Statement	1
1.1.1 Soil-Gas Monitoring	2
1.1.2 <i>In Situ</i> Bioremediation	3
1.2 Experimental Objectives	4
1.3 Proposed Publications	6
1.4 References	7
2. THE TRANSPORT OF TRICHLOROETHYLENE ACROSS THE CAPILLARY FRINGE	9
2.1 Introduction	9
2.2 Experimental	13
2.2.1 Physical Modeling	13
2.2.2 Sampling, Analyses, and Preparation of Standards	15
2.3 Results and Discussion	16
2.3.1 Drainage Experiment	16
2.3.2 Water-Table Drop Experiment	17

2.3.3	Imbibition Experiment	18
2.4	Numerical Modeling	19
2.4.1	Two-Dimensional Advection-Diffusion Model	19
2.4.2	One-Dimensional Diffusion-Dispersion Model	22
2.5	Conclusions	24
2.6	References	27
3.	MEASUREMENT OF TRICHLOROETHYLENE DIFFUSION IN SOIL WITH A CONTINUOUSLY-VARYING MOISTURE CONTENT	38
3.1	Introduction	38
3.2	Experimental	41
3.3	Results and Discussion	43
3.3.1	Calculation of Effective Diffusion Coefficients	44
3.3.2	Comparison of Experimental and Theoretical Effective Diffusion Coefficients	46
3.3.3	Numerical Modeling	47
3.4	Conclusions	49
3.5	References	50
4.	DEVELOPMENT OF A TWO-DIMENSIONAL PARTICLE-TRACKING MODEL	61
4.1	Introduction	61
4.2	Physical Basis and Governing Equations	62
4.3	Model Evaluation	67
4.4	Example Simulations	68
4.5	Conclusions	69
4.6	References	70
5.	SUMMARY, CONCLUSIONS, AND IMPLICATIONS	78
5.1	Summary of Research	78
5.2	Conclusions of Research	79

5.2.1	Mass-Transfer Experiments	79
5.2.2	Diffusion Experiments	80
5.2.3	Numerical Modeling	80
5.3	Implications	81
5.3.1	Soil-Gas Monitoring	82
5.3.2	<i>In Situ</i> Bioremediation	84
5.3.3	Numerical Modeling	85
5.4	References	86
Appendix A.	Selected Experimental Data from the Mass-Transfer Experiments	92
Appendix B.	One-Dimensional Numerical-Model Code	106
Appendix C.	Selected Experimental Data from the Diffusion Experiments	114
Appendix D.	Two-Dimensional Numerical-Model Code	128
Vita		169

LIST OF FIGURES

- 2.1 The shallow subsurface environment. a) Hydrologic components, b) soil-moisture content as a function of depth, and c) pressure head as a function of depth (after Freeze and Cherry [1979]). 30
- 2.2 Schematic drawing of the aquifer model. 31
- 2.3 a) Schematic drawing of the experimental set-up used for the mass transfer experiments; b) cross-sectional view showing the locations of selected sampling bundles and ports. 32
- 2.4 a) Steady-state profiles of depth versus TCE concentration under drainage (■) and imbibition (+) conditions. b) Moisture content versus depth under drainage (■) and imbibition (+) conditions. [Concentrations are reported relative to influent concentration.] 33
- 2.5 Water-table drop experiment. a) TCE concentration versus time at sampling bundle A ($x = 0.3$ m), b) TCE concentration versus time at a depth of 0.46 m, and c) water level versus time. [Concentrations are reported relative to influent concentration.] 34

2.6	Superposed results from the two-dimensional numerical model (lines) and experimental data (symbols) from sampling bundle C ($x = 0.7$ m). [Concentrations are reported relative to the maximum concentration at bundle A ($x = 0.3$ m).]	35
2.7	Results from the one-dimensional numerical model (lines) and experimental data (symbols) from sampling bundle C ($x = 0.7$ m). [Concentrations are reported relative to the maximum concentration at bundle A ($x = 0.3$ m).]	36
3.1	Column design.	53
3.2	Experimental setup.	54
3.3	Effluent concentration versus time for a column section with low moisture content. [Effluent concentration is reported relative to bottom-reservoir concentration].	55
3.4	Effluent concentration versus time for a column section with high moisture content. [Effluent concentration is reported relative to bottom-reservoir concentration].	56
3.5	Measured ^a (■) and theoretical ^b (+) effective diffusion coefficients versus gas-filled porosity. a) Arithmetic scale, and b) semi-logarithmic scale.	57
	^a Calculated using equation 3.6.	
	^b Calculated using equation 3.8.	

3.6	Measured soil-moisture profile.	58
3.7	Calculated soil-moisture profiles for the experimental (solid line) and finer-grained (dotted line) sands used in the numerical simulations.	59
3.8	Results from the numerical simulation of transport through the experimental (solid line) and finer-grained (dotted line) sands.	60
4.1	Experimentally determined TCE concentrations, soil-moisture contents, and effective diffusion coefficients versus depth.	72
4.2	Simulation results from the one-dimensional model (solid line) and superposed simulation results from the two-dimensional model (dashed lines).	73
4.3	The modeled domain.	74
4.4	Properties of the modeled domain. a) Moisture content versus depth; b) effective diffusion coefficient versus depth.	75
4.5	Vertical particle displacements resulting from ten time steps versus vertical particle position. a) Entire domain; b) near the fine-grained layer.	76
4.6	Simulation results from the two-dimensional model for a domain a) with the fine-grained layer, and b) without the fine-grained layer.	77

5.1	Results from the one-dimensional numerical simulation of transport from a dissolved TCE source located 1-m below the water table.	88
5.2	Steady-state profile of depth versus oxygen concentration from the one-dimensional numerical model.	89
5.3	Simulation results from the one- and two-dimensional models for a domain a) with the fine-grained layer, and b) without the fine-grained layer. Results from the one-dimensional model are shown as dotted lines; results from the two-dimensional model are shown as solid lines.	90

LIST OF TABLES

2.1	Numerical model input parameters for TCE at 20 C.	37
5.1	Numerical model input parameters for oxygen at 10 C.	91

ABSTRACT

THE TRANSPORT OF VOLATILE COMPOUNDS ACROSS THE CAPILLARY FRINGE

Kathleen A. McCarthy, Ph.D.

Oregon Graduate Institute of Science & Technology, 1992

Supervising Professor: Richard L. Johnson

Mass transfer between ground water and the unsaturated zone plays an important role in many subsurface processes. In this study, the mechanism(s) responsible for the movement of a dissolved, volatile organic compound (VOC) from ground water to the unsaturated zone were identified and quantitated. The study consisted of large-scale mass-transfer experiments, small-scale diffusion experiments, and numerical modeling.

The mass-transfer experiments were conducted in a large physical model of the subsurface (1.0-m long, 1.0-m deep, and 0.75-m wide). Ground water containing dissolved trichloroethylene (TCE) flowed through the model and transport from ground water to the unsaturated zone was monitored as a function of the soil-moisture profile and water-table position.

The diffusion experiments were conducted on discrete sections of gravity-drained sand columns in which the soil-moisture content ranged from field capacity to saturation. These experiments provided values for the effective diffusion coefficient of TCE through

a zone representative of the interface between the saturated and unsaturated zones and were used to evaluate a mathematical expression for the effective diffusion coefficient [Millington, 1959].

Two numerical models were developed to simulate mass exchange between the saturated and unsaturated zones. The first was a two-dimensional particle-tracking model that simulates longitudinal and vertical transport due to advection and molecular diffusion. A one-dimensional finite-difference model that simulates vertical transport due to molecular diffusion and mechanical dispersion was also developed. The models were evaluated with experimental data and were used to simulate a variety of subsurface scenarios.

Data from the physical experiments and numerical simulations showed that molecular diffusion was the primary vertical transport process responsible for mass exchange between the saturated and unsaturated zones and that vertical mechanical dispersion was negligible. As a result, even slight changes in soil properties that result in changes in soil-moisture content were shown to alter concentration profiles by three orders of magnitude. Finally, comparisons of results from the one- and two- dimensional numerical models showed that a one-dimensional approximation of vertical transport in the subsurface can be useful when conditions are appropriate.

CHAPTER 1

INTRODUCTION

1.1 PROBLEM STATEMENT

In the past several decades, much effort has been spent studying water flow and contaminant transport in the saturated zone of the subsurface. The majority of this work has focused on movement *within* the ground-water zone and thus on the processes of advection and longitudinal dispersion.

Substantial research effort has also been directed toward the problems of flow and transport in the unsaturated zone. Agricultural interests have provided much of the incentive for this research and the primary emphasis has thus been on the upper soil horizons and the transport of pesticides and fertilizers resulting from irrigation flow and natural infiltration within this zone.

In each of the zones described above, several transport mechanisms have been investigated in depth and mathematically formulated. As a result, understanding of subsurface transport has increased and sophisticated computer models have been developed to evaluate the movement of water and contaminants within each of these zones.

Due to the complex nature of the interface between the saturated and unsaturated zones, however, few investigators have studied the subsurface as a continuum. Vertical processes in the saturated zone, transport in the deep unsaturated zone and mass exchange

between the two zones have received attention only recently and quantitative data on these processes remain scarce. This lack of information seriously limits our understanding of the interfacial zone and therefore our ability to accurately model transport there. In addition, the success of many methods for detecting, characterizing, monitoring and remediating subsurface contamination is limited by the lack of data available on mass exchange between the saturated and unsaturated zones. Two examples of such methods are soil-gas monitoring and *in situ* bioremediation.

1.1.1 SOIL-GAS MONITORING

One key motivation for an improved understanding of mass exchange between the saturated and unsaturated zones is the widespread popularity of soil-gas surveys. Due to the high cost of installing ground-water wells, soil-gas monitoring is often used as a preliminary technique to determine the presence and extent of underlying ground-water contamination and to assist in the design of monitoring-well networks. This practice is based on the assumption that volatile contaminants in ground water are transported upward in sufficient quantity to be detected in the overlying soil gas. Several field studies have indicated that mass exchange between the saturated and unsaturated zones does occur [e.g., Lappala and Thompson, 1983; Davis et al., 1986; Davis and Matthews, 1989; Barber et al., 1990; Rivett and Cherry, 1991; Conant, et al., 1992], but the relationship between concentrations in ground water and soil gas is not well understood.

Rivett and Cherry [1991] investigated the effectiveness of soil-gas monitoring in the field and concluded that the method may be useful only at sites with unsaturated-zone sources or very shallow ground-water contamination. Their data show that soil-gas concentrations of trichloroethylene (TCE) resulting from a dissolved solvent plume located just 1 m below the water table were very low, often below the detection limit. Therefore, they suggested that even very shallow ground-water contamination may be effectively isolated from the unsaturated zone by infiltration of clean recharge water. In addition to field data, Rivett and Cherry [1991] presented several conceptual models of

ground-water and soil-gas contamination resulting from a variety of sources and concluded that it may not be possible to distinguish the location or nature of subsurface contamination using soil-gas data.

Results from physical experiments and numerical model simulations that show the relationship between contaminant concentrations in ground water and overlying soil gas for a variety conditions are presented in later chapters. Those examples illustrate the complex nature of this relationship and the difficulties involved in interpreting soil-gas data.

1.1.2 IN SITU BIOREMEDIATION

A second incentive for investigating mass transport between the saturated and unsaturated zones is the continuing interest in *situ* bioremediation of subsurface contamination. In order for aerobic microorganisms to successfully biodegrade contaminants in ground water, a continuous supply of oxygen is necessary. Conversely, the efficient removal of potentially toxic metabolic products such as carbon dioxide may be critical to sustain microbial activity. Transport of gases into and out of the saturated zone is therefore an important consideration for any *in situ* bioremediation scheme.

Borden and Bedient [1986] developed a numerical model to simulate aerobic biodegradation of hydrocarbons in ground water. Through a series of sensitivity analyses, they determined that vertical dispersion in the saturated zone and its effect on exchange with the unsaturated zone had a dominant effect on the rate of hydrocarbon degradation. They concluded that the exchange of oxygen and hydrocarbons between the saturated and unsaturated zones may significantly enhance biodegradation, but pointed out that the large uncertainties typically associated with vertical dispersion coefficients can result in errors of several orders of magnitude for biodegradation rates.

The model developed by Rifai et al. [1987], *BIOPLUME II*, is based on the work of Borden and Bedient [1986] and is one of few commercially available for simulating the transport and biodegradation of dissolved contaminants. In this model, vertical

transport of oxygen between the saturated and unsaturated zones is mathematically formulated as a first-order decay in hydrocarbon concentration using a "reaeration coefficient" supplied by the user. Although analyses performed by the authors of the model showed results to be highly sensitive to this parameter, few data are available to assist users in choosing a realistic value. Consequently, the term often becomes a "fitting parameter" with limited physical significance.

It is apparent from the preceding discussion that a need exists for quantitative information on the mechanisms and rates of mass exchange between the saturated and unsaturated zones.

1.2 EXPERIMENTAL OBJECTIVES

The primary objective of the research presented here was to identify and quantitate the transport mechanism(s) responsible for movement of a dissolved, volatile organic compound (VOC) from ground water to the unsaturated zone. TCE was chosen as a representative VOC because it is a common subsurface contaminant and its physical and chemical properties are well documented. Three major tasks were completed to meet the objective of this research:

1. *Mass-transfer experiments.*

These experiments were conducted in a physical model of the subsurface that included both saturated and unsaturated zones. The model was 1.0 m in length, 1.0 m in depth, and 0.75 m in width. Ground water containing dissolved TCE flowed through the model, and the movement of TCE from ground water to the unsaturated zone was monitored as a function of the soil-moisture profile and water-table position. These experiments are discussed in Chapter 2.

2. Small-scale diffusion experiments.

Data from the mass-transfer experiments suggested that molecular diffusion was the dominant mechanism of mass transport between the saturated and unsaturated zones. Therefore, additional experiments were conducted to investigate the diffusion process as a function of depth. The effective diffusion coefficient of TCE was measured through discrete sections of gravity-drained sand columns in which the soil-moisture content ranged from field capacity to saturation. These experiments are discussed in Chapter 3.

3. Numerical modeling.

A two-dimensional particle-tracking model was developed to simulate transport due to advection and molecular diffusion. The model was used to simulate the mass-transfer experiments. The similarity between experimental data and the model results showed that molecular diffusion was the vertical transport mechanism governing transport of TCE from ground water to the unsaturated zone. Development of the two-dimensional model is discussed in Chapter 4.

A one-dimensional finite-difference model was developed to simulate vertical transport due to molecular diffusion and mechanical dispersion. This model was also used to simulate the mass-transfer experiments. The results agreed well experimental data and with results from the two-dimensional model and showed that vertical mechanical dispersion overestimates mass transfer between the saturated and unsaturated zones. Development of the one-dimensional model is discussed in Chapter 2.

A secondary objective of this research was to extrapolate the conclusions of the experimental work to other subsurface conditions. To meet this objective, information gained from the mass-transfer and diffusion experiments was incorporated into the numerical models and a variety of simulations were conducted to illustrate the influence

of different soil and source conditions on mass exchange between the saturated and unsaturated zones. These simulations are discussed primarily in Chapter 5.

1.3 PROPOSED PUBLICATIONS

A slightly modified version of Chapter 2 has been submitted for publication in *Water Resources Research*. Chapters 3, 4, and 5 are planned for submission to *Journal of Contaminant Hydrology*, *Water Resources Research*, and *Groundwater*, respectively.

1.4 REFERENCES

Barber, C., G. B. Davis, D. Briegel and J. K. Ward, Factors controlling the concentration of methane and other volatiles in groundwater and soil-gas around a waste site, **J. Contaminant Hydrology**, **5**, 155-169, 1990.

Borden, R. C., and P. B. Bedient, Transport of dissolved hydrocarbons influenced by oxygen-limited biodegradation, 1, Theoretical development, **Water Resour. Res.**, **22**, 1973-1982, 1986.

Conant, B. H., R. W. Gillham, and C. A. Mendoza, Field experiments and modelling of vapour transport of trichloroethylene in the unsaturated zone, in abstract volume, American Geophysical Union Spring 1992 Meeting, Montreal, Canada, May 12-16, 1992.

Davis, G. B., B. Math and C. Barber, Modeling the volatilization of methane from contaminated groundwaters, in Proceedings, Conference on Water Quality Modelling in the Inland Natural Environment, Bournemouth, England, June 10-13, 1986.

Davis, R. W., and E. W. Matthews, Chloroform contamination in part of the alluvial aquifer, Southwest Louisville, Kentucky, U. S. Geological Survey Water-Supply Paper 2202, 1989.

Lappala, E. G., and G. M. Thompson, Detection of groundwater contamination by shallow soil gas sampling in the vadose zone, in Proceedings, NWWA/API Conference on Characterization and Monitoring of the Vadose Zone, Las Vegas, Nevada, December, 1983.

Rifai, H. S., P. B. Bedient, R. C. Borden, and J. F. Haasbeek, BIOPLUME II: Computer model of two-dimensional contaminant transport under the influence of oxygen limited biodegradation in ground water, user's manual version 1.0, National Center for Ground Water Research, Rice University, Houston, Texas, 1987.

Rivett, M. O., and J. A. Cherry, The effectiveness of soil gas surveys in delineation of groundwater contamination: Controlled experiments at the Borden field site, in Proceedings, NWWA/API Conference on Petroleum Hydrocarbons and Organic Chemicals in Ground Water: Prevention, Detection, and Restoration, Houston, Texas, November 20-22, 1991.

CHAPTER 2

THE TRANSPORT OF TRICHLOROETHYLENE ACROSS THE CAPILLARY FRINGE

2.1 INTRODUCTION

Mass transport between the unsaturated and saturated zones plays an important role in controlling many subsurface processes. This is particularly the case for volatile organic contaminants. Because many contaminant sources occur at the land surface or within the unsaturated zone, mass transport from the unsaturated zone to the saturated zone is a common mechanism of ground-water contamination. Conversely, volatilization of contaminants from ground water and subsequent transport to the atmosphere can provide a natural remediation pathway. Microorganisms active in the saturated zone may also rely on this transport pathway either to provide oxygen or other compounds essential for their growth, or to rid their environment of potentially toxic metabolic products. Finally, the success of technologies such as soil-gas monitoring to detect underlying ground-water contamination, and enhanced in situ volatilization to remediate existing pollution problems will require quantitative knowledge of the movement of contaminants across the interface between the saturated and unsaturated zones.

In order to better understand mass transfer between the saturated and unsaturated zones, it is necessary to more clearly understand the nature of the interface between the two zones (Figure 2.1). This interface, referred to subsequently as the *capillary fringe*,

includes both the tension-saturated porous medium above the water table (in which water pressure is less than atmospheric) and the deep part of the unsaturated zone (in which soil-moisture content varies as a function of depth). Because moisture content and hence air-filled porosity in this region vary with depth, the cross-sectional area available for mass flux and the pathway tortuosity for both phases vary. The variation in water-filled porosity also produces a variation in relative permeability for the aqueous phase and therefore leads to changes in water velocity with depth.

The processes involved in mass exchange between the saturated and unsaturated zones include aqueous- and gas-phase molecular diffusion, mechanical dispersion, aqueous- and gas-phase advection and partitioning among the aqueous, gas and solid phases. The extent to which each of these processes contributes to mass transfer between the saturated and unsaturated zones depends on both the properties of the compound and the conditions within the subsurface. Although numerous investigators have reported field data that indicate exchange between the two zones can be significant [Swallow and Gschwend, 1983; Lappala and Thompson, 1983; Hincbee and Reisinger, 1985; Davis et al., 1986; Davis and Matthews, 1989; Pionke and Glotfelty, 1990], few have specifically examined the transport mechanisms involved.

Swallow and Gschwend [1983] formulated a one-dimensional steady-state mathematical model to describe the volatilization of compounds from unconfined aquifers. The three-box model was based on vertical dispersion in the saturated zone, Henry's Law phase partitioning at the interface, and gas-phase diffusion in the unsaturated zone. In an associated laboratory experiment they measured dye dispersion below the water table and calculated a vertical dispersivity of 0.33 cm. In another experiment, they measured concentration gradients resulting from a saturated-zone source of TCE, but were unable to detect TCE in the unsaturated zone, possibly due to the limited scale of their physical model. They therefore used mass-balance calculations to estimate flux through the unsaturated zone. By comparing model results with flux estimates from the experiments, they concluded that their model adequately described the vertical transport of TCE from ground water.

Barber et al. [1990] investigated the transport of methane from ground water to the unsaturated zone at a field site and concluded that the process was dominated by diffusion and that diffusivity in the saturated zone was the limiting mechanism. However, due to the scale of their field study, a detailed investigation of the interface between the saturated and unsaturated zones was not possible. Using a simple, one-dimensional diffusion model, they obtained reasonably good agreement with their data, but changes in diffusivity within the unsaturated zone were neglected.

Numerical modeling of transport in and exchange between the saturated and unsaturated zones poses significant problems resulting from: 1) The abrupt change in spatial and temporal scales of transport at the interface between the zones; 2) the large difference between horizontal (usually advection dominated) and vertical (usually dispersion dominated) transport parameters in the saturated zone; and 3) the paucity of data available on vertical dispersion, particularly above the water table, and mass-exchange rates between the two zones. As a result, the few existing models that incorporate mass exchange between the zones rely on assumptions that have not previously been validated in the laboratory or in the field.

In a study of oxygen-limited hydrocarbon biodegradation, Borden and Bedient [1986] modeled the exchange of hydrocarbons and oxygen between the saturated and unsaturated zones. In their simulations, it was assumed that the moisture content throughout the unsaturated zone was constant and that the interface between the unsaturated and saturated zones occurred at the water table. Thus, the zone of increasing water content in the deep unsaturated zone and the zone of tension-saturated porous medium above the water table were not accounted for. It was further assumed that soil-gas concentrations immediately above the water table were in equilibrium with ground water immediately below the water table.

Sleep and Sykes [1989] developed a numerical model to simulate the transport of volatile organic compounds in both the saturated and unsaturated zones. Their model allowed for variations in water content near the water table, so diffusive vapor transport could be accurately represented in that region. To simulate the movement of volatile

organics across the interface between the saturated and unsaturated zones, they used a range of mass-transfer coefficients. They also modeled infiltration of water into the subsurface, partitioning of the volatile organics between the vapor and infiltrating water phases, and incorporation of the infiltrating water into ground water. For the conditions simulated, they concluded that aqueous-phase transport into the ground water was the primary transport pathway *into* the saturated zone.

Mendoza and Frind [1990] reported a model that simulates diffusive and advective vapor transport in unsaturated porous media. As with the model of Sleep and Sykes [1989], their model allows increasing water content and decreased vapor diffusion rates near the water table. Transport from the unsaturated zone to the ground water was once again simulated using mass-transfer coefficients. Mendoza and McAlary [1990] investigated the potential for ground-water contamination resulting from an unsaturated-zone vapor source by using an unsaturated-zone transport model to define the source function for a saturated-zone transport model. In their unsaturated-zone simulations, mass transport at the upper and lower boundaries was governed by mass-transfer coefficients and the soil-moisture content was assumed to be constant throughout the domain. Their saturated-zone simulations indicate that the potential for ground-water contamination is significant; however, this may be due to the large value used for vertical dispersivity (0.1 m).

Vertical dispersion has been examined in the field by a number of researchers (e.g., Feenstra [1990], Garabedian et al., [1991], LeBlanc et al., [1991], and Rajaram and Gelhar [1991]). At low ground-water velocities (< 0.5 m/d), they observed vertical dispersion to be on the order of molecular diffusion, rather than more commonly used values based on dispersivities in the range 0.01-1 m. For reference, at a ground-water velocity of 0.1 m/d, a vertical dispersivity of 0.0005 m results in a vertical dispersion equal in magnitude to molecular diffusion.

The assumption of a constant soil-moisture content throughout the unsaturated zone, omission of the tension-saturated zone, and the use of unrealistically high values of saturated-zone vertical dispersivity all serve to overestimate mass flux between the

saturated and unsaturated zones. In addition, few data are available to quantify the rate coefficients commonly used to represent mass exchange at the interface between the zones. The objective of the physical and numerical model studies reported was to examine and quantify transport within the capillary fringe under conditions of low ground-water velocity and no infiltration.

2.2 EXPERIMENTAL

2.2.1 PHYSICAL MODELING

The aquifer model used in these experiments was 0.75 m wide, 1.0 m long and 1.0 m deep (Figure 2.2). It was constructed with glass bottom and side panels and acrylic-sheet end panels, all supported by a steel frame. Rigid screens were installed parallel to and approximately 0.025 m in from the ends of the model to form end reservoirs (Figure 2.3). To prevent direct communication between the soil gas of the unsaturated zone and the headspace of the reservoirs, aluminum plates extending from the top of the model to a depth of approximately 0.55 m were installed at the inner sides of the screens. The outflow port from the downstream reservoir was connected via tubing to an adjustable constant-head reservoir that controlled the water level in the model.

A two-dimensional sampling network was installed along the longitudinal axis of the model. Nine bundles of 1.6-mm outside diameter (o.d.), 0.8-mm inside diameter Teflon tubing attached to 3.2-mm o.d. stainless steel support rods provided 0.1-m horizontal sampling resolution. Each bundle consisted of twenty lengths of tubing, providing 0.03-m vertical sampling resolution in the middle portion of the tank and 0.06-m vertical resolution in the upper and lower parts. The upper end of each tube was fitted with an 18-gauge syringe needle and plugged with a Teflon stopper.

The main part of the aquifer model was carefully filled with #8 flintshot Ottawa sand in 1-mm horizontal layers. The water level was adjusted to be just below the working surface throughout the filling procedure. As each third of the final depth was

achieved, a portable concrete vibrator was used to ensure that sand was packed uniformly into the spaces between the tubing and support rods of the sampling bundles. The end reservoirs were filled with pea gravel. Clean, helium-sparged water was then flushed continuously through the entire model for several weeks. The water level was then lowered to a depth of 0.61 m below the top of the model and clean, helium-sparged water continued to flow through the model for several weeks before the first experiment began.

The flow system used for the mass-transfer experiments is shown in Figure 2.3a. A peristaltic pump delivered helium-sparged deionized water to a 2-liter glass bottle where it was continuously stirred with trichloroethylene (TCE). The resulting TCE-saturated aqueous solution then flowed through the aquifer model.

Data from three of the nine sampling bundles are reported here. These sampling bundles and the vertical positions of the associated sampling ports are shown in Figure 2.3b. Bundles A, B, and C, were located 0.3, 0.5, and 0.7 m, respectively, from the influent reservoir.

The first experiment was designed to investigate the movement of dissolved TCE from the ground water to the unsaturated zone under drainage conditions produced by *lowering* the water table 0.61 m. The resulting drainage capillary fringe included a tension-saturated zone that extended approximately 0.14 m above the water table (Figure 2.4b). The average ground-water velocity through the model was maintained at approximately 0.1 m/d. After 16 days, concentrations throughout the model stabilized, indicating steady-state conditions had been established. Steady-state conditions were maintained for 42 days.

After steady-state conditions had been established under drainage conditions, a second experiment was conducted to investigate the transport of TCE from ground water during a water-table drop. The water table was lowered an additional 0.15 m at a rate of 0.05 m/d and allowed to remain at that level for three days. During this period, TCE concentrations in the saturated and unsaturated zones were monitored.

A third experiment was conducted to examine the movement of TCE from ground water under imbibition conditions. After the water-table drop, the water level was raised

back to its original depth of 0.61 m at a rate of 0.05 m/d. This resulted in an imbibition capillary fringe in which the tension-saturated zone extended approximately 0.09 m above the water table. Again, an average ground-water velocity of approximately 0.1 m/d was maintained through the model and steady-state conditions were reestablished in both the saturated and unsaturated zones. This experiment was continued for 58 days.

At the conclusion of the experiments, soil cores were taken from the aquifer model under both drainage and imbibition conditions. The cores were cut into 3-cm sections for determination of the soil bulk density, porosity, and depth-dependent moisture content.

2.2.2 SAMPLING, ANALYSES, AND PREPARATION OF STANDARDS

Samples were collected by attaching a Hamilton gas-tight syringe (Hamilton Inc, Reno NV) to the needle fitted into the sampling port tubing. Two sampling tube volumes were drawn to purge the sampling line before the sample was collected (purge volumes ranged from 0.2 to 1.1 ml).

Aqueous samples (2.0 ml) were collected from the saturated zone in 5-ml syringes. The samples were placed in 5-ml glass vials fitted with Teflon Mininert valves (Pierce, Rockford, IL), and allowed to equilibrate, with periodic vigorous shaking, for a minimum of one hour. (Preliminary tests showed that this method resulted in equilibration between the aqueous phase and headspace within 30 minutes.) A 0.75-ml sample of headspace was then drawn from the vial using a 1-ml gas-tight syringe and analyzed by gas chromatography (GC). Aqueous-phase standards were prepared in 45-ml vials equipped with Mininert valves. The vials were initially cleaned with methanol and rinsed with deionized water. The vials were then weighed and a known quantity (by weight) of deionized water was injected through the valve. A known quantity (by weight) of a TCE-saturated aqueous stock solution was then injected into the bottom of the vial. The vials were stored in an inverted position and periodically shaken vigorously. Aqueous-phase standards were allowed to equilibrate for a minimum of 24 hours before use and were prepared approximately every three days.

Soil-gas samples (0.75-ml) were collected from the unsaturated zone in 1.0-ml gas-tight syringes and were analyzed directly by GC. Gas-phase standards were prepared in 0.8-l stainless-steel canisters equipped with stainless-steel bellows valves (Whitey Co., Highland Heights, OH). The canisters were initially cleaned by alternately evacuating and pressurizing to ten atmospheres with nitrogen gas. A known quantity (by volume) of TCE was then injected into each canister with a gas-tight syringe. Each canister was then pressurized with nitrogen gas to obtain the desired TCE concentrations. Gas-phase standards were prepared approximately once per month.

All analyses were performed using a six-port gas-sampling valve connected to a Hewlett-Packard HP 5890 GC (Hewlett-Packard Co., Avondale, PA) equipped with a flame ionization detector. Standards were run at the beginning of all sampling sessions and again at the end of selected sampling sessions. The combined coefficient of variation of data from three successive samplings of bundle A over an eight-day period during the drainage experiment was 4.8%. For a 13-day period during the imbibition experiment, the combined coefficient of variation for data collected from bundle A was 7.6%.

2.3 RESULTS AND DISCUSSION

2.3.1 DRAINAGE EXPERIMENT

During the drainage experiment, TCE concentrations decreased nearly three orders of magnitude between the water table and the top of the capillary fringe. The steady-state depth versus concentration profile that developed at 0.3 m into the aquifer model (bundle A) is shown as a solid line in Figure 2.4a and Figure 2.4b shows the corresponding soil-moisture profile. A significant change in the vertical concentration gradient occurred near the water table, resulting in a pronounced gradient across the tension-saturated zone. Moving upward through the capillary fringe, concentrations continued to drop, but at a decreasing rate. A nonlinear steady-state concentration gradient such as this is to be

expected in a region of changing water content. This can be seen from the one-dimensional form of Fick's First Law:

$$F_z = - \left[\theta_w D_{ew} \left(\frac{\partial C_w}{\partial z} \right) + \theta_g D_{eg} \left(\frac{\partial C_g}{\partial z} \right) \right] \quad (2.1)$$

where F_z is the vertical mass flux; θ_w and θ_g are the water- and gas-filled porosities; D_{ew} and D_{eg} are the effective diffusion coefficients, in the water and gas phases, for the species of interest; and $\partial C_w/\partial z$ and $\partial C_g/\partial z$ are the vertical concentration gradients in the water and gas phases. If molecular diffusion was the dominant vertical transport mechanism (as will be shown in the modeling section) and the gas- and water-filled porosities changed with depth (as shown in Figure 2.4b), it is clear from equation 2.1 that a constant vertical flux would occur only if the concentration gradients changed with depth.

2.3.2 WATER-TABLE DROP EXPERIMENT

Changes in TCE concentration that occurred at four different depths during the water-table drop experiment are shown in Figure 2.5. At depths of 0.16, 0.28, and 0.40 m in the unsaturated zone (Figure 2.5a), concentrations rose markedly and had approximately doubled by the time the water table reached its lowest level. This can be explained by the redistribution of water and soil gas which occurred over the course of this experiment. In response to the declining water table, the water content in what had originally been the capillary fringe decreased and water which had previously been part of the saturated zone (and hence contained high concentrations of TCE) was increasingly exposed to the gas phase. The gas and water phases quickly approached concentration equilibrium, resulting in elevated soil-gas concentrations. However, because transport in the gas phase is rapid, the high concentrations quickly dissipated. Within one day, elevated concentrations began falling toward previous levels. After the water table was

raised to its original position, TCE concentrations throughout most of the unsaturated zone returned to near-initial values.

In contrast to the shallow unsaturated zone, at a depth of 0.46 m, TCE concentrations showed an overall decrease during the water-table drop and did not return to initial values (Figure 2.5b). This behavior can also be explained by the soil-moisture profile. Before the water-table drop, the 0.46-m sampling ports were less than 0.01 m above the top of the tension-saturated zone and thus in a region of very high moisture content. Because the soil-moisture profile is not linear, the *relative* increase in gas-filled porosity and, hence, gas-phase transport was much greater at this depth than at shallower depths. As illustrated in Figure 2.5b, the lowered concentrations persisted even after the water table was raised to its original level. This can also be attributed to the soil-moisture profile. The vertical extent of the *imbibition* tension-saturated zone that developed after the water-table drop was approximately .05 m less than that of the previous *drainage* tension-saturated zone (Figure 2.5c). As a consequence, the moisture content at a depth of 0.46 m decreased from approximately 0.29 (prior to the water-table drop) to approximately 0.23 (after the water table was raised to its original position). As will be shown in Chapter 3, this corresponds to more than an order of magnitude increase in the effective diffusion coefficient at this depth.

2.3.3 IMBIBITION EXPERIMENT

Similar to the drainage experiment, data from the imbibition experiment were also characterized by a pronounced concentration gradient within the tension-saturated zone and a decrease in concentration of nearly three orders of magnitude between the water table and the top of the capillary fringe (Figure 2.4a, dotted line). However, in contrast to the drainage case, concentrations above the water table dropped more abruptly. This is consistent with what would be expected based on the imbibition moisture-content profile (Figure 2.4b) which is characterized by a less extensive tension-saturated zone within the capillary fringe.

2.4 NUMERICAL MODELING

2.4.1 TWO-DIMENSIONAL ADVECTION-DIFFUSION MODEL

The physical-model experiments discussed previously were simulated using a two-dimensional, advection-diffusion numerical model. As mentioned earlier, the spatial and temporal scales of transport within the capillary fringe span more than three orders of magnitude. This necessitates prohibitive discretization in standard finite-difference and finite-element numerical models in order to prevent numerical dispersion. To partially overcome discretization requirements, random-walk particle-tracking was chosen as the numerical technique for this model. The model development is presented in detail in Chapter 4 and will be discussed only briefly here.

For a three-phase system in which aqueous- and gas-phase diffusion and horizontal ground-water advection are the dominant transport mechanisms, the transport equation may be written:

$$\begin{aligned} \frac{\partial C_T}{\partial t} = & \frac{\partial}{\partial x} \left[(D_{fw}\theta_w\tau_w) \left(\frac{\partial C_w}{\partial x} \right) \right] + \frac{\partial}{\partial x} \left[(D_{fg}\theta_g\tau_g) \left(\frac{\partial C_g}{\partial x} \right) \right] - \frac{\partial}{\partial x} [v_w\theta_w C_w] \\ & + \frac{\partial}{\partial z} \left[(D_{fw}\theta_w\tau_w) \left(\frac{\partial C_w}{\partial z} \right) \right] + \frac{\partial}{\partial z} \left[(D_{fg}\theta_g\tau_g) \left(\frac{\partial C_g}{\partial z} \right) \right] \end{aligned} \quad (2.2a)$$

where

$$C_T = C_w\theta_w + C_g\theta_g + C_s\rho_b \quad (2.2b)$$

In these expressions, C_T is the total concentration; t is time; x and z are the horizontal (longitudinal) and vertical coordinates; D_{fw} and D_{fg} are the free-water and free-gas diffusion coefficients; θ_w and θ_g are the water- and gas-filled porosities; τ_w and τ_g are the water- and gas-phase tortuosity factors; C_w , C_g , and C_s are the water-, gas-, and solid-

phase concentrations; v_w is the ground-water velocity; and ρ_b is the soil bulk density. If equilibrium phase partitioning is assumed,

$$C_g = HC_w \quad (2.3a)$$

and

$$C_s = K_d C_w \quad (2.3b)$$

where H is Henry's Constant and K_d is the soil-water partition coefficient, both in their dimensionless forms. Using the relationships given by equations 2.3, equation 2.2a may be rewritten as:

$$\begin{aligned} \frac{\partial C_T}{\partial t} = \frac{\partial}{\partial x} \left[(D^*) \left(\frac{\partial C_w}{\partial x} \right) \right] - \frac{\partial}{\partial x} [v_w \theta_w C_w] \\ + \frac{\partial}{\partial z} \left[(D^*) \left(\frac{\partial C_w}{\partial z} \right) \right] \end{aligned} \quad (2.4a)$$

where

$$D^* = D_{fw} \theta_w \tau_w + D_{fg} \theta_g \tau_g H \quad (2.4b)$$

As discussed in Chapter 4, in order to satisfy the requirements of particle tracking theory, the governing transport equation (2.4a) must be expressed in the form of the Ito Fokker-Planck equation. Appropriate rearrangement leads to:

$$\begin{aligned} \frac{\partial C_T}{\partial t} = \frac{\partial^2}{\partial x^2} (D^* R C_T) - \frac{\partial}{\partial x} \left[R C_T \left(\frac{\partial D^*}{\partial x} \right) \right] - \frac{\partial}{\partial x} (v_w \theta_w R C_T) \\ + \frac{\partial^2}{\partial z^2} (D^* R C_T) - \frac{\partial}{\partial z} \left[R C_T \left(\frac{\partial D^*}{\partial z} \right) \right] \end{aligned} \quad (2.5a)$$

where

$$R = (\theta_w + \theta_g H + K_d \rho_b)^{-1} \quad (2.5b)$$

The two-dimensional numerical model was based on equation 2.5a.

For the simulations presented, tortuosity factors for each phase were calculated based on the method of Millington [1959]:

$$\tau_i = \frac{\theta_i^{7/3}}{\theta_T} \quad (2.6)$$

where θ_T is total porosity. The values used for porosity, bulk density, and depth-dependent soil-moisture content were those measured from the soil cores taken from the aquifer model. The values used for free-water and free-gas diffusion coefficients, Henry's Constant, and the soil-water partition coefficient are given in Table 1. A rectangular domain was defined to approximate the experimental conditions (Figure 2.3). Data collected from sampling bundle A were used to define a constant-flux upstream boundary at $x = 0.3$ m. The top boundary ($z = 0.0$ m) was open and the bottom boundary ($z = 1.0$ m) was reflective. The downstream boundary ($x = 1.0$ m) was reflective above $z = 0.55$ m and open below this level. The length of time simulated was four days which corresponded to 0.4 m of horizontal ground-water movement in the physical model.

The results from four identical simulations are shown superposed in Figure 2.6. These results are vertical profiles of concentration from 0.4 m downstream of the constant-flux boundary and represent the simulated concentrations at sampling bundle C. The experimental data shown in Figure 2.6 are from sampling bundle C and were collected four days after the data used as initial conditions. The model results agree well with the experimental data considering that no fitting parameters were used in the simulations. The values used for all variables were either experimentally determined or obtained from the literature. The results indicate that molecular diffusion was the dominant vertical transport process.

The particle-tracking model provided an accurate means for simulating transport across the capillary fringe while partially overcoming the discretization requirements of standard finite-difference and finite-element models. However, the large changes in concentration that occur across the capillary fringe necessitate the use of very large numbers of particles in order to obtain meaningful results. As a consequence, the model is numerically very intensive. A simpler means of simulating transport across the capillary fringe is therefore desirable.

2.4.2 ONE-DIMENSIONAL DIFFUSION-DISPERSION MODEL

In the physical experiments, the ground-water velocity was low and flow was horizontal. In addition, horizontal concentration gradients were small. This is illustrated in Figure 2.5b which shows that concentrations decreased only slightly between sampling bundles A and C. It was hypothesized that, under these conditions, vertical transport was not significantly affected by horizontal processes and could therefore be adequately approximated in one dimension. To test this hypothesis, a one-dimensional finite-difference model was developed.

For a three-phase system in which molecular diffusion and aqueous-phase mechanical dispersion are the dominant vertical transport mechanisms, the one-dimensional form of the transport equation is:

$$\frac{\partial C_T}{\partial t} = \frac{\partial}{\partial z} \left[(D_{fw} + \alpha v_w) \theta_w \tau_w \left(\frac{\partial C_w}{\partial z} \right) \right] + \frac{\partial}{\partial z} \left[D_{fg} \theta_g \tau_g \left(\frac{\partial C_g}{\partial z} \right) \right] \quad (2.7)$$

where α is mechanical dispersivity and all other variables are as defined in the previous section. Recalling equations 2.2b and 2.3, and assuming θ_w , H , θ_g , ρ_b , and K_d do not

change over time, equation 2.7 may be written:

$$\frac{\partial C_w}{\partial t} = \frac{\partial}{\partial z} \left[\frac{[(D_{fw} + \alpha v_w) \theta_w \tau_w + D_{fg} \theta_g \tau_g H] \left(\frac{\partial C_w}{\partial z} \right)}{(\theta_w + \theta_g H + \rho_b K_d)} \right] \quad (2.8)$$

The one-dimensional numerical model was based on a finite-difference approximation of equation 2.8 and incorporated Dirichlet boundary conditions.

For the simulations presented, tortuosity factors were again calculated using equation 2.6 and the values used for all other variables were the same as those used in the two-dimensional simulations. Data collected from sampling bundle A were used as initial conditions and the length of time simulated was once again four days.

The results from three simulations of the drainage experiment are shown in Figure 2.7 along with experimental data. The experimental data points shown are the same as those shown in Figure 2.6, collected from sampling bundle C four days after the data used as initial conditions. The solid line in Figure 2.6 is the result of a simulation based on molecular diffusion alone (dispersivity = 0). The dotted line is the result of a simulation which incorporated a saturated-zone dispersivity of .001 m, and the dashed line is the results of a simulation which incorporated a saturated-zone dispersivity of .01 m. The similarity between the experimental data and the numerical model results based on molecular diffusion indicates that molecular diffusion is the dominant transport process responsible for mass exchange between the saturated and unsaturated zones under the conditions tested. Using a saturated-zone mechanical dispersivity of 0.01 m greatly overestimated vertical mass transport. This is consistent with recent field observations of vertical dispersion at similar ground-water velocities [Feenstra, 1990; Garabedian et al., 1991; Rajaram and Gelhar, 1991]. For the experimental conditions, even a mechanical dispersivity of .001 m overestimated flux to the unsaturated zone.

The good agreement between the experimental data and the results of the one-dimensional model indicates that the physical experiment was adequately approximated in one-dimension. This suggests that a simple, one-dimensional approximation of vertical

transport across the capillary fringe can be useful, at least in a qualitative sense, when conditions are appropriate. For many cases in which ground-water velocities are low, flow is predominantly horizontal, and horizontal concentration gradients are small, a one-dimensional approximation may be adequate. Because the one-dimensional model does not allow for lateral transport, the condition of small horizontal concentration gradients is critical. This condition will often be satisfied, however, when depths are small relative to the lateral extent of the species of interest. For example, transport of oxygen from the atmosphere to ground water, or volatilization from within a shallow, laterally extensive ground-water plume will not typically produce strong horizontal concentration gradients.

2.5 CONCLUSIONS

In the mass-transfer experiments described above, strong vertical concentration gradients developed in the capillary fringe and very low concentrations were observed in the unsaturated zone. Because gas-phase diffusion coefficients are approximately four orders of magnitude greater than aqueous-phase diffusion coefficients, unsaturated-zone transport of TCE was relatively rapid. This maintained soil-gas concentrations at low levels and resulted in large concentration gradients in the tension-saturated zone. TCE concentrations decreased nearly three orders of magnitude between the water table and the top of the capillary fringe. Even soil-gas concentrations measured from 0.01 m above the tension-saturated zone were approximately two orders of magnitude lower than concentrations at the water table.

Data from the water-table drop experiment illustrate two mechanisms that affected transport from the saturated zone to the unsaturated zone during a water-table fluctuation. First, as the water table dropped, the soil-moisture profile partially drained. As water-filled porosity decreased and gas-filled porosity increased in the new capillary fringe, water which had previously been part of the saturated zone (and hence contained high concentrations of TCE) was increasingly exposed to the gas phase. The gas and water phases quickly approached concentration equilibrium, and soil-gas concentrations

increased. However, because transport in the gas phase is rapid, the high concentrations quickly dissipated. This was the dominant effect observed throughout most of the unsaturated zone. A second effect was observed in the deep part of the unsaturated zone where an overall decrease in concentrations was observed. This was because the *relative* increase in gas-filled porosity was greater at this depth than at the shallower depths. In addition, due to the affects of hysteresis on the soil-moisture profile, the vertical extent of the tension-saturated zone was reduced by approximately .05 m as the water table was raised to its original level. As a result, the reduced concentrations deep in the unsaturated zone persisted even after the water table was returned to its original level. This has implications for field work where the position of the water table is routinely monitored, but the extent of the tension-saturated zone and the affects of hysteresis are generally unknown.

The agreement between experimental data and the numerical model simulations based on molecular diffusion was very good. This indicates that at low ground-water velocities (e.g., 0.1 m/d) and in the absence of infiltration, molecular diffusion, rather than mechanical dispersion, is the dominant mechanism for mass transfer between ground water and the unsaturated zone. The agreement between the one-dimensional diffusion model and the two-dimensional advection-diffusion model suggests that vertical transport may be adequately simulated with a one-dimensional diffusion model when the conditions are appropriate. Such conditions include low ground-water velocities, predominantly horizontal flow, and weak horizontal concentration gradients.

The conclusion that aqueous-phase diffusion controls mass transport from the saturated zone to the unsaturated zone has a number of important implications, including: 1) Mass flux from the ground-water zone will be relatively small and, even after very long transport times, will be confined to the uppermost part of the saturated zone; 2) numerical simulations that incorporate vertical mechanical dispersion in the saturated zone, particularly above the water table, may significantly overestimate the importance of mass transfer across the capillary fringe; 3) soil-gas concentrations in the unsaturated zone are strongly dependent upon moisture conditions in the porous medium and the

physical properties of the material being transported; 4) as the result of 3), the relationship between ground-water concentrations and soil-gas concentrations is not straightforward; and 5) the assumption of concentration equilibrium between soil gas and underlying ground water is not valid.

2.6 REFERENCES

Barber, C., G. B. Davis, D. Briegel and J. K. Ward, Factors controlling the concentration of methane and other volatiles in groundwater and soil-gas around a waste site, **J. Contaminant Hydrology**, **5**, 155-169, 1990.

Borden, R. C., and P. B. Bedient, Transport of dissolved hydrocarbons influenced by oxygen-limited biodegradation, 1, Theoretical development, **Water Resour. Res.**, **22**, 1973-1982, 1986.

Davis, G. B., B. Math and C. Barber, Modeling the volatilization of methane from contaminated groundwaters, in Proceedings, Conference on Water Quality Modelling in the Inland Natural Environment, Bournemouth, England, June 10-13, 1986.

Davis, R. W., and E. W. Matthews, Chloroform contamination in part of the alluvial aquifer, Southwest Louisville, Kentucky, U. S. Geological Survey Water-Supply Paper 2202, 1989.

Feenstra, S., Unpublished Data, University of Waterloo, Waterloo, Ontario, 1990.

Freeze, R. A. and J. A. Cherry, Groundwater, Prentice-Hall, 604 pp., Englewood Cliffs, New Jersey, 1979.

Garabedian, S. P., D. R. LeBlanc, L. W. Gelhar, and M. A. Celia, Large-scale natural gradient tracer test in sand and gravel, Cape Cod, Massachusetts, 2. Analysis of spatial moments for a nonreactive tracer, **Water Resour. Res.**, **27**, 911-924, 1991.

Hinchee, R. E., and H. J. Reisinger, Multi-phase transport of petroleum hydrocarbons in the subsurface environment: Theory and practical application, in Proceedings, NWWA/API Conference on Petroleum Hydrocarbons and Organic Chemicals in Ground Water: Prevention, Detection and Restoration, Houston, Texas, November 13-15, 1985.

Lappala, E. G., and G. M. Thompson, Detection of groundwater contamination by shallow soil gas sampling in the vadose zone, in Proceedings, NWWA/API Conference on Characterization and Monitoring of the Vadose Zone, Las Vegas, Nevada, December, 1983.

LeBlanc, D. R., S. P. Garabedian, K. M. Hess, L. W. Gelhar, R. D. Quadri, K. G. Stollenwerk, and W. W. Wood, Large-scale natural gradient tracer test in sand and gravel, Cape Cod, Massachusetts, 1. Experimental design and observed tracer movement, **Water Resour. Res.**, **27**, 895-910, 1991.

Lyman, W. J., W. F. Reehl, and D.H. Rosenblatt, Handbook of Chemical Property Estimation Methods: Environmental Behavior of Organic Compounds, McGraw-Hill, New York, 1982.

Mabey, W. R., J. H. Smith, R. T. Podoll, H. L. Johnson, T. Mill, T. W. Chou, J. Gates, I. W. Partridge, H. Jaber, and D. Vandenberg, Aquatic fate process data for organic priority pollutants, EPA Report 440/4-81-014, 1982.

Mendoza, C.A., and E.O. Frind, Advective-Dispersive Transport of Dense Organic Vapors in the Unsaturated Zone. 1. Model Development, **Water Resour. Res.**, **21**, 379-387, 1990.

Mendoza, C. A., and T. A. McAlary, Modeling of ground-water contamination caused by organic solvent vapors, **Ground Water**, **28**, 199-206, 1990.

Millington, R. J., Gas diffusion in porous media, **Science**, **130**, 100-102 (1959)

Pionke, H. B., and D. W. Glotfelty, Contamination of groundwater by atrazine and selected metabolites, **Chemosphere**, **21**, 813-822, 1990.

Rajaram, H., and L. W. Gelhar, Three-dimensional spatial moments analysis of the Borden tracer test, **Water Resour. Res.**, **27**, 1239-1251, 1991.

Sleep, B. E., and J. F. Sykes, Modeling the transport of volatile organics in variably saturated media, **Water Resour. Res.**, **25**, 81-92, 1989.

Swallow, J. A., and P. M. Gschwend, Volatilization of organic compounds from unconfined aquifers, in Proceedings, NWWA/API Third National Symposium on Aquifer Restoration and Groundwater Monitoring, Columbus, Ohio, May, 1983.

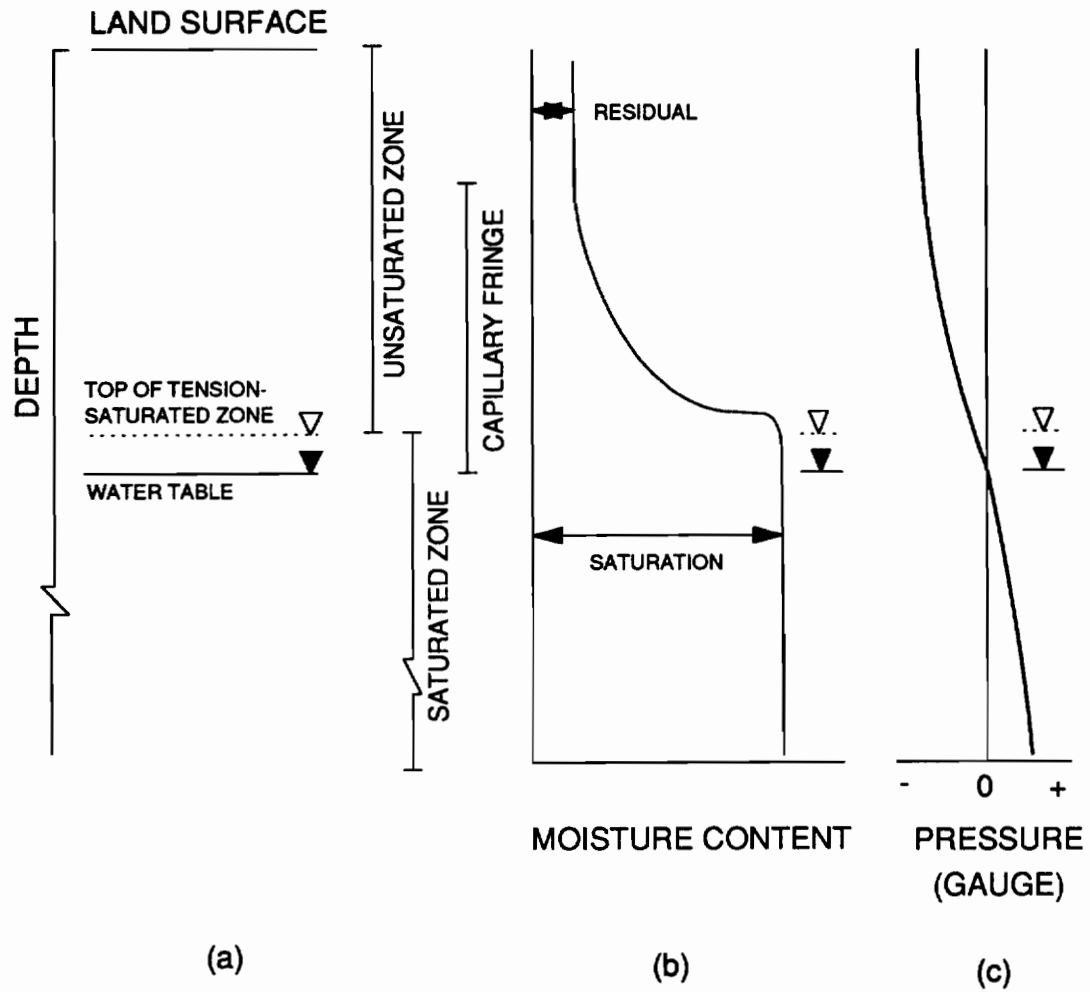


Figure 2.1. The shallow subsurface environment. a) Hydrologic components, b) soil-moisture content as a function of depth, and c) pressure head as a function of depth (After Freeze and Cherry [1979]).

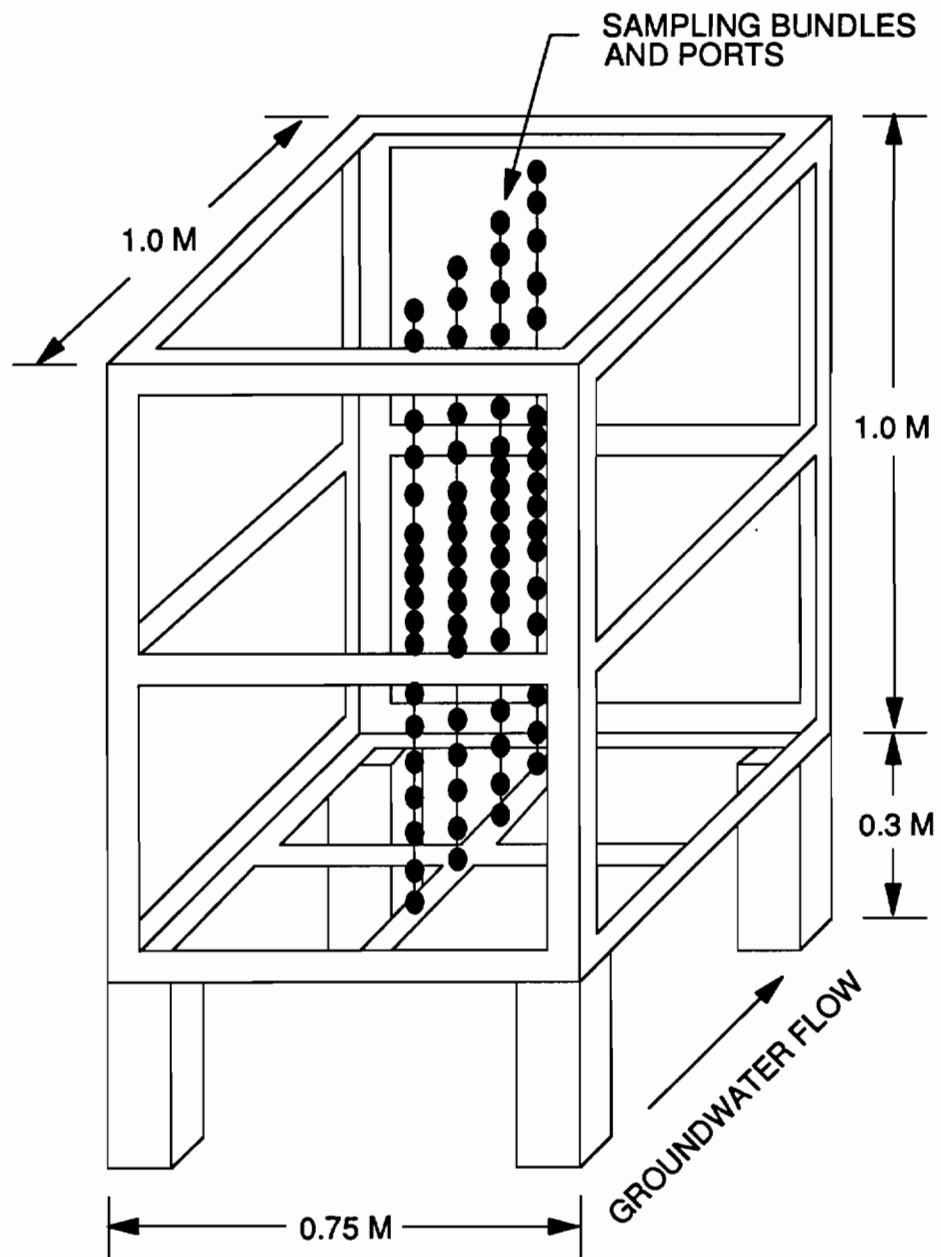


Figure 2.2. Schematic drawing of the aquifer model.

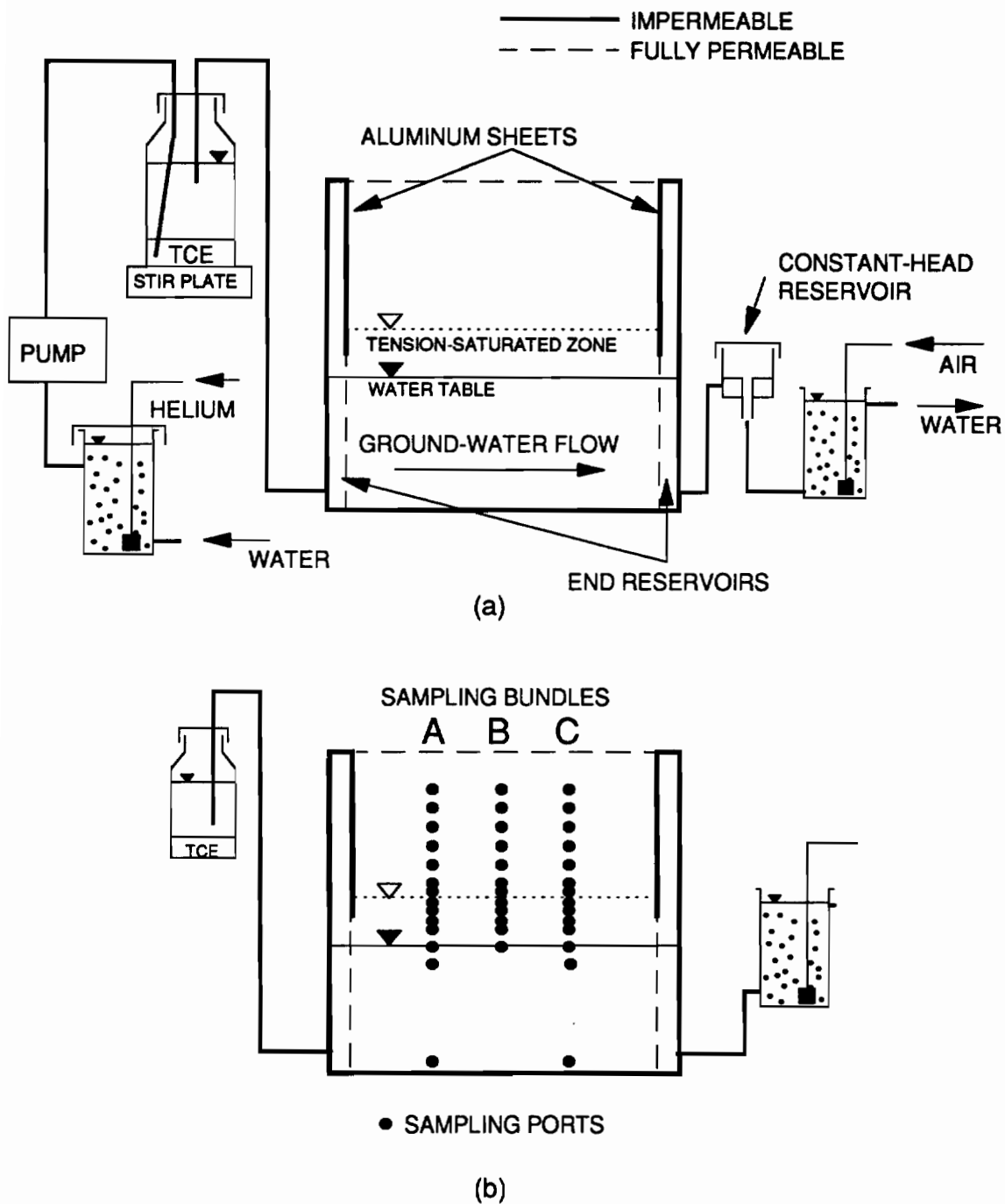


Figure 2.3. a) Schematic drawing of the flow system used for the mass transfer experiments; b) cross-sectional view showing the locations of selected sampling bundles and ports.

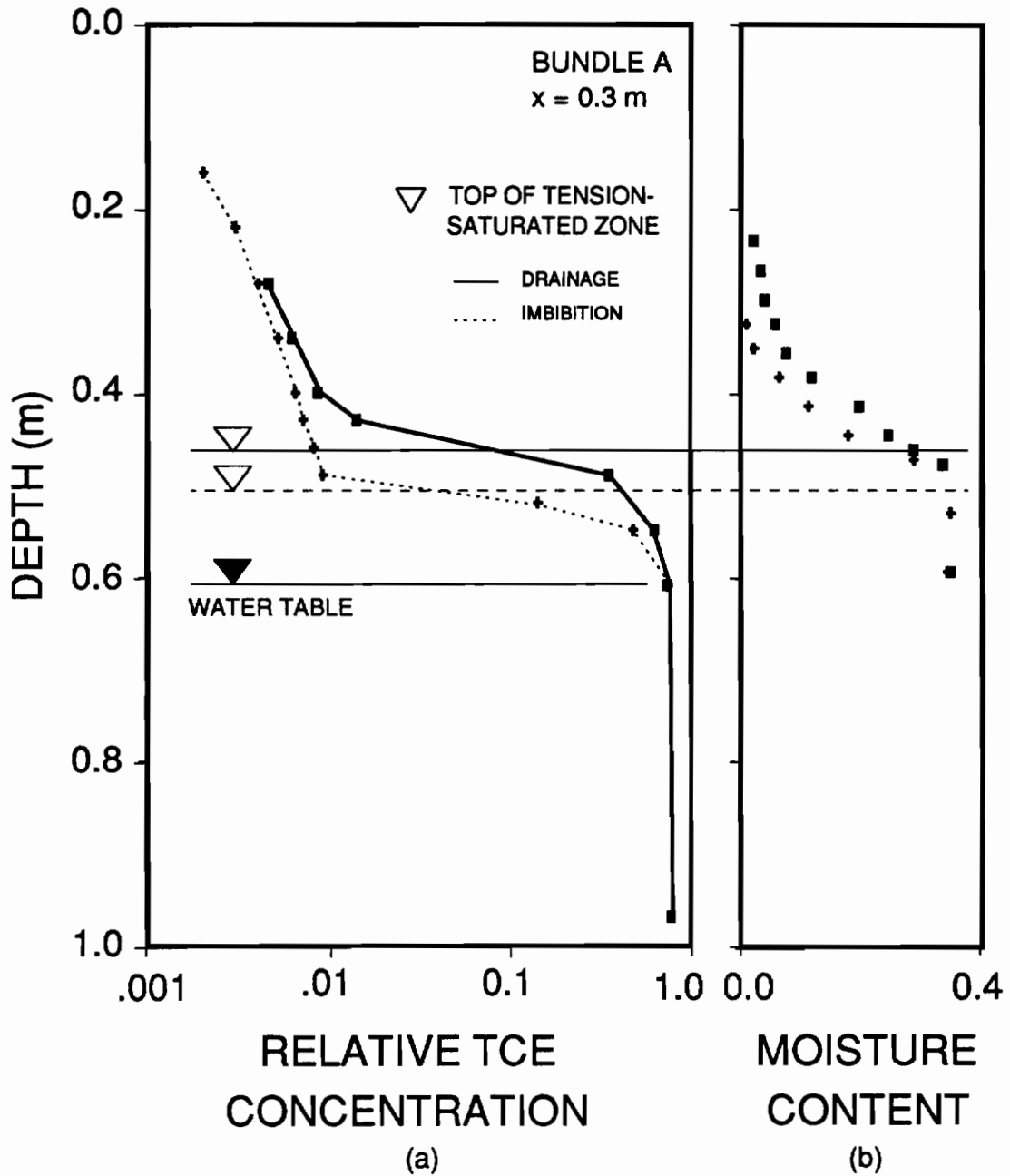


Figure 2.4. a) Steady-state profiles of depth versus TCE concentration under drainage (■) and imbibition (+) conditions. b) Moisture content versus depth under drainage (■) and imbibition (+) conditions. [Concentrations are reported relative to influent concentration.]

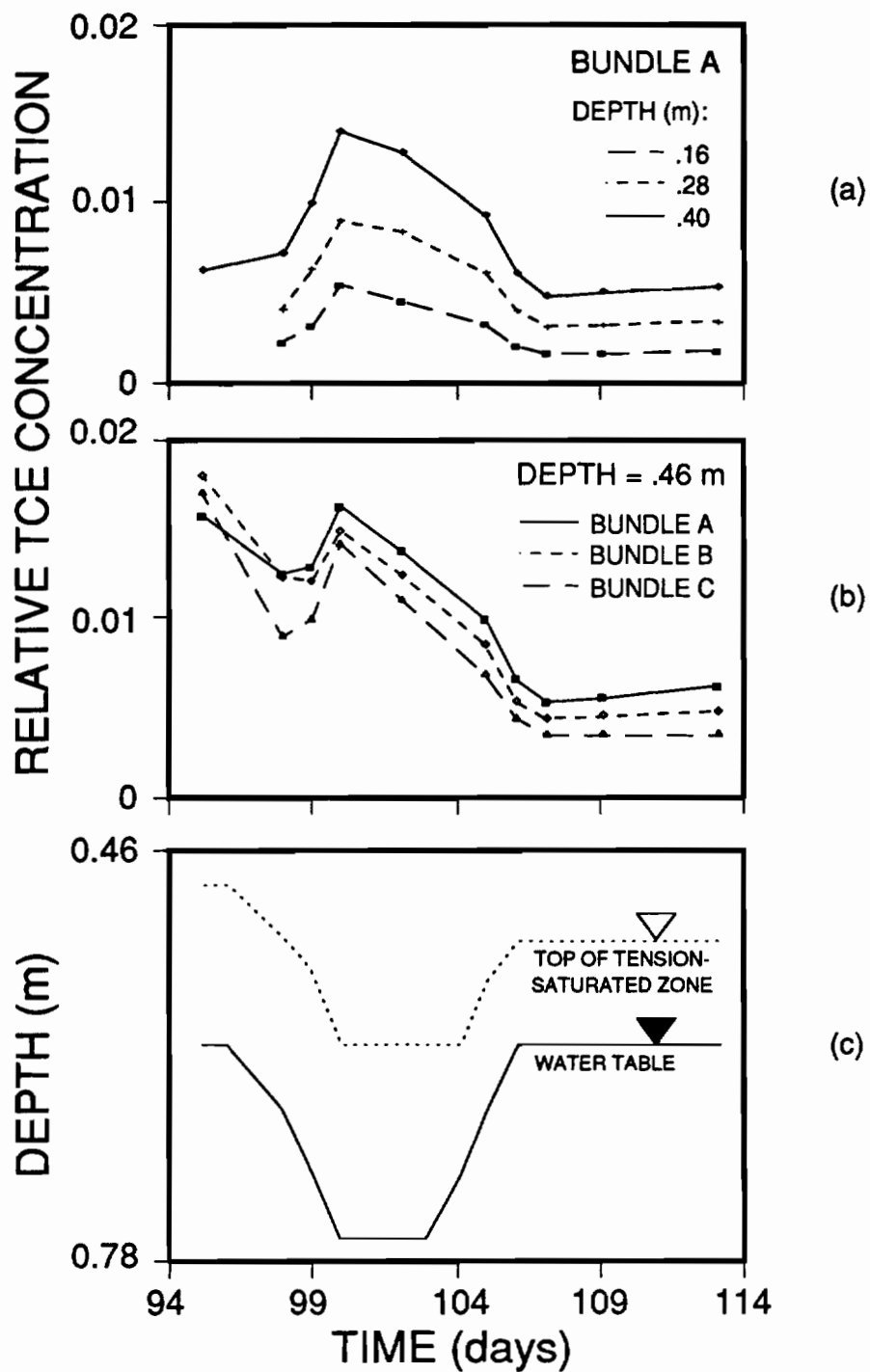


Figure 2.5. Water-table drop experiment. a) TCE concentration versus time at sampling bundle A ($x = 0.3$ m), b) TCE concentration versus time at a depth of 0.46 m, and c) water level versus time. [Concentrations are reported relative to influent concentration.]

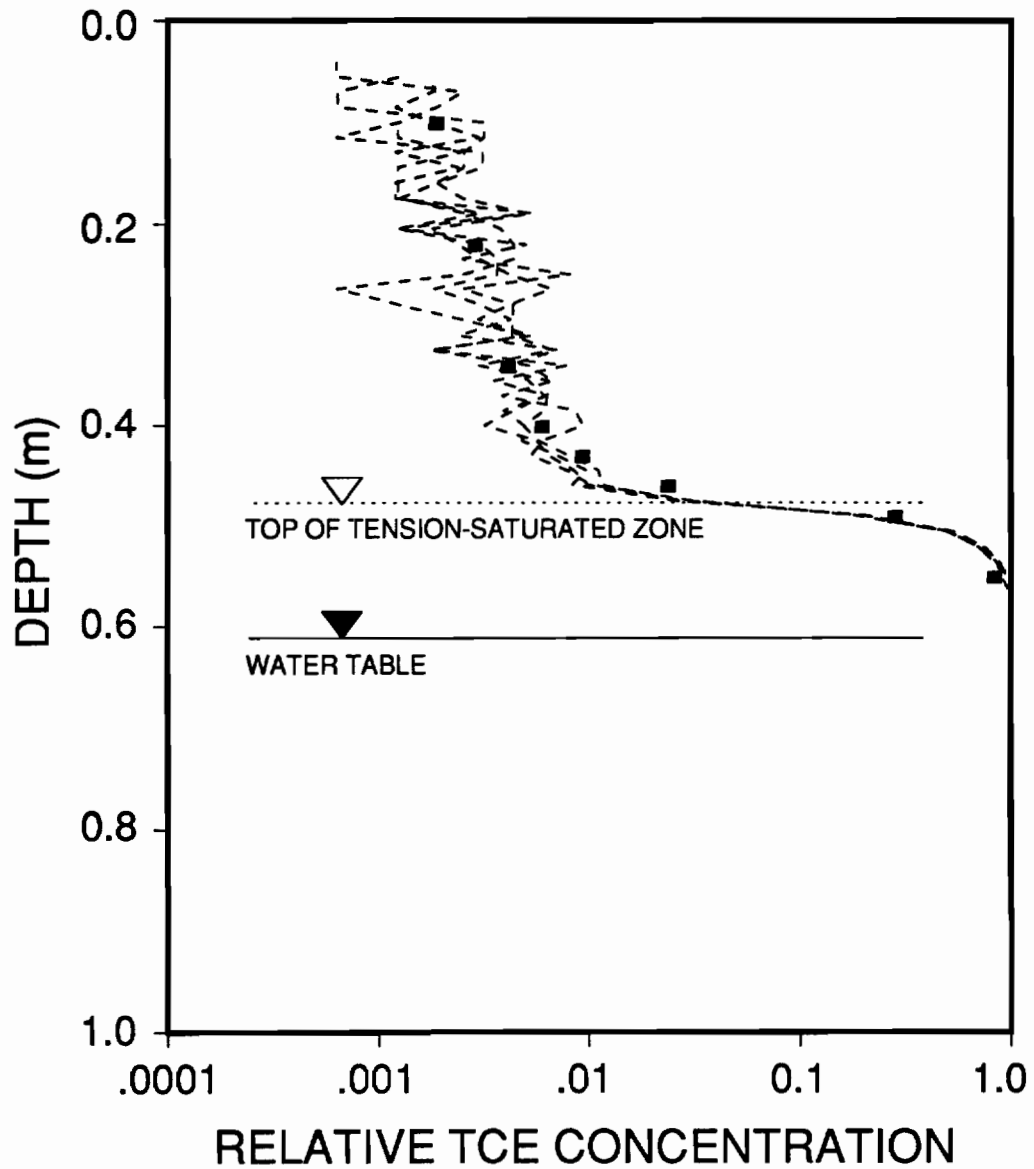


Figure 2.6. Superposed results from the two-dimensional numerical model (lines) and experimental data (symbols) from sampling bundle C ($x = 0.7$ m). [Concentrations are reported relative to the maximum concentration at bundle A ($x = 0.3$ m).]

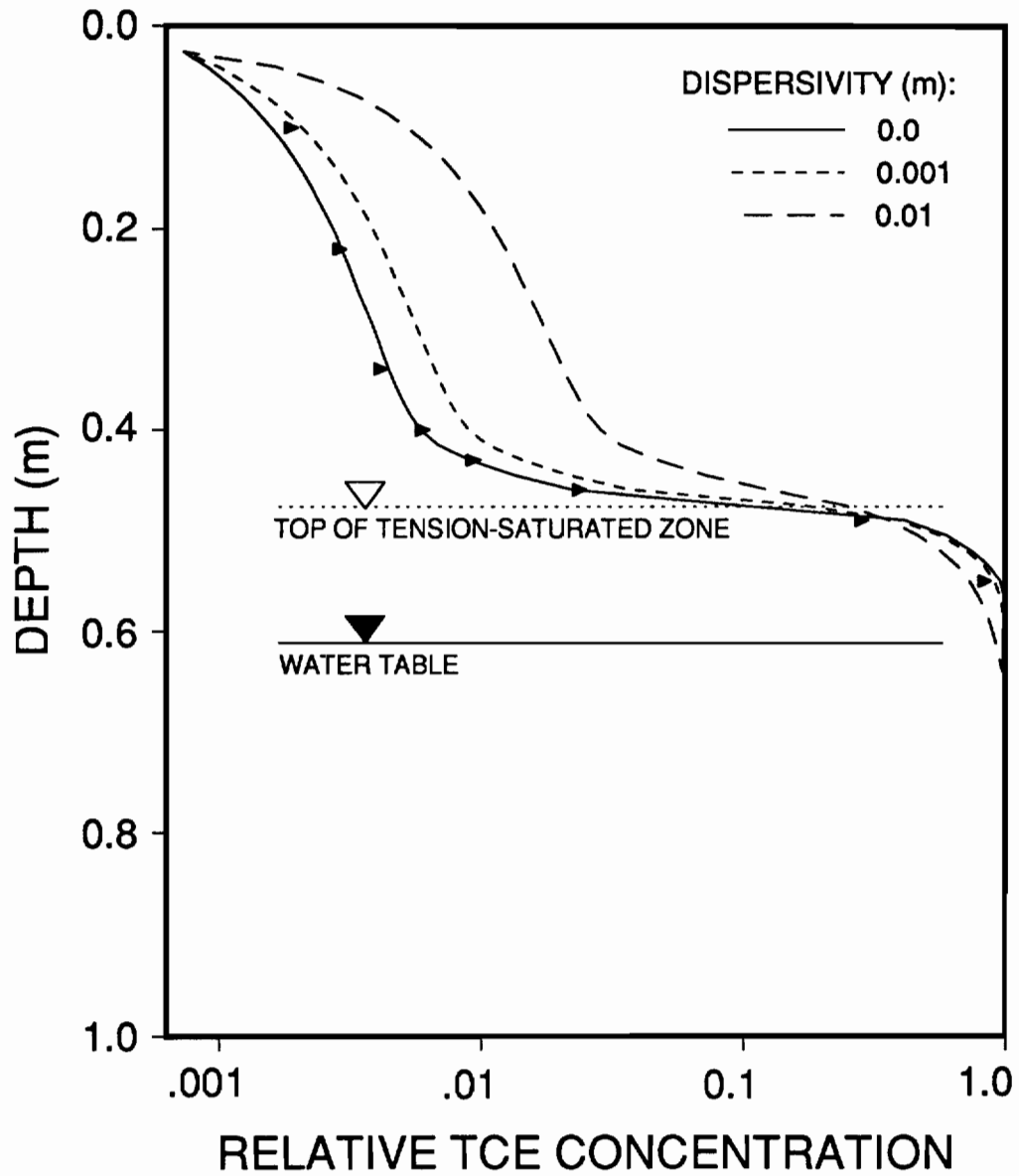


Figure 2.7. Results from the one-dimensional numerical model (lines) and experimental data (symbols) from sampling bundle C ($x = 0.7$ m). [Concentrations are reported relative to the maximum concentration at bundle A ($x = 0.3$ m).]

TABLE 2.1. Numerical model input parameters for TCE at 20 C.

PARAMETER	VALUE
FREE-WATER DIFFUSION COEFFICIENT (m ² /s)	9.1 x 10 ⁻¹⁰ ^a
FREE-GAS DIFFUSION COEFFICIENT (m ² /s)	8.3 x 10 ⁻⁶ ^b
HENRY'S CONSTANT (dimensionless)	0.38 ^c
SOIL-WATER PARTITION COEFFICIENT (dimensionless)	0.126 ^c

^a Estimated by the Hayduk and Laudie Method [Lyman et al., 1982]

^b Estimated by the Fuller, Schettler and Giddings Method [Lyman et al., 1982]

^c Mabey et al., 1982

CHAPTER 3

MEASUREMENT OF TRICHLOROETHYLENE DIFFUSION IN SOIL WITH A CONTINUOUSLY-VARYING MOISTURE CONTENT

3.1 INTRODUCTION

Molecular diffusion in porous media has been a subject of study for several decades. In virtually all of these investigations, the concept of tortuosity has been used to describe the impedance to diffusion resulting from the porous medium. The tortuosity factor is customarily expressed as:

$$\tau = \frac{D_e}{D} \quad (3.1)$$

where D_e is the effective diffusion coefficient in the porous medium, and D is the diffusion coefficient in the absence of the porous medium. In fully-saturated materials, impedance to diffusion results from the structure of the porous medium only, and the range of accepted values of the tortuosity factor is relatively small. For example, a tortuosity factor of $\frac{2}{3}$, or approximately 0.7, is generally accepted for saturated sand [de Marsily, 1986; Bear, 1972]. In partially-saturated materials, however, impedance to diffusion results not only from the porous medium, but also from the presence of a second fluid phase. Under such conditions, the value of the tortuosity factor can range over several orders of magnitude. The resulting change in the effective diffusion coefficient

can significantly affect transport across the capillary fringe and hence control the relationship between concentrations in ground water and overlying soil gas. In addition, changes in the effective diffusion coefficient can strongly influence the movement of vapors within the unsaturated zone.

Reible and Shair [1982], Weeks et al. [1982], and Troeh et al. [1982] provide concise reviews of several of the expressions that have been developed to describe the tortuosity factor in partially-saturated porous media. While no single expression can precisely account for all of the factors that influence diffusion through all types of porous media, reliable approximations are necessary for investigations of the transport and fate of compounds in the subsurface, especially in variably-saturated media.

The relationship between total and air-filled porosity developed by Millington [1959] to approximate the tortuosity factor has been widely used for several decades:

$$\tau_g = \frac{\theta_g^{7/3}}{\theta_T^2} \quad (3.2)$$

In this expression, τ_g is the gas-phase tortuosity factor, θ_g is the gas-filled porosity, and θ_T is the total porosity. To arrive at this expression, Millington [1959] developed the expression for the planar area "available" for transport in a dry porous medium and coupled this with the expression for the probability of continuity between adjacent planes proposed by Childs and Collis-George [1950]. He then expanded this expression to account for the presence of water within the pores. One advantage of this theoretical approach is that the expression is generally applicable over a broader range of moisture levels than expressions based on empirical data. Other estimation methods have subsequently been developed to improve on this expression (e.g., Millington and Shearer [1971], for aggregated porous media; van Brakel and Heertjes [1974]; Troeh et al. [1982]; and Nielson et al. [1984]) but they are more mathematically complex and often require additional data that are not readily available (e.g., pore-size distributions).

A number of investigators have compared experimentally determined and estimated diffusion coefficients. Sallam et al. [1984] measured Freon diffusion through soils with relatively high water contents and compared their measured diffusion coefficients with predictions from several models available in the literature. While they suggest a minor modification to Millington's [1959] expression, they found it to be the most accurate of the models employed. Karimi et al. [1987] measured benzene diffusion through soils with relatively low water contents and found Millington's [1959] expression for the tortuosity factor adequately predicted flux through the soil. Collin and Rasmuson [1988] used a number of methods to estimate effective diffusion coefficients and compared the results with experimental diffusion data available in the literature. They concluded that the method of Millington and Shearer [1971] provided the best estimate of effective diffusion coefficients. The simpler Millington [1959] expression was not included in their comparisons.

In the experimental work referenced above, soil samples were prepared to achieve a particular, uniform water content. This is a common practice and is often accomplished by mechanically mixing known volumes of soil and water together. The resulting soil-moisture distribution is undoubtedly different than in naturally-drained soils. The first objective of the current study was to measure the effective diffusion coefficient of trichloroethylene (TCE) in a gravity-drained soil where the moisture content varied from field capacity to saturation. The technique used was designed to achieve moisture conditions that closely approximate those encountered in the field. The second objective was to investigate the applicability of a single expression for the tortuosity factor to this range of moisture conditions. Although the underlying theory strictly applies only to conditions of constant moisture content, Millington's [1959] expression for the tortuosity factor was chosen as a basis for comparison due to its previous success, its relatively simple formulation, and the fact that it is applicable over a wide range of moisture contents.

Shackelford [1991] provides a review of the various transient and steady-state methods that have been used to measure diffusion coefficients in the laboratory. Steady-

state methods permit the use of relatively simple mathematical expressions for determining effective diffusion coefficients and allow the effects of sorption and phase partitioning between the gas and aqueous phases to be neglected. Therefore, a steady-state approach, similar to that used by Penman [1940], was chosen for this study.

The experiments were performed on discrete sections of gravity-drained sand columns and thus provide a measure of diffusion through a continuously-varying soil-moisture profile. In addition, the vertical resolution achieved in these experiments (2.5 cm) provides insight into the spatial variability of subsurface molecular diffusion.

3.2 EXPERIMENTAL

Three columns of sand were prepared for the diffusion experiments. The column design is shown in Figure 3.1. Each aluminum column was 3.8 cm in diameter and approximately 30 cm in length. An aluminum end cap containing a 10-ml reservoir and access port was sealed to the bottom of each column with caulk. The reservoir was separated from the column by a circular piece of screen supported on a circular piece of perforated metal. The columns were packed vertically with dry #8 flintshot Ottawa sand in 0.5-cm increments with gentle tamping between lifts. A circular piece of screen was placed on the sand surface and this was covered by another circular piece of perforated metal to increase rigidity. End caps similar to those on the bottom, but with two access ports, were then sealed to the tops with caulk. To promote thorough water saturation, approximately 20 pore volumes of CO₂ were flushed upward through each column followed by approximately 50 pore volumes of helium-sparged water. Constant-head reservoirs were then connected to the bottom ports and the saturated columns were allowed to drain for several weeks with the water table maintained near the bottom of the sand. This resulted in soil-moisture profiles within each column ranging from field capacity near the top to complete saturation near the bottom.

For the first diffusion experiment, a tubing cutter was used to cut a 2.5-cm section from the top of one of the columns. Once the aluminum column was severed, a thin

piece of stainless steel was inserted through the cut and the 2.5-cm section was lifted from the column. Aluminum end caps fitted with screen and perforated metal disks, similar to those described previously, were then sealed to the exposed surfaces at the bottom of the section and the top of the remaining column. Column sections for subsequent experiments were prepared in the same way and ranged in length from 2.5 to 2.9 cm. Thus, each column provided several sections for independent diffusion experiments.

The setup used for the diffusion experiments is shown in Figure 3.2. Humidified air was continuously flushed through the top reservoir of the diffusion cell at a constant rate. Flow rates used for the various experiments ranged between two and ten ml/min. At the beginning of each experiment, one ml of TCE was placed in the bottom reservoir using a syringe. Care was taken to ensure that the system remained at ambient pressure during this step. The reservoir port was then sealed and the entire diffusion cell was placed in a constant-temperature bath. The temperature was maintained between 24 and 25 C.

During the experiments, effluent from the top reservoir flowed to a vent and was also connected to an eight-port valve that allowed sampling to be automated. In the "passive" mode, flow through the valve followed the dotted-line path (Figure 3.2). Effluent from the diffusion cell flowed to the vent. A vacuum pump was connected to a 0.5-ml "evacuation chamber." In the "sampling" mode, effluent from the diffusion cell was drawn into the evacuation chamber, filling a 0.1-ml sample loop. When the valve once again switched to the "passive" mode, the contents of the sample loop were flushed via carrier gas to a Hewlett-Packard HP 5890 Gas Chromatograph (Hewlett-Packard Co., Avondale, PA) equipped with a flame ionization detector. Data acquisition and the valve were controlled by a Nelson Analytical 3000 Series Chromatography Data System (Nelson Analytical, Inc., Cupertino, CA). Using this system, effluent samples were analyzed every 3, 15, 30, or 60 minutes, depending on the individual experiment. Regardless of sampling frequency, the valve remained in the sampling mode for 30 seconds. A water manometer connected to the effluent line showed that the system remained at atmospheric pressure

at all times. Each experiment was continued until the effluent concentration stabilized. The concentration in the headspace of the bottom reservoir was measured periodically and at the end of each experiment and remained essentially constant throughout each experiment.

Once the experiment was concluded, the end caps were removed and the column section was weighed, air-dried for several days, then reweighed periodically until no further changes in weight were observed. The loss in weight was assumed to be due to water evaporation and was used to determine the moisture content of the section. The dry sand was then removed from the column section and weighed, yielding the dry bulk density of the section, ρ_b . Using the grain density supplied by the vendor (Ottawa Industrial Sand Company, Ottawa, IL), the total porosity of the section was calculated from ρ_b .

3.3 RESULTS AND DISCUSSION

Figures 3.3 and 3.4 show examples of experimental data collected from two of the column sections. Data in Figure 3.3 are from a relatively dry section with a water content of 0.04 (volume of water/bulk volume of soil). TCE breakthrough occurred within minutes and the effluent concentration stabilized after approximately one hour. Data in Figure 3.4 are from a nearly-saturated section (water content = 0.32) and clearly show the effect of the higher water content on the effective diffusion coefficient. TCE breakthrough was much slower through this section and several days were required for the effluent concentration to stabilize. In addition, the stabilized flux through this section was approximately three orders of magnitude lower than through the drier section. All column sections showed similar behavior with breakthrough and approach to steady state occurring more slowly and flux decreasing as the water content increased.

3.3.1 CALCULATION OF EFFECTIVE DIFFUSION COEFFICIENTS

Calculation of effective diffusion coefficients from experimental data was based on Fick's First Law, modified to account for diffusion through a porous medium:

$$F_T = - \left[\theta_w \tau_w D_{fw} \left(\frac{\partial C_w}{\partial z} \right) + \theta_g \tau_g D_{fg} \left(\frac{\partial C_g}{\partial z} \right) \right] \quad (3.3)$$

where F_T is the total flux; θ_w and θ_g are the water- and air-filled porosities; τ_w and τ_g are the water- and gas-phase tortuosity factors; D_{fw} and D_{fg} are the free-water and free-gas diffusion coefficients; C_w and C_g are the water- and gas-phase concentrations; and z is the vertical coordinate. Because the experimental conditions approximated steady state, equilibrium between the aqueous and gas phases can be assumed and equation 3.3 can be expressed as:

$$F_T = - \left[\frac{\theta_w \tau_w D_w}{H} + \theta_g \tau_g D_g \right] \left(\frac{\partial C_g}{\partial z} \right) \quad (3.4)$$

where H is the dimensionless form of Henry's Constant (gas-phase concentration/aqueous-phase concentration). The expression in brackets in equation 3.4 represents the overall effective diffusion coefficient, and can be expressed simply as:

$$D_e^* = - F_T \left(\frac{\partial C_g}{\partial z} \right)^{-1} \quad (3.5)$$

D_e^* strictly accounts only for the reduced cross-sectional area available for flux and the effects of tortuosity. Other impedances to diffusion encountered in porous media such as constrictivity (e.g., Dullien [1975] and van Brakel and Heertjes [1974]) and pore-wall effects (e.g., Thorstenson and Pollock [1989]) are assumed to be relatively negligible.

Substituting measured experimental values into equation 3.5 yields the following expression for the effective diffusion coefficient for each column section:

$$D_e^* = \frac{\frac{C_1 Q}{A}}{\frac{C_2 - C_1}{L}} \quad (3.6)$$

where C_1 is the effluent concentration; Q is the effluent flow rate; A is the cross-sectional area of the section; C_2 is the gas-phase concentration in the bottom reservoir; and L is the length of the section. The numerator on the right side of equation 3.6 represents the flux from the section and the denominator represents the vertical concentration gradient within the section.

The application of equation 3.6 requires the following assumptions:

- 1) Effluent and bottom-reservoir concentrations are constant over the period of interest.
- 2) The concentration gradient within each section is linear.
- 3) Transport of TCE within each section is by molecular diffusion only.

The first assumption is valid because only data from late in each experiment, after the effluent concentration had stabilized, were used in calculations. Because moisture content varies with depth, the second assumption is not strictly valid. However, due to the short length of each section, it is a reasonable approximation. To insure that diffusion was the only transport process, the diffusion cell was designed to prevent continuous advective flow through the column sections. The bottom of the cell was sealed and the pressure in the effluent line was maintained at a constant value (monitored with a manometer). The third assumption is therefore sound.

3.3.2 COMPARISON OF EXPERIMENTAL AND THEORETICAL EFFECTIVE DIFFUSION COEFFICIENTS

As mentioned previously, one objective of this study was to investigate the applicability of Millington's [1959] expression for the tortuosity factor to continuously-varying moisture conditions. As given in equation 3.2, Millington's [1959] expression for the gas-phase tortuosity factor is:

$$\tau_g = \frac{\theta_g^{7/3}}{\theta_T^2} \quad (3.7)$$

Because aqueous-phase diffusion does become significant at high moisture contents, the effective diffusion coefficients used throughout this study were based on diffusion through both the gas and aqueous phases. Therefore, an expression analogous to equation 3.7 was used for the water-phase tortuosity factor. Recalling equations 3.4 and 3.5, D_e^* may now be written:

$$D_e^* = \frac{\frac{\theta_w^{10/3} D_w}{H} + \theta_g^{10/3} D_g}{\theta_T^2} \quad (3.8)$$

Figure 3.5 shows the experimentally determined effective diffusion coefficients, calculated using equation 3.6, along with theoretical effective diffusion coefficients, calculated using equation 3.8. The free-water diffusion coefficient used in equation 3.8 was estimated by the Hayduk and Laudie method [Lyman et al., 1982] and the free-gas diffusion coefficient was estimated by the Fuller, Schettler and Giddings method [Lyman et al., 1982]. The water-filled porosities used were those determined for each section as described previously. The total porosity used was the average of all values determined for each individual section. Gas-filled porosity was assumed to be the difference between

total porosity and water-filled porosity. Experimental values agree reasonably well with calculated values, though there is scatter in the data.

The observed scatter in the data can be largely attributed to the moisture conditions investigated. Figure 3.6 shows the soil-moisture profile measured in one of the columns. The soil-moisture profiles in all three columns were similar. Because the values of moisture content used to calculate effective diffusion coefficients are those measured from finite sections of gravity-drained columns, they reflect only the *average* moisture content for that section. The experimental error of this *average* measurement is small relative to the difference between *average* and *actual* moisture content within each section. The *actual* moisture content varied from a somewhat lower value in the shallow part of the section to a somewhat greater value in the deeper part. Diffusion was limited by the layer of highest water content encountered and therefore measured values of the effective diffusion coefficient are expected to be slightly lower than those calculated based on the average moisture content. This probably explains why equation 3.8 slightly underestimated diffusion coefficients at higher gas-filled porosities. As gas-filled porosity decreases, the diffusion process becomes sensitive to moisture *distribution* and will be dominated by any pathway through the column section with a moisture content less than the average value. This probably explains the scatter in the data at higher saturation levels. Considering the inherent nonideality of all moist porous media, however, the approximations of equation 3.8 appear quite adequate for a wide range of applications. For the purposes of numerical modeling, however, it should be noted that the continuous function described by this expression has a minimum near 96% water saturation rather than 100% water saturation.

3.3.3 NUMERICAL MODELING

While the transition from saturation to residual moisture content occurred over a distance of less than 0.3 m in the sand used for these experiments, finer grained materials will be characterized by much more vertically extensive capillary fringes [van Genuchten,

1978; Bumb et al., 1992]. As a result, the effects of high moisture content on the effective diffusion coefficient will be more significant. To demonstrate the relevance of this to subsurface transport, the one-dimensional numerical model developed in Chapter 2 was used. Two simulations were conducted with identical, continuous sources of dissolved TCE at the water table, located at a depth of 3.5 m. The soil-moisture profiles for each simulation were calculated using van Genuchten's [1978] equation:

$$\theta = \theta_r + \frac{\theta_s - \theta_r}{\left[1 + (\alpha |h|)^n\right]^{\left(1 - \frac{1}{n}\right)}} \quad (3.9)$$

where θ is the moisture content; θ_r and θ_s are the residual and saturation moisture contents; α and n are soil-dependent parameters; and h is the suction pressure head (in cm), taken here to be the distance above the water table. For the first simulation, the soil-moisture profile closely approximated the sand used in the experiments ($\alpha = 0.61$, $n = 6.51$). For the second simulation, parameters from van Genuchten [1978] were used to develop a soil-moisture profile characteristic of a finer-grained sand ($\alpha = .012$, $n = 3.0$). The two soil-moisture profiles are shown in Figure 3.7.

Figure 3.8 shows the simulated concentration profiles that developed in the two sands after one year of transport. Concentrations in the unsaturated zone are markedly different for the two sands and illustrate the strong impedance to diffusion that results from the higher moisture contents in the finer-grained sand. For example, at a depth of 2.0 meters, the concentrations in the two sands differ by nearly three orders of magnitude.

While these two sands are characterized by very different soil-moisture profiles, it should be noted that their properties span a very narrow range relative to soils typically encountered in the environment. For example, to compare the two sands in terms of a more familiar property, the hydraulic conductivity of the sand used in the experiments is approximately 75 m/d [Anderson, 1988] and van Genuchten [1978] reports a hydraulic conductivity of 4 m/d for the sand used for the second simulation. This suggests that

even moderately heterogeneous soils will be characterized by significant differences in moisture content, and hence effective diffusivity, within the unsaturated zone.

3.4 CONCLUSIONS

The experimental data reported here show the effect of changing moisture content in a continuous, gravity-drained soil profile. The effective diffusion coefficient was measured over the entire soil-moisture range from field capacity to complete saturation. As a result of water-content changes, the effective diffusion coefficient decreased three orders of magnitude over a vertical distance of only 15 cm.

The experimental data reported here also show that the Millington [1959] expression, modified to include the effects of aqueous-phase diffusion, provides a good approximation of tortuosity in unconsolidated porous media for moisture conditions ranging from field capacity to complete saturation. A primary advantage of this expression is that it requires only total porosity and moisture content as input parameters, values that can often be measured or estimated with relative ease. In addition, due to its simple formulation, this expression can easily be incorporated into field investigations or numerical models to represent the subsurface as a continuum rather than a collection of discrete zones of uniform water content.

The numerical simulations show the strong influence of the soil-moisture profile on vertical transport from the saturated zone. After one year of diffusive transport, concentrations in the unsaturated zones of two sands differed by nearly three orders of magnitude.

3.5 REFERENCES

Anderson, M. R., The dissolution and transport of dense non-aqueous phase liquids in saturated porous media, Ph.D. Dissertation, 260 pp., Oregon Graduate Institute, Beaverton, Oregon, 1988.

Bear, J., Dynamics of Fluids in Porous Media, 764 pp., Dover Publications, Inc., New York, 1972.

Bumb, A. C., C. L. Murphy, and L. G. Everett, A comparison of three functional forms for representing soil moisture characteristics, **Ground Water**, **30**, 177-185, 1992.

Dullien, F. A. L., Prediction of "tortuosity factors" from pore structure data, **American Institute of Chemical Engineers Journal**, **21**, 820-822, 1975.

Childs, E. C., and N. Collis-George, The permeability of porous materials, **Proc. R. Soc. London A.**, **201**, 392-405, 1950.

Collin, M., and A. Rasmuson, A comparison of gas diffusivity models for unsaturated porous media, **Soil Sci. Soc. Am. J.**, **52**, 1559-1565, 1988.

de Marsily, G., Quantitative Hydrogeology, 440 pp., Academic Press, Inc., Orlando, 1986. Translated from the French by G. de Marsily.

Karimi, A. A., W. J. Farmer, and M. M. Cliath, Vapor-phase diffusion of benzene in soil, **J. Environ. Qual.**, **16**, 38-43, 1987.

Lyman, W. J., W. F. Reehl, and D. H. Rosenblatt, Handbook of Chemical Property Estimation Methods: Environmental Behavior of Organic Compounds, McGraw-Hill, New York, 1982.

Millington, R. J., Gas diffusion in porous media, **Science**, **130**, 100-102, 1959.

Millington, R. J., and R. C. Shearer, Diffusion in aggregated porous media, **Soil Sci.**, **111**, 372-378, 1971.

Nielson, K. K., V. C. Rogers, and G. W. Gee, Diffusion of radon through soils: A pore distribution model, **Soil Sci. Soc. Am. J.**, **48**, 482-487, 1984.

Penman, H. L., Gas and vapour movements in the soil, 1, The diffusion of vapours through porous solids, **J. Agric. Sci.**, **30**, 437-462, 1940.

Reible, D. D., and F. H. Shair, A technique for the measurement of gaseous diffusion in porous media, **J. Soil. Sci.**, **33**, 165-174, 1982.

Sallam, A., W. A. Jury, and J. Letey, Measurement of gas diffusion coefficient under relatively low air-filled porosity, **Soil Sci. Soc. Am. J.**, **48**, 3-6, 1984.

Shackelford, C. D., Laboratory diffusion testing for waste disposal--a review, **J. Contam. Hydrol.**, **7**, 177-217, 1991.

Thorstenson, D. C., and D. W. Pollock, Gas transport in unsaturated porous media: The adequacy of Fick's law, **Reviews of Geophysics**, **27**, 61-78, 1989.

Troeh, F. R., J. D. Jabro, and D. Kirkham, Gaseous diffusion equations for porous materials, **Geoderma**, **27**, 239-253, 1982.

van Brakel, J., and P. M. Heertjes, Analysis of diffusion in macroporous media in terms of a porosity, a tortuosity and a constrictivity factor, **Int. J. Heat Mass Transfer**, **17**, 1093-1103, 1974.

van Genuchten, M. Th., Numerical solutions of the one-dimensional saturated-unsaturated flow equation, Research Report 78-WR-09, Water Resources Program, Department of Civil Engineering, Princeton University, Princeton, New Jersey, 1978.

Weeks, E. P., D. E. Earp, and G. M. Thompson, Use of atmospheric fluorocarbons F-11 and F-12 to determine the diffusion parameters of the unsaturated zone in the Southern High Plains of Texas, **Water Resour. Res.**, **18**, 1365-1378, 1982.

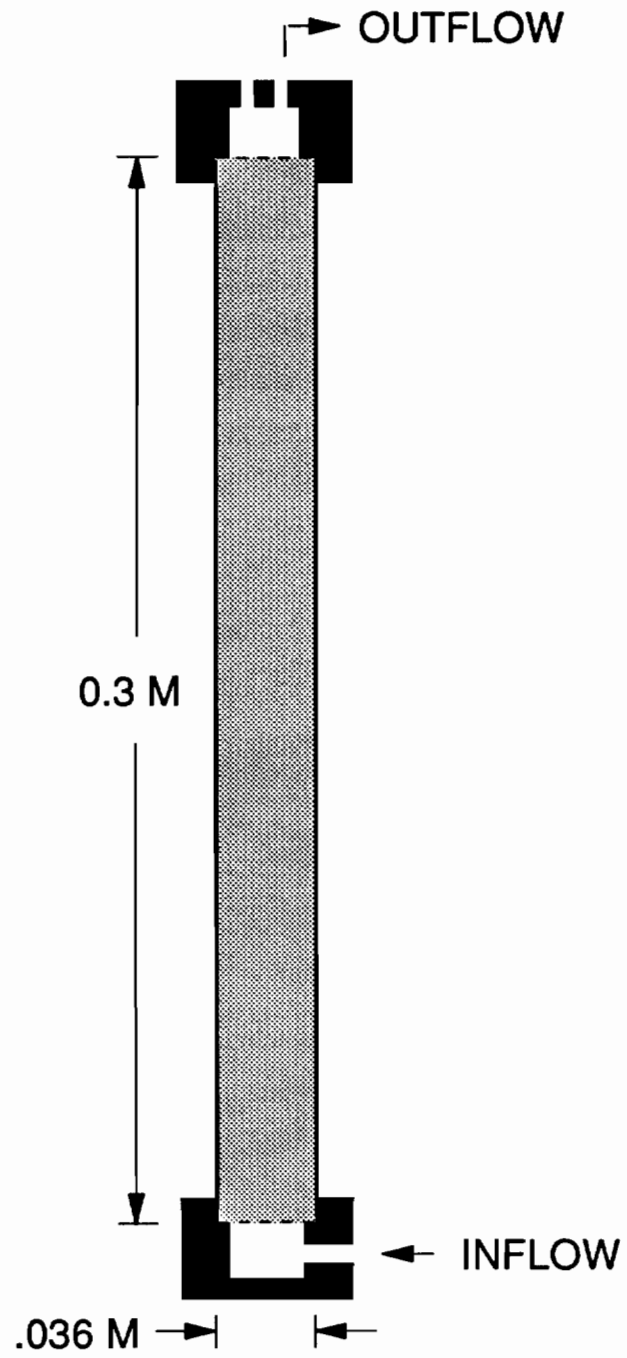


Figure 3.1. Column design.

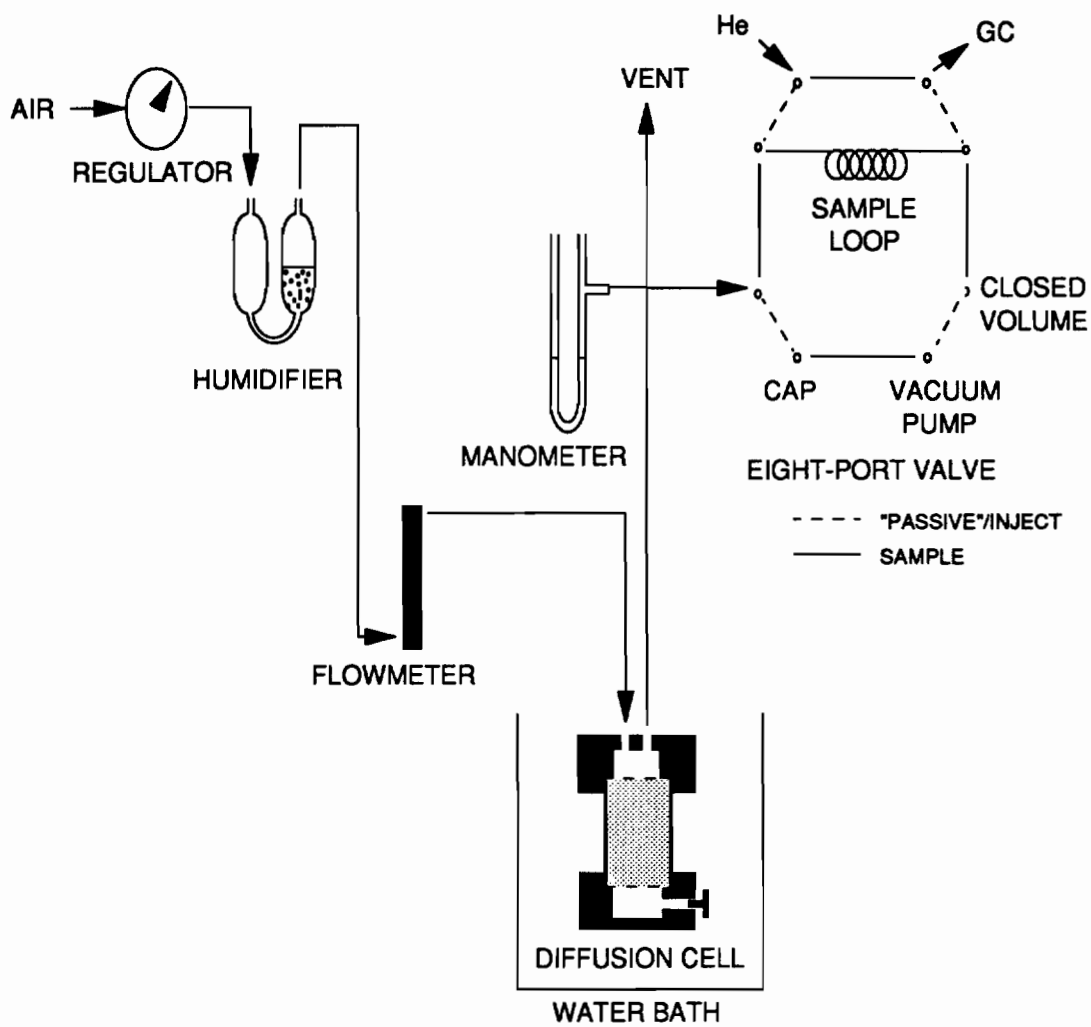


Figure 3.2. Experimental setup.

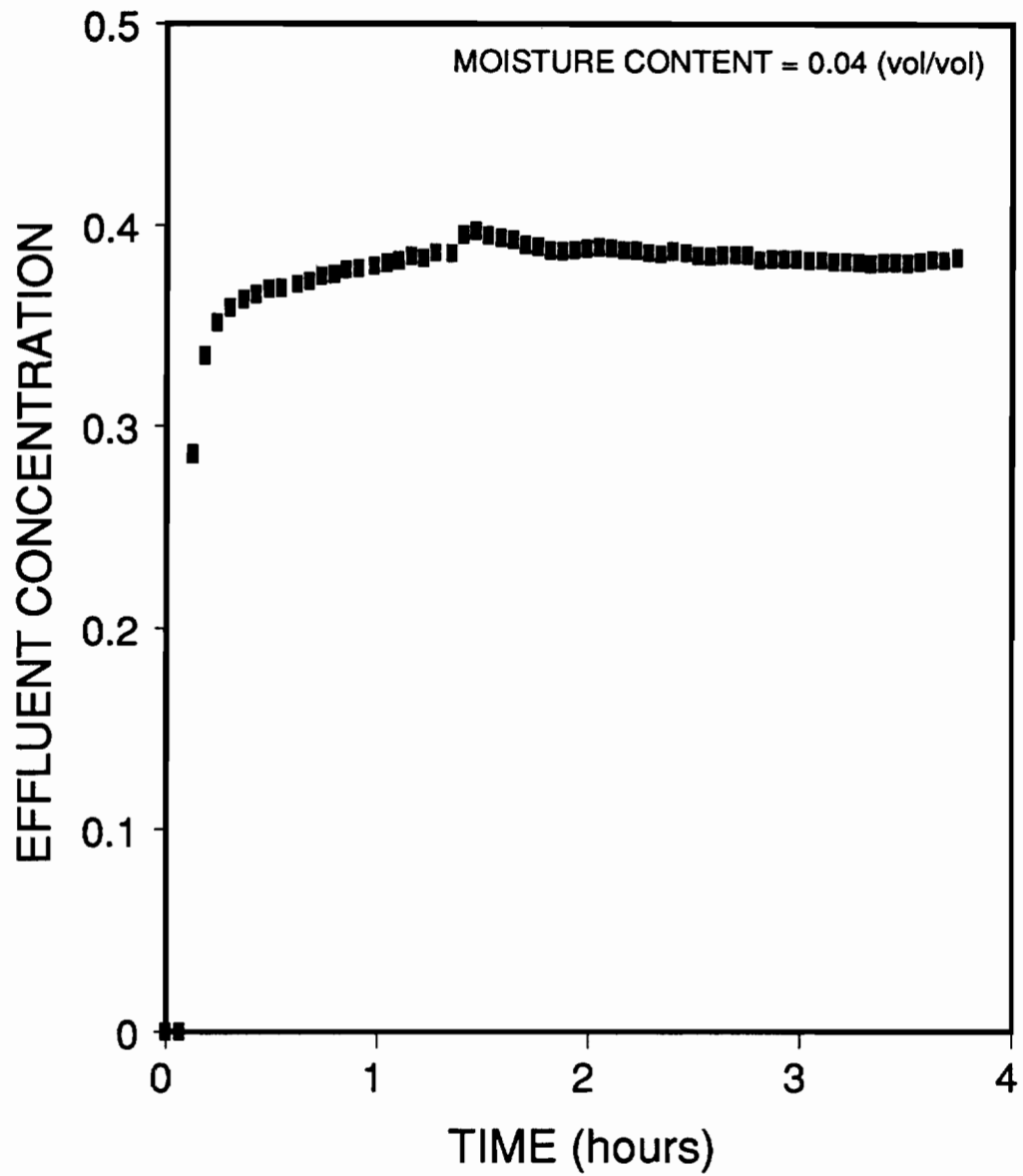


Figure 3.3. Effluent concentration versus time for a column section with low moisture content. [Effluent concentration is reported relative to bottom-reservoir concentration].

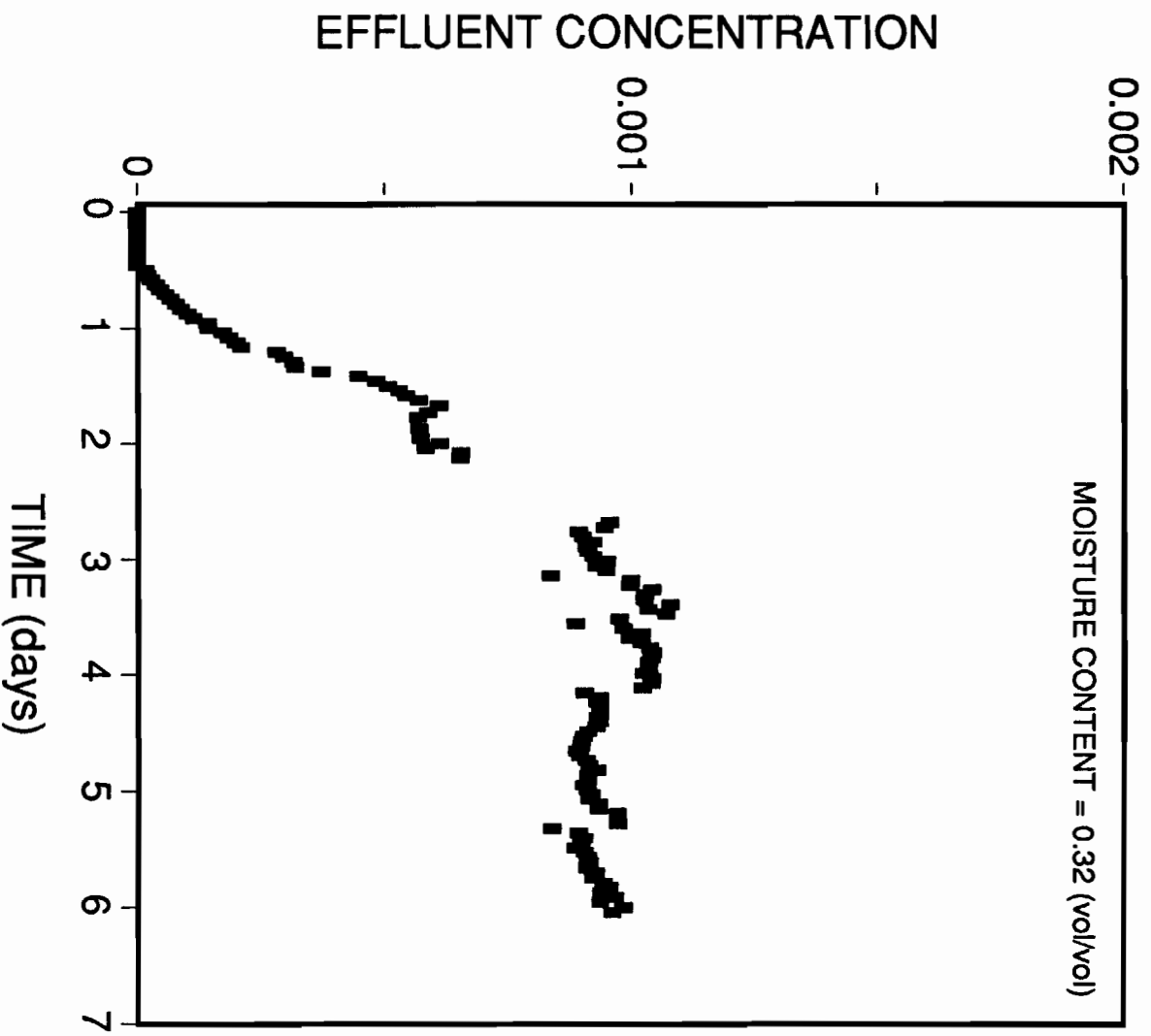


Figure 3.4. Effluent concentration versus time for a column section with high moisture content. [Effluent concentration is reported relative to bottom-reservoir concentration].

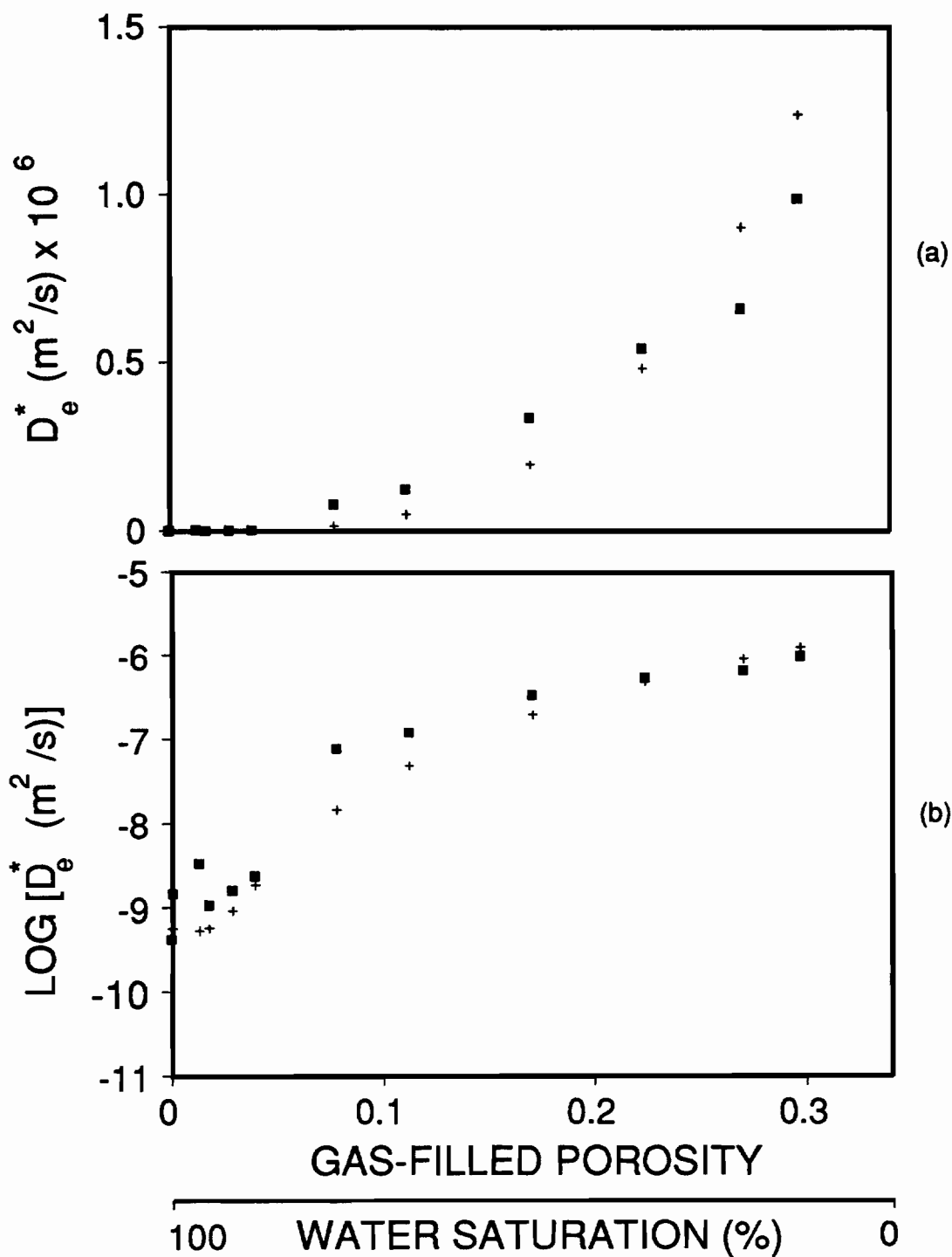


Figure 3.5. Measured^a (■) and theoretical^b (+) effective diffusion coefficients versus gas-filled porosity. a) Arithmetic scale, and b) Semi-logarithmic scale.

^aCalculated using equation 3.6.

^bCalculated using equation 3.8.

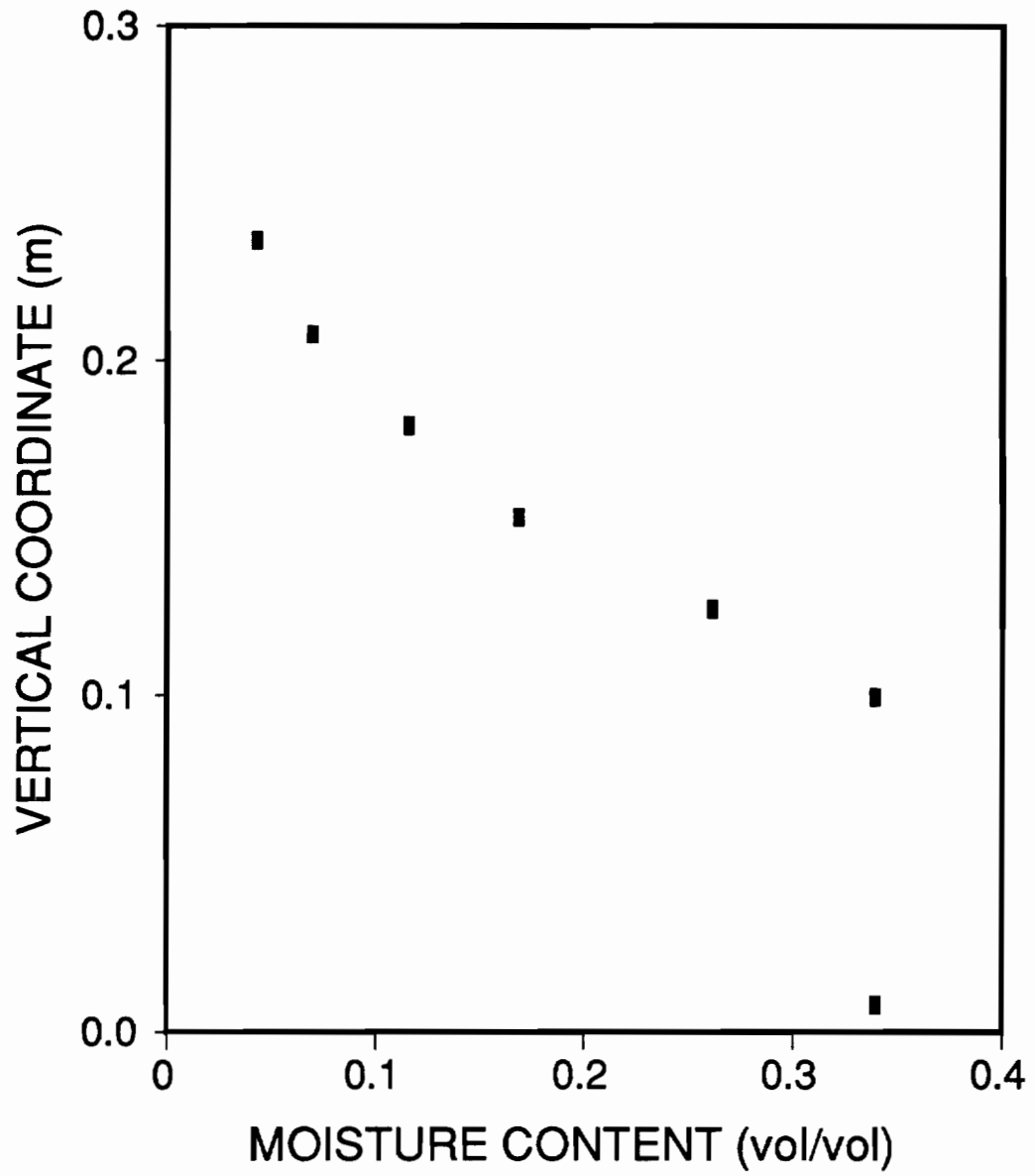


Figure 3.6. Measured soil-moisture profile.

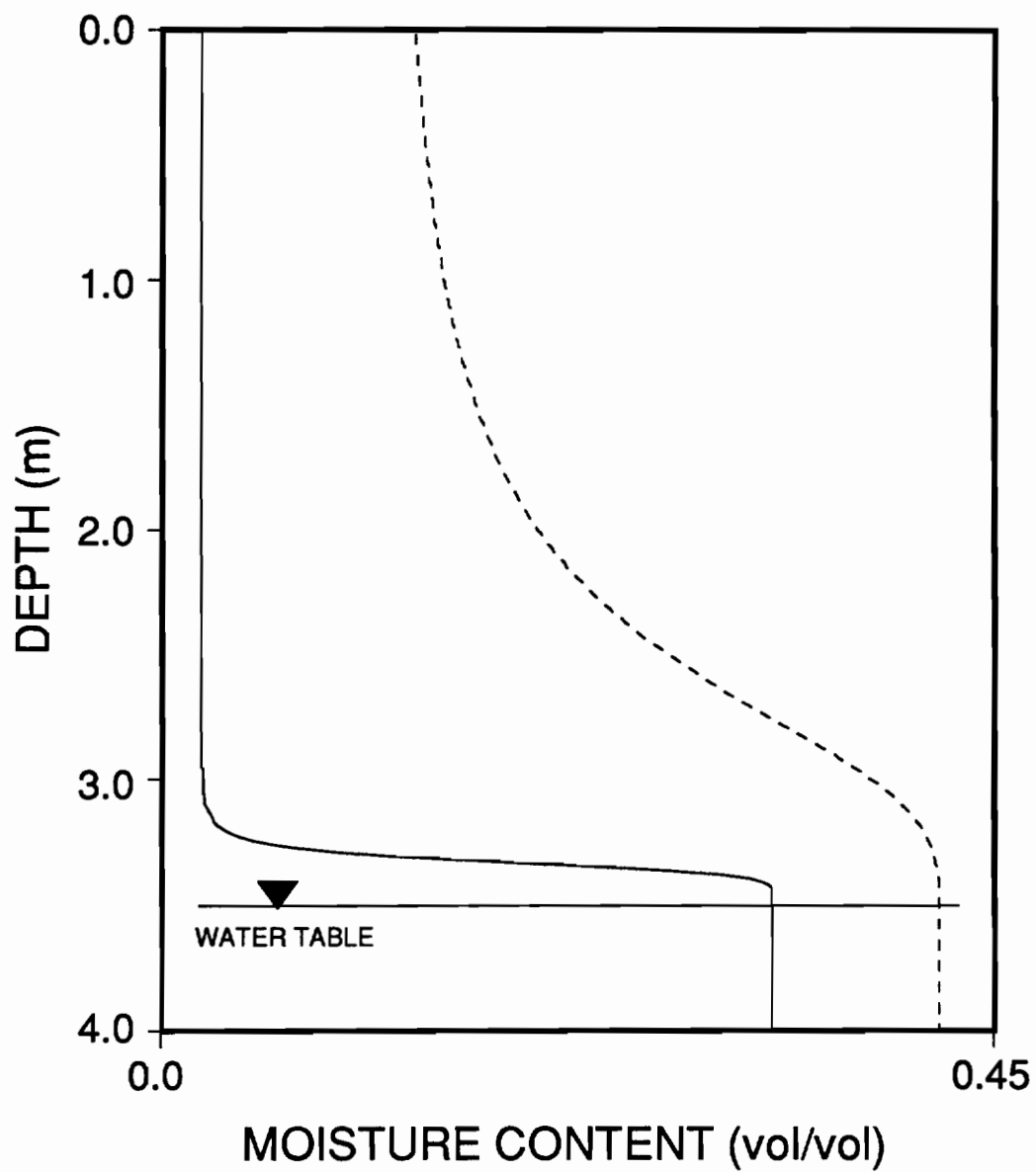


Figure 3.7. Calculated soil-moisture profiles for the experimental (solid line) and finer-grained (dotted line) sands used in the numerical simulations.

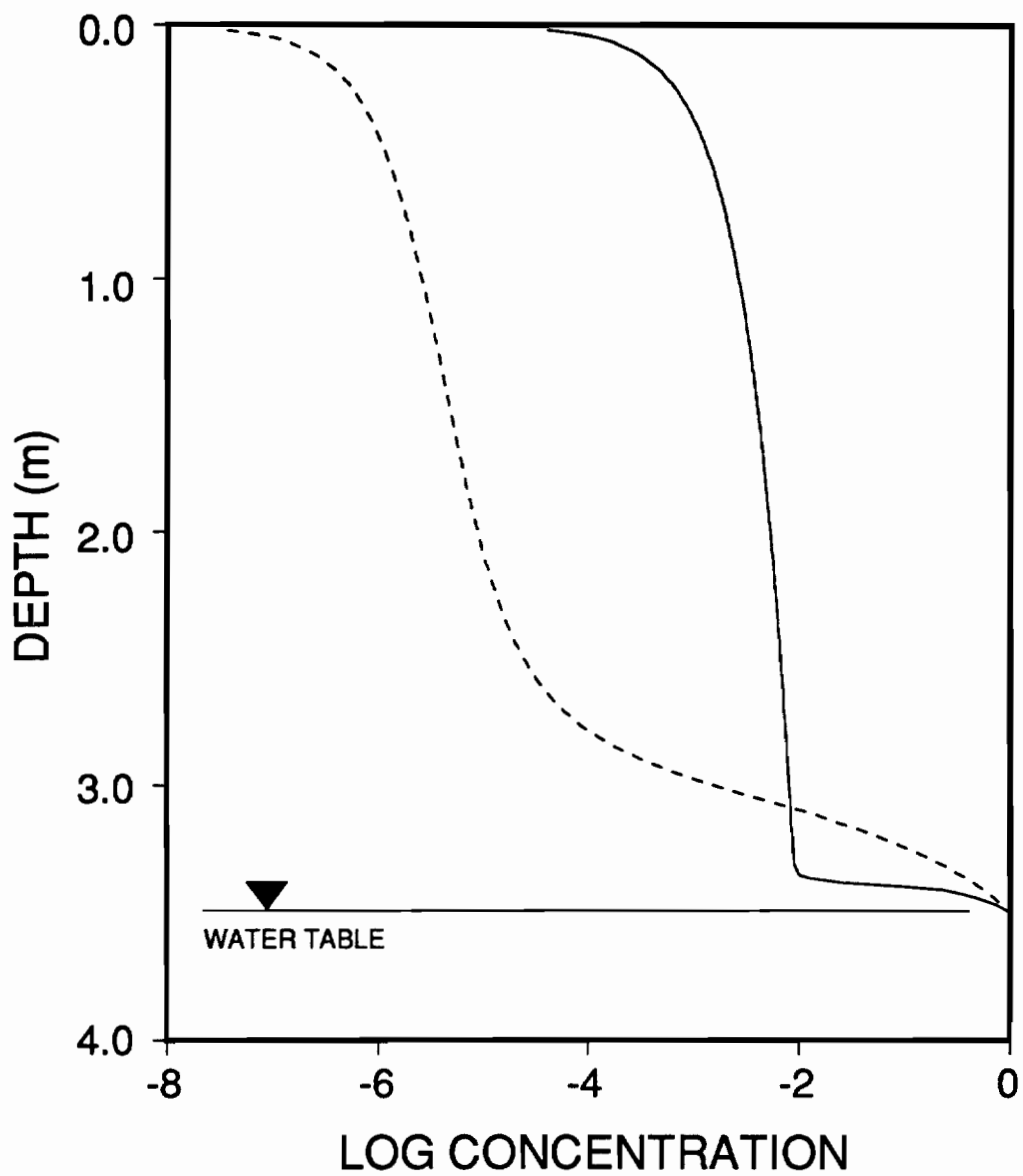


Figure 3.8. Results from the numerical simulation of transport through the experimental (solid line) and finer-grained (dotted line) sands.

CHAPTER 4

DEVELOPMENT OF A TWO-DIMENSIONAL PARTICLE-TRACKING MODEL

4.1 INTRODUCTION

Mass transfer of volatile organics between the saturated and unsaturated zones of the subsurface is often controlled by vertical transport processes within the capillary fringe. As shown in Chapter 2, very large vertical concentration gradients can occur in this region due to the nature of the soil-moisture profile and its affect on the effective diffusion coefficient. Experimental data from Chapters 2 and 3 are shown in Figure 4.1 which illustrates the large changes in the magnitudes of TCE concentrations, soil-moisture contents, and effective diffusion coefficients that occur within the capillary fringe.

In order to mathematically model mass exchange between the saturated and unsaturated zones, transport within the capillary fringe must be included. However, because the values of transport parameters typically change three to four orders of magnitude within this region, the spatial and/or temporal discretization requirements necessary to avoid numerical dispersion in standard finite-element and finite-difference models are impractical [Kinzelbach, 1990]. For this reason, the majority of available subsurface numerical models do not incorporate transport within the capillary fringe. One robust numerical technique that relaxes discretization restrictions is particle tracking; this technique often includes a random-walk component.

The random nature of solute transport through porous media has been recognized for several decades. Scheidegger [1954] and De Josselin de Jong [1958], for example, employed stochastic mathematical methods to investigate diffusive and dispersive phenomena. More recently, stochastic methods have been used to numerically model contaminant transport (e.g., Ahlstrom, et. al., 1977; Prickett et al., 1981; Uffink, 1985; Ackerer, 1988; Valocchi and Quinodoz, 1989; Kinzelbach, 1990; Tompson and Gelhar, 1990). Until recently, however, computational limitations restricted applications to relatively simple systems. Now, due to considerable increases in computational capabilities, particle-tracking simulations with the large numbers of particles necessary to characterize more complex systems are a viable alternative for many more applications. Even for cases in which the concentrations of interest range up to six orders of magnitude, particle tracking is now a practical tool. In this study, the random-walk method was employed to develop a two-dimensional particle-tracking model to simulate mass exchange between the saturated and unsaturated zones.

4.2 PHYSICAL BASIS AND GOVERNING EQUATIONS

For the sake of simplicity, the development of a one-dimensional form of the model will be presented here. For a three-phase system, total concentration may be expressed as:

$$C_T = C_w\theta_w + C_g\theta_g + C_s\rho_b \quad (4.1)$$

where C_T is the total mass per unit volume of the system; C_w , C_g , and C_s are the aqueous-, gas-, and solid-phase concentrations; θ_w and θ_g are the water- and gas-filled porosities; and ρ_b is the soil bulk density. If diffusion and aqueous-phase advection are

the only significant transport mechanisms, the transport equation may be written:

$$\frac{\partial C_T}{\partial t} = \frac{\partial}{\partial z} \left[D_{fw} \theta_w \tau_w \left(\frac{\partial C_w}{\partial z} \right) + D_{fg} \theta_g \tau_g \left(\frac{\partial C_g}{\partial z} \right) - v_w \theta_w C_w \right] \quad (4.2)$$

where t is time, D_{fw} is the free-water diffusion coefficient, τ_w and τ_g are the water- and gas-phase tortuosity factors, D_{fg} is the free-gas diffusion coefficient, and v_w is the aqueous-phase velocity.

Van Kampen [1981], Kinzelbach [1986], and Tompson et. al. [1987] provide discussions of the theory of the random-walk method as applied to transport problems. This theory states that for sufficiently large numbers of particles, the density distribution resulting from random steps of the form:

$$z_p(t + \Delta t) = z_p(t) + u\Delta t + Z(2B\Delta t)^{1/2} \quad (4.3)$$

where z_p is the particle coordinate and Δt is the time step, and Z is a normally distributed random variable with average 0 and standard deviation 1, fulfills the Ito Fokker-Planck equation:

$$\frac{\partial f}{\partial t} = \frac{\partial^2}{\partial z^2} (Bf) - \frac{\partial}{\partial z} (uf) \quad (4.4)$$

In order to apply a random-walk method to approximate the solution of equation 4.2, therefore, the equation must take the form of equation 4.4. The following equilibrium partition coefficients will be used to facilitate the transformation of (4.2):

$$H = \frac{C_g}{C_w} \quad (4.5a)$$

and

$$K_d = \frac{C_s}{C_w} \quad (4.5b)$$

where H is Henry's constant and K_d is the soil-water partition coefficient, both in their dimensionless forms. In the absence of infiltration, water-table fluctuations, or significant gas-phase velocities, it is reasonable to assume that gas-, aqueous-, and solid-phase concentrations are in equilibrium [Johnson et al., 1987], so use of equations 4.5 will not prove overly restrictive in the context of this model. Equation 4.1 may now be written:

$$C_T = \frac{C_w}{R} \quad (4.6a)$$

where,

$$R = \frac{1}{\theta_w + H\theta_g + K_d\rho_b} \quad (4.6b)$$

and equation 4.2 becomes:

$$\frac{\partial C_T}{\partial t} = \frac{\partial}{\partial z} \left[D^* \frac{\partial (C_T R)}{\partial z} \right] - \frac{\partial}{\partial z} [v_w \theta_w C_T R] \quad (4.7a)$$

where,

$$D^* = D_{fw} \theta_w \tau_w + D_{fg} \theta_g \tau_g H \quad (4.7b)$$

By making the following variable substitutions:

$$f = C_T \quad (4.8a)$$

$$B = D^* R \quad (4.8b)$$

$$u = R \left[v_w \theta_w + \frac{\partial D^*}{\partial z} \right] \quad (4.8c)$$

equation 4.4 becomes:

$$\frac{\partial C_T}{\partial t} = \frac{\partial^2}{\partial z^2} [D^* R C_T] - \frac{\partial}{\partial z} \left[\left(v_w \theta_w R + \frac{R \partial D^*}{\partial z} \right) C_T \right] \quad (4.9)$$

With expansion of the second derivative term and rearrangement of equation 4.9, this form of the Ito Fokker-Planck equation is equivalent to the transport equation given by equation 4.7a. Therefore, the particle steps used in the model are of the form:

$$z_p(t + \Delta t) = z_p(t) + R \left[v_w \theta_w + \frac{\partial D^*}{\partial z} \right] \Delta t + Z [2D^* R \Delta t]^{1/2} \quad (4.10)$$

where the variables R , v_w , θ_w , and D^* are all dependent on the position of the particle at time t . For a sufficiently large number of particles, the steps represented by equation 4.10 will result in a density distribution that fulfills the form of the transport equation given by equation 4.7a. The derivative in the second term of the particle step (4.10) was not included in earlier random-walk models such as those developed by Ahlstrom [1977] and Prickett et al. [1981], and is still often neglected in order to simplify models [e.g., Ackerer, 1988; Valocchi and Quinodoz, 1989]. More rigorous developments [Kinzelbach, 1986; Tompson et al., 1987; Tompson and Dougherty, 1988; Kinzelbach, 1990; Tompson and Gelhar, 1990] include the derivative term and thus allow for spatially varying dispersion and diffusion. In addition, a second derivative term involving the porosity is typically incorporated into the particle step to account for spatially varying total or water-filled porosity. The need for this second derivative term is avoided in equation 4.10 by the formulation of D^* (4.7b) in which total, water-filled, and gas-filled porosities are incorporated. This allows the simulation of two-phase transport through a domain of spatially-varying properties with relatively simple particles steps.

In Chapter 3 it was shown that Millington's [1959] expression for the tortuosity factor, modified to account for aqueous-phase transport, provides a good approximation of the effective diffusion through soil-moisture profiles typical of the capillary fringe.

Therefore, the tortuosity factors used in the model are:

$$\tau_w = \frac{\theta_w^{7/3}}{\theta_T^2} \quad (4.11a)$$

and

$$\tau_g = \frac{\theta_g^{7/3}}{\theta_T^2} \quad (4.11b)$$

where θ_T is total porosity.

For many problems involving mass exchange between the saturated and unsaturated zones, transport is dominated by molecular diffusion and horizontal groundwater advection, and horizontal variations in properties are negligible relative to vertical variations. For such cases, adherence to the assumptions inherent in the above mathematical development are not overly restrictive. Furthermore, if time steps are kept small, molecular diffusion may be considered an isotropic process and the expansion of the model to two or three dimensions is straightforward. In the example simulations presented here, it was further assumed that *all* domain characteristics, including groundwater velocity, are horizontally uniform. This allowed all parameters to be represented numerically as one-dimensional vertical arrays, greatly simplifying the model and substantially reducing computational effort. The effective diffusion coefficient arrays also provided a simple means to calculate a central-difference approximation of the derivative term in equation 4.10.

Both permeable and impermeable boundaries and a variety of source conditions can be simulated with the model. At permeable boundaries, particles are allowed to move freely across the boundary. They are then lost from the domain and no longer tracked. At impermeable boundaries, the particles are reflected. Specified-concentration or specified-flux sources may be defined anywhere within the domain by supplying the coordinates that bound the source region. For specified-concentration sources, particles are either added to or removed from the defined region at each time step so that the

region contains the specified number of particles at each time step. For specified-flux sources, the appropriate number of particles are introduced into the region at each time step. Sources may be constant or may vary with time.

At the end of each simulation, the domain is spatially discretized into cells and the number of particles in each cell is counted to yield concentrations in terms of C_T . Using the relationships defined by equations 4.1 and 4.5, calculation of aqueous-, gas-, and solid-phase concentrations is straightforward. Because the model is based on a stochastic process, resulting concentration fields are generally irregular rather than smooth. In some cases, the irregularities may be great enough to interfere with interpretation of the results. This problem can be rectified by increasing the number of particles in a given simulation, or superposing the results of several simulations.

The choice of spatial discretization depends on the characteristics of the domain and the degree of detail desired in the concentration field. The time step also depends on domain characteristics and is generally chosen such that several particles steps are required to cross a cell. Prickett et al. [1981] found that time discretization resulting in five to ten particles steps per cell gave good results.

4.3 MODEL EVALUATION

The model was tested on problems with analytical solutions. For example, pulse injections of particles were introduced at various locations in domains in which all boundaries were reflective. Following the transient period, the resulting steady-state concentration fields were uniform, as expected. These tests were conducted under a variety of moisture conditions.

The model was further evaluated by conducting four simulations of the mass-transfer experiment discussed in Chapter 2 and comparing the superposed results with results from the one-dimensional finite-difference model. This comparison is shown in Figure 4.2.

4.4 EXAMPLE SIMULATIONS

The example diffusion simulations presented here were conducted to investigate the effects of a relatively fine-grained layer in the unsaturated zone. The modeled domain, shown in Figure 4.3, is 3.0-m deep and 2.0-m long. The lower boundary of the domain is reflective and the land-surface boundary is open. The upstream and downstream boundaries are open in the saturated zone and reflective in the unsaturated zone. A constant-flux source of TCE is located at the upstream boundary. The source is 0.15-m thick and spans the interface between the saturated and unsaturated zones. Except for the fine-grained layer, the porous medium is the Ottawa sand used in the mass-transfer experiments. The fine-grained layer is located at a depth of 1.0 m, is 0.1-m thick, and extends laterally across the entire domain. The soil-moisture conditions for the system were calculated using van Genuchten's [1978] equation:

$$\theta = \theta_r + \frac{\theta_s - \theta_r}{\left[1 + (\alpha |h|)^n\right]^{1 - \frac{1}{n}}} \quad (4.12)$$

where θ is the moisture content, θ_r and θ_s are the residual and saturation moisture contents, α and n are soil-dependent parameters, and h is the suction pressure head (cm), taken here to be the distance above the water table. For the Ottawa sand, values of 0.61 and 6.51 were used for α and n , respectively. For the fine-grained layer, the values used for α and n were .01 and 2.80, respectively. All other variables used in the simulation are the same as those given in Table 2.1. Vertical profiles of the moisture content and effective diffusion coefficient, D^* , are shown in Figure 4.4.

To help in conceptualizing the behavior of particles in the modeled system, Figure 4.5a shows the *vertical* displacement resulting from ten particle steps for 25,000 particles located at various random positions throughout the domain. Figure 4.5b focuses on the fine-grained layer and illustrates the effects of the derivative term in equation 4.10 on the magnitude and direction of vertical particle steps. Just below the layer, the derivative

term is negative and just above the layer, the derivative term is positive. This serves to hinder the movement of particles *into* the layer and favor the movement of particles *out of* the layer. If the derivative term was neglected, particle steps into and out of the layer would be based solely on transport properties characteristic of the particle's initial position and a false stagnation zone would result within the layer.

Results of the simulation are shown in Figure 4.6a. Figure 4.6b shows results from a similar simulation in which the fine-grained layer was absent. The results shown are vertical concentration profiles from 0.25 m downstream of the source after 12 days of transport. A concentration drop of approximately one order of magnitude occurs across the fine-grained layer and its effects on concentrations are apparent both above and below the layer. Relative to the case with no layer, concentrations below the layer are elevated and concentrations above the layer are reduced. While the effects are not extreme, it should be noted that the fine-grained layer is very thin (0.15 m). In addition, in terms of soils typically encountered in the environment, the properties of the fine-grained layer differ only slightly from those of the Ottawa sand. It is very likely, in fact, that even the most careful site assessment would not reveal the presence of such a layer in a field-scale investigation.

4.5 CONCLUSIONS

As discussed in Chapter 2, agreement between experimental data and the two-dimensional numerical model simulations was very good (Figure 2.7). Furthermore, as shown in Figure 4.2, results from the two-dimensional model agree well with those from the one-dimensional finite-difference model for the conditions simulated.

Results from the example simulations show that even minor changes in subsurface conditions can significantly alter concentration profiles in the unsaturated zone. Concentrations dropped approximately one order of magnitude across a thin (0.15 m) fine-grained layer in the unsaturated zone even though the properties of the layer differed only slightly from those of the rest of the domain.

4.6 REFERENCES

Ackerer, Ph., Random-walk method to simulate pollutant transport in alluvial aquifers or fractured rocks, In: Groundwater flow and quality modelling, D. Reidel Publishing Company, Dordrecht, Holland, 475-486, 1988.

Ahlstrom, S., H. Foote, R. Arnett, C. Cole, and R. Serne, Multi-component mass transport model: Theory and numerical implementation, Rep. BNWL 2127, Battelle Pac. Northwest Lab., Richland, Wash., 1977.

De Josselin de Jong, G., Longitudinal and transverse diffusion in granular deposits, Trans. AGU 39, 67-74, 1958.

Johnson, R. L., C. D. Palmer, and J. F. Keely, Mass transfer of organics between soil, water and vapor phases: Implications for monitoring, biodegradation and remediation, Proc. NWWA/API Conf. on Petroleum Hydrocarbons and Organic Chemicals in Ground Water: Prevention, Detection and Restoration, Houston, Texas, November 17-19, 1987.

Kinzelbach, W., Groundwater Modelling: An Introduction with Sample Programs in Basic, 333 pp., Elsevier, Amsterdam, 1986.

Kinzelbach, W., Simulation of pollutant transport in groundwater with the random walk method, In: *Groundwater Monitoring and Management* (Proc. Dresden Symp., March 1987), IAHS Publ., 173, 265-279, 1990.

Millington, R. J., Gas diffusion in porous media, *Science*, **130**, 100-102, 1959.

Prickett, T. A., T. Naymik, and C. G. Lonquist, A "random walk" solute transport model for selected groundwater quality evaluations, Illinois State Water Survey Bull. 65, 1981.

Scheidegger, A. E., Statistical hydrodynamics in porous media, **J. Appl. Phys.**, **25**, 994-1001, 1954.

Tompson, A. F. B., and L. W. Gelhar, Numerical simulation of solute transport in three-dimensional, randomly heterogeneous porous media, **Water Resour. Res.**, **26**, 2541-2562, 1990.

Tompson, A. F. B., and D. E. Dougherty, On the use of particle tracking methods for solute transport in porous media, in Computational Methods in Water Resources, Vol. 2, Numerical Methods for Transport and Hydrologic Processes, edited by M. Celia, L. Ferrand, C. Brebbia, W. Gray, and G. Pinder, pp. 227-232, Elsevier, New York, 1988.

Tompson, A. F. B., E. G. Vomvoris, and L. W. Gelhar, Numerical simulation of solute transport in randomly heterogeneous porous media: Motivation, model development, and application, Rep. UCID-21281, Lawrence Livermore Natl. Lab., Livermore, Calif., 1987.

Uffink, G. J. M., A random walk method for the simulation of macrodispersion in a stratified aquifer, in Relation of Groundwater Quantity and Quality, Proceedings of the Hamburg Symposium, August 1983, IAHS Publ., 146, 103-114, 1985.

Valocchi, A. J., and H. A. M. Quinodoz, Application of the random walk method to simulate the transport of kinetically adsorbing solutes, in Groundwater Contamination, Proceedings of the Baltimore Symposium, May 1989, IAHS Publ., 185, 35-42, 1989.

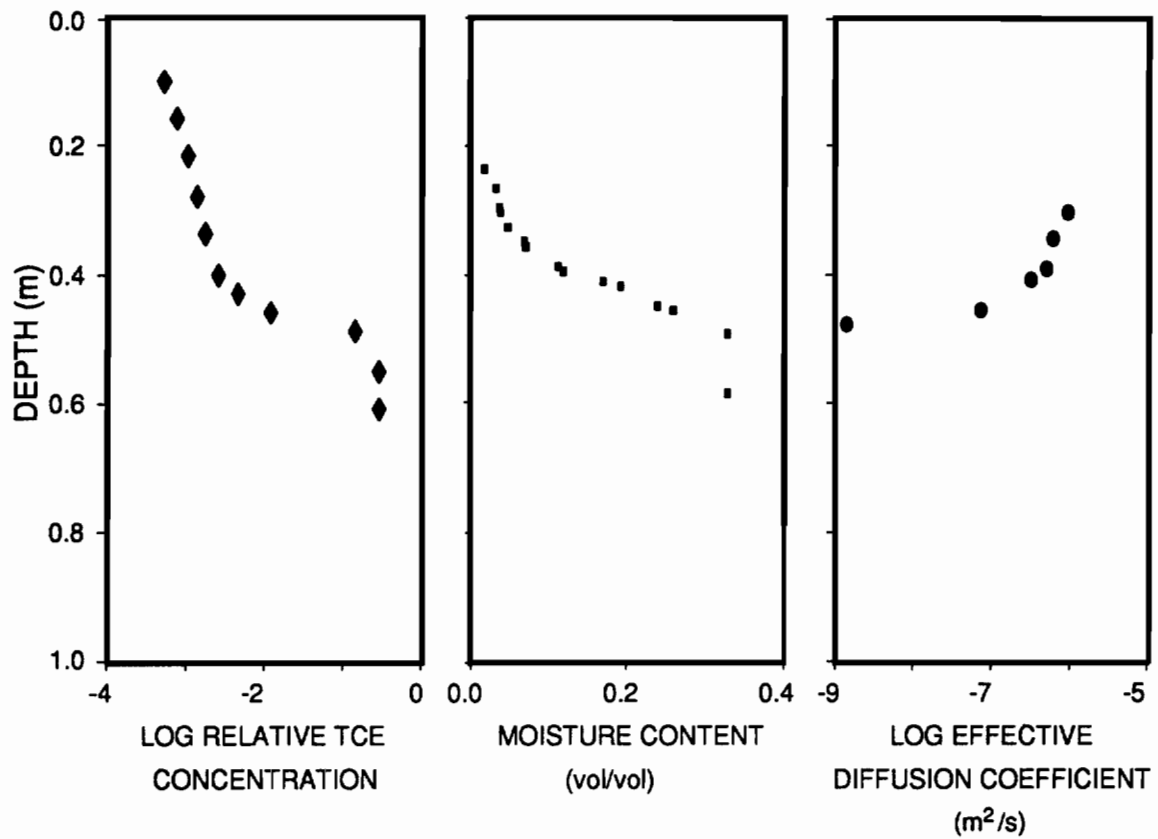


Figure 4.1. Experimentally determined TCE concentrations, soil-moisture contents, and effective diffusion coefficients versus depth.

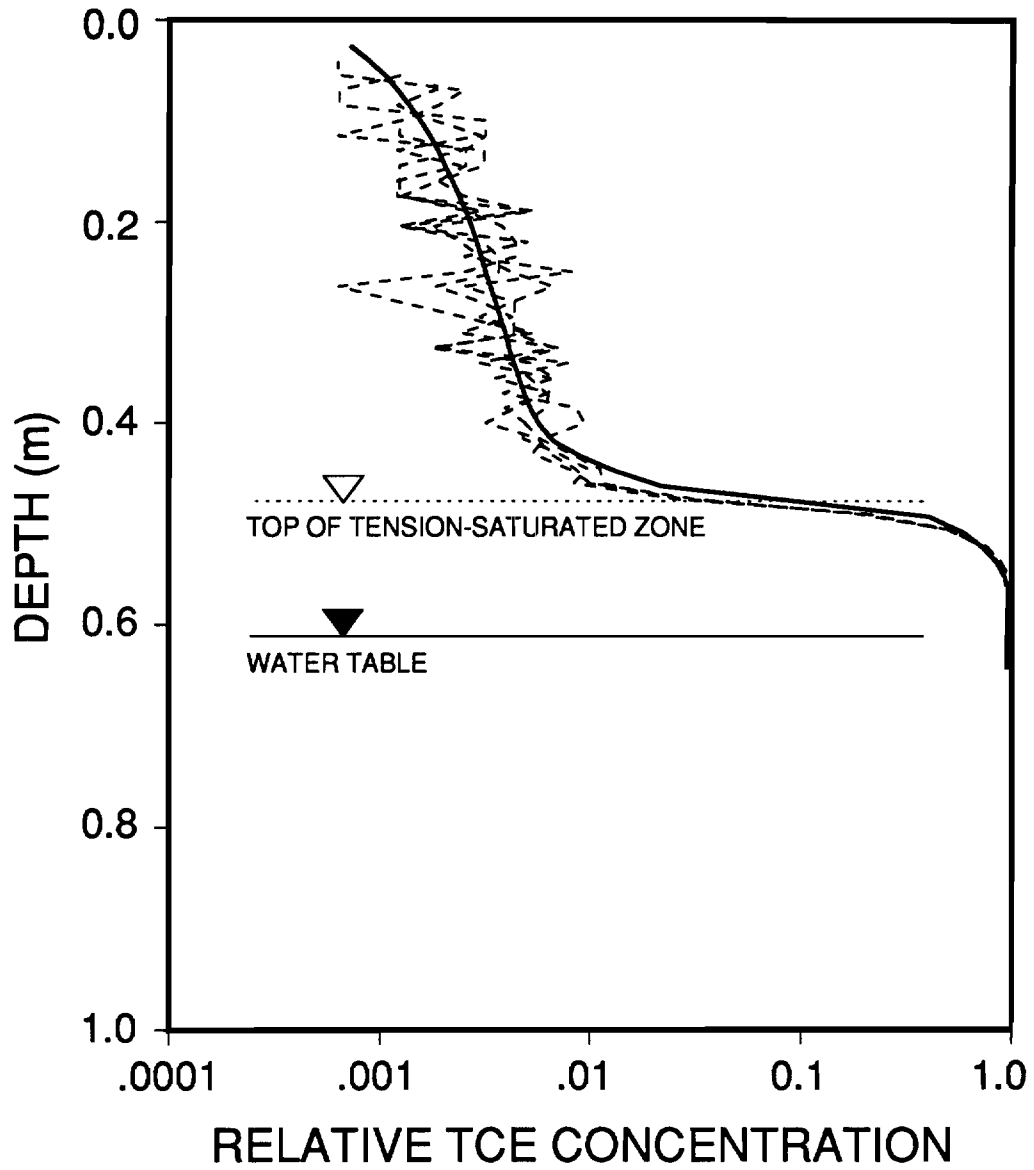


Figure 4.2. Simulation results from the one-dimensional model (solid line) and superposed simulation results from the two-dimensional model (dashed lines).

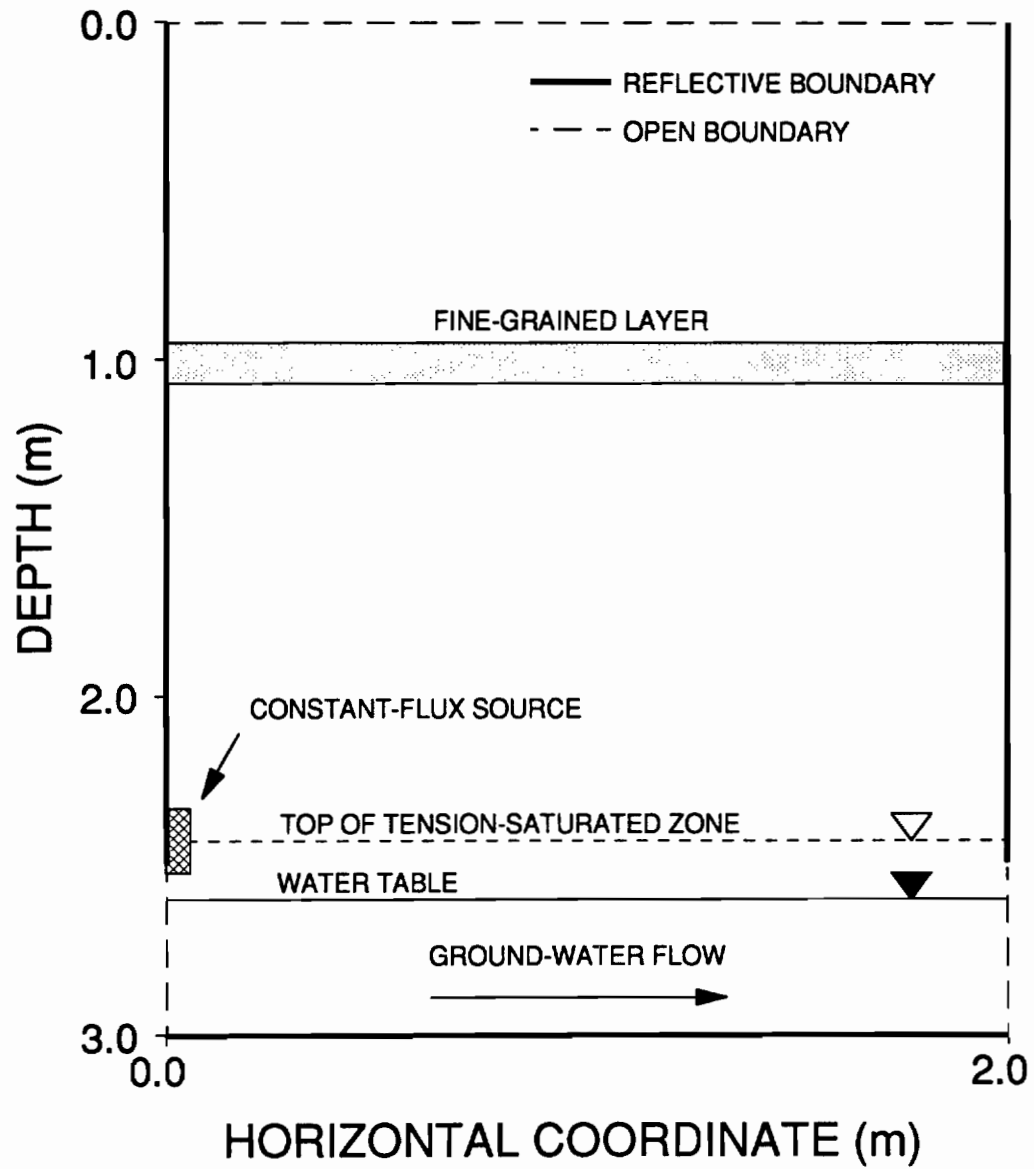


Figure 4.3. The modeled domain.

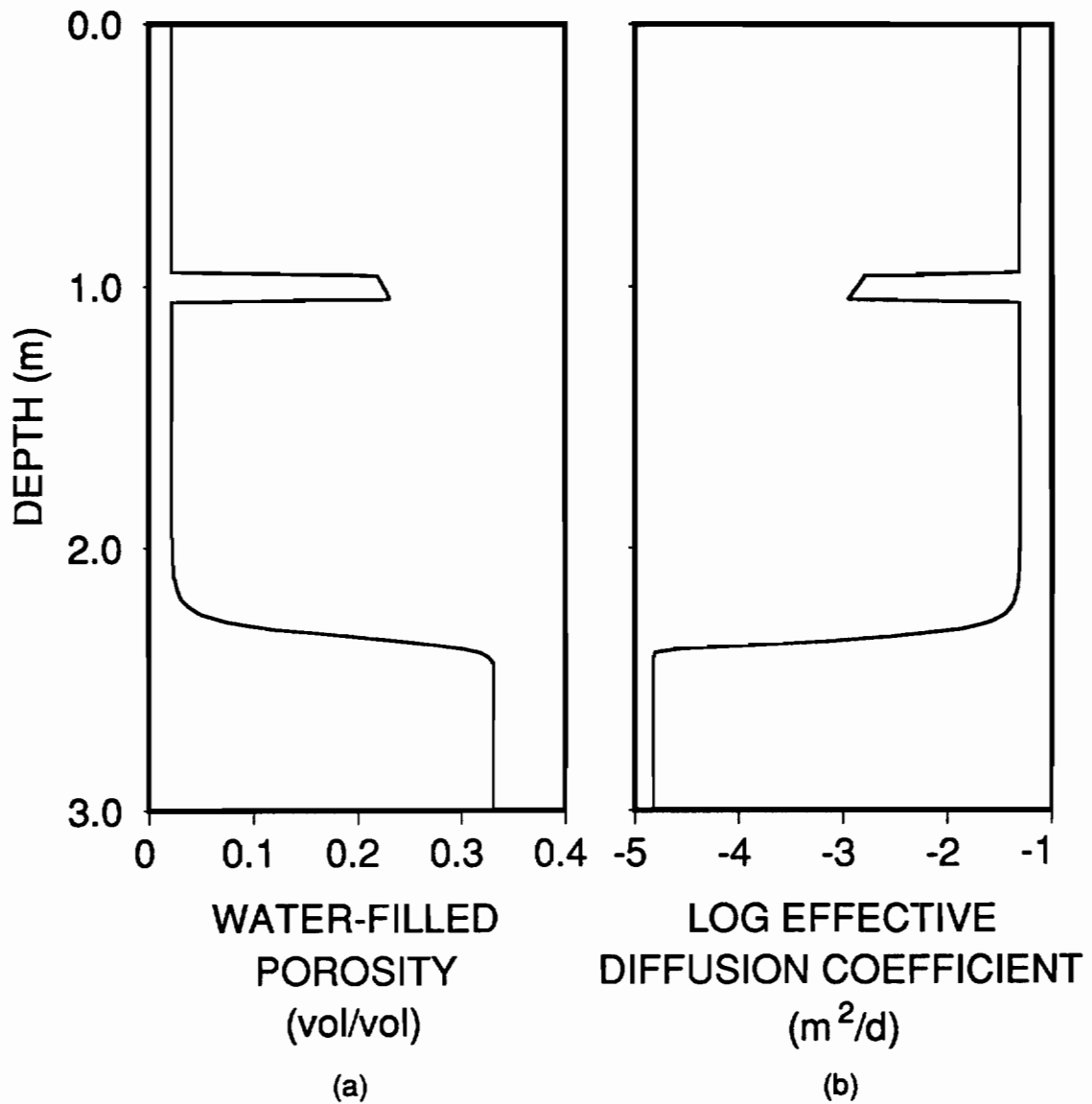


Figure 4.4. Properties of the modeled domain. a) Moisture content versus depth; b) effective diffusion coefficient versus depth.

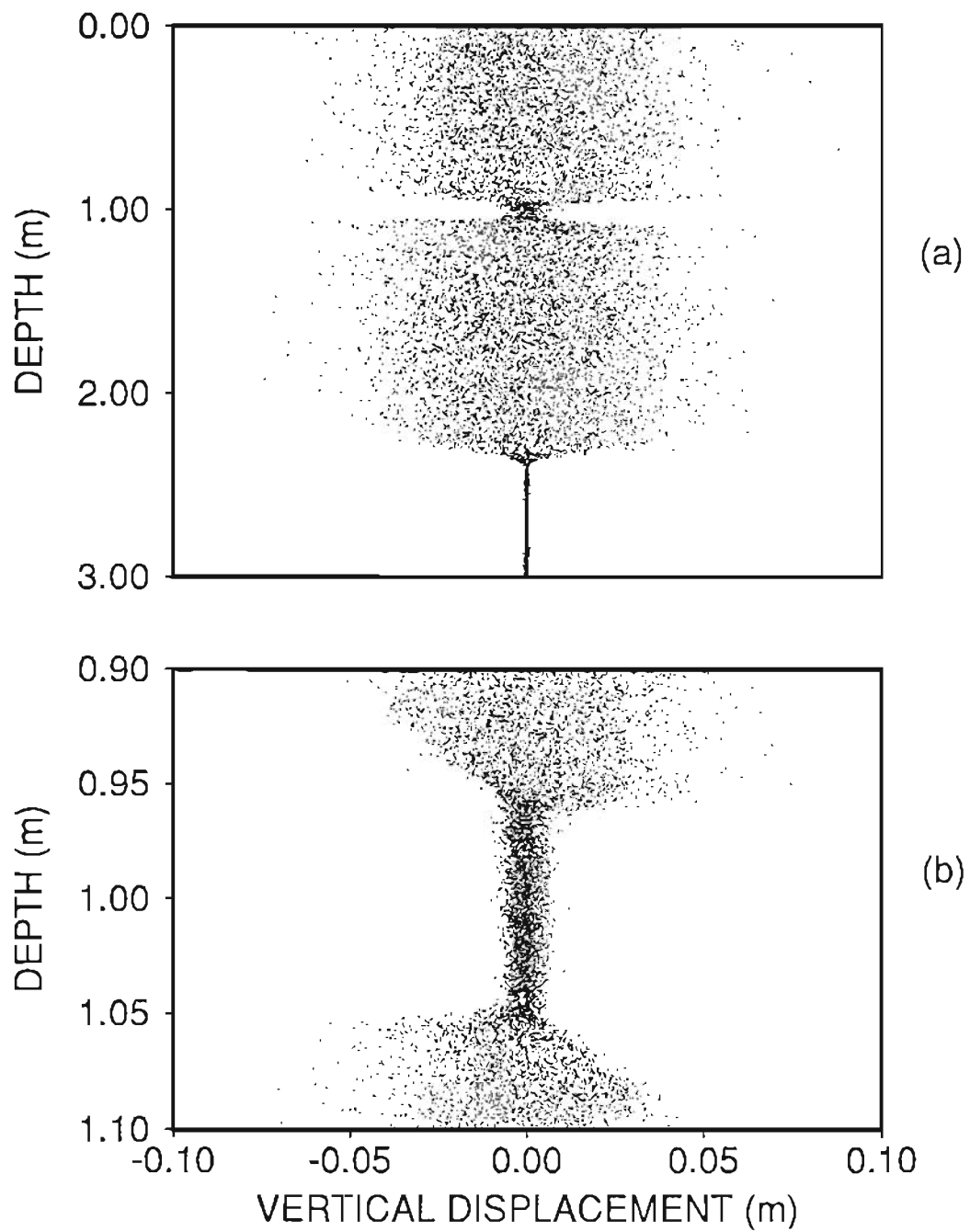


Figure 4.5. Vertical particle displacements resulting from ten time steps versus vertical particle position. a) Entire domain; b) near the fine-grained layer.

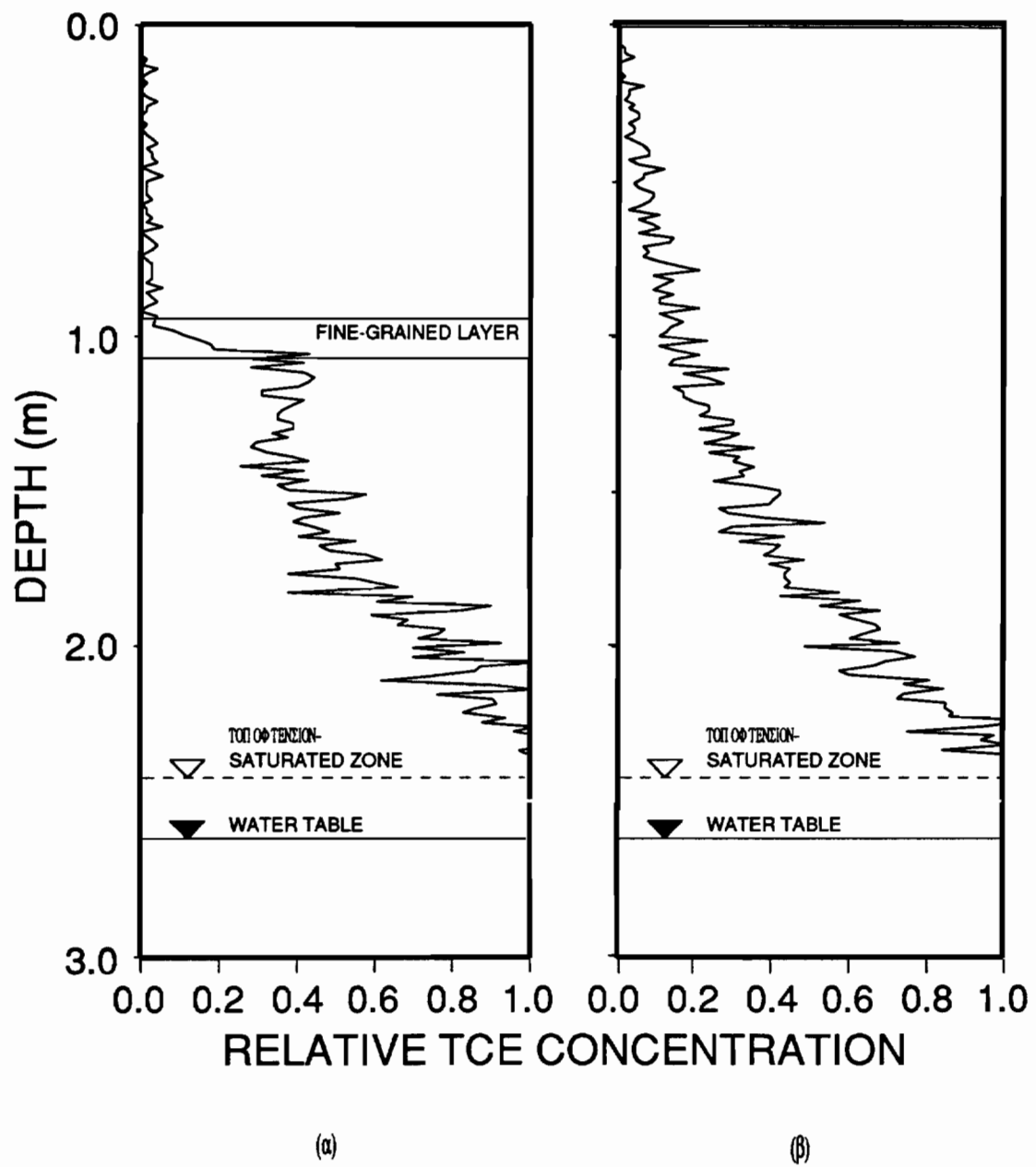


Figure 4.6. Simulation results from the two-dimensional model for a domain a) with the fine-grained layer, and b) without the fine-grained layer.

CHAPTER 5

SUMMARY, CONCLUSIONS, AND IMPLICATIONS

5.1 SUMMARY OF RESEARCH

The research reported here has three principal components: 1) Physical modeling of mass transfer of TCE from ground water to the unsaturated zone, 2) experimental determination of effective diffusion coefficients in a variably-saturated porous medium, and 3) numerical modeling of both the mass-transfer experiments and a number of relevant examples.

Laboratory experiments to examine mass transfer from ground water to the unsaturated zone were conducted in a physical model of the subsurface that included both saturated and unsaturated zones. The model was 1.0-m deep, 1.0-m long, and 0.75-m wide. The transport of TCE resulting from a dissolved ground-water source was monitored as a function of the soil-moisture profile and water-table position.

The effective diffusion coefficient for TCE was measured as a function of depth in gravity-drained sand columns designed to reproduce conditions in the mass-transfer experiments mentioned above. Individual diffusion measurements were conducted on 2.5-cm column sections with moisture contents ranging from field capacity to saturation. Measured values of the effective diffusion coefficient were compared with values obtained using Millington's [1959] expression.

A two-dimensional particle-tracking model was developed to simulate molecular diffusion and advection in the subsurface. This model was used to simulate the mass transfer experiments. In addition, the effects of a heterogeneous unsaturated zone were investigated by simulating the transport resulting from a dissolved source of TCE in both a homogeneous domain and a domain with a fine-grained layer.

A one-dimensional, explicit finite-difference model was also developed. This model simulated mass exchange between the saturated and unsaturated zones due to molecular diffusion and vertical hydraulic dispersion. It was used to simulate the mass-transfer experiments and to compare transport through soils characterized by different soil-moisture profiles.

5.2 CONCLUSIONS OF RESEARCH

5.2.1 MASS-TRANSFER EXPERIMENTS

The mass-transfer experiments showed that a dissolved ground-water source of TCE resulted in strong concentration gradients in the capillary fringe and very low concentrations in the unsaturated zone under conditions of steady ground-water flow and constant water-table position. TCE concentrations decreased nearly three orders of magnitude between the water table and the top of the capillary fringe.

Data from the water-table drop experiment showed two effects on transport from ground water to the unsaturated zone. The first effect was a transient increase in TCE concentrations throughout most of the unsaturated zone. As water-filled porosity decreased and gas-filled porosity increased in the new, deeper capillary fringe, water which had previously been part of the saturated zone (and hence contained high concentrations of TCE) was increasingly exposed to the gas phase. The gas and water phases quickly approached concentrations equilibrium, resulting in elevated gas-phase concentrations. Due to rapid gas-phase transport, however, the elevated concentrations rapidly dissipated. The second effect was observed in the deep part of the unsaturated

zone where an overall decrease in concentrations was observed. This was because the *relative* increase in gas-filled porosity (and, therefore, the effective diffusion coefficient) was greater at this depth than at shallower depths. Also, due to the effects of hysteresis on the soil-moisture profile, the vertical extent of the tension-saturated zone was reduced by approximately .05 m after the water table was raised to its original level. This resulted in increased gas-filled porosity in the deep unsaturated zone and, therefore, a higher effective diffusion coefficient. Consequently, the reduced concentrations in the deep unsaturated zone persisted even after the water table was returned to its original level.

5.2.2 DIFFUSION EXPERIMENTS

Results of the diffusion experiments showed the strong dependence of the diffusion process on air-filled porosity. In continuous, gravity-drained soil-moisture profiles, the effective diffusion coefficient decreased three orders of magnitude over a vertical distance of 0.15 m. The data also showed that Millington's [1959] expression for tortuosity, modified to include aqueous-phase diffusion, provides reliable estimates of the effective diffusion coefficient in sand with moisture contents ranging from field capacity to saturation. The applicability of the Millington [1959] expression is important because of its simplicity. It requires only knowledge of the total porosity and soil-moisture content, parameters that are easily determined from field samples.

5.2.3 NUMERICAL MODELING

Numerical simulations of the mass-transfer experiments using both the two-dimensional particle-tracking and one-dimensional finite-difference models showed that molecular diffusion was the dominant mechanism responsible for mass transport from ground water to the unsaturated zone. Simulations that incorporated vertical dispersivities of .001 and .01 m, in addition to molecular diffusion, substantially overestimated mass flux to the unsaturated zone. This indicates that in the absence of infiltration or water-

table fluctuations, and when ground-water velocities are low (~ 0.1 m/d), mass transport from ground water to the unsaturated zone will be significantly less than has been previously assumed.

Comparison of results from the relatively simple, one-dimensional diffusion model with those from the more rigorous, two-dimensional advection-diffusion model showed that when conditions are appropriate, a one-dimensional approximation of mass exchange between the saturated and unsaturated zones can be useful at least as a preliminary tool. This is significant because the one-dimensional model is much less numerically intensive and therefore less costly to operate than the two-dimensional model.

In addition to corroborating the results of the one-dimensional approximation, the two-dimensional model allows the simulation of more complex systems. Although it is numerically intensive, it provides an accurate means to simulate transport in the subsurface as a continuum while overcoming the prohibitive discretization requirements of standard finite-difference and finite-element models. Finally, the particle-tracking method is based on discrete particle steps that mimic the movements of real gases and solutes. It therefore provides an attractive alternative to standard finite-difference and finite-element techniques, particularly as an investigative or teaching tool.

5.3 IMPLICATIONS

The data presented here were collected during laboratory-scale experiments conducted under controlled conditions. The conclusions are therefore limited to the scale and conditions investigated. However, careful extrapolation of the conclusions to other subsurface conditions is possible. The implications of limited mass transfer for field-scale soil-gas monitoring, *in situ* bioremediation, and numerical modeling are discussed in the following sections.

5.3.1 SOIL-GAS MONITORING

The practice of soil-gas monitoring to investigate underlying ground-water contamination was discussed in Chapter 1. The experimental data and numerical modeling results presented here have four important implications for this practice. First, concentrations in the unsaturated zone will, in many cases, be very low relative to underlying ground water. In the experiments, the water table was shallow (~ 0.6 m) and very high concentrations of TCE were maintained very near the water table. Nevertheless, except in the deepest part of the unsaturated zone, concentrations in the soil gas were two to three orders of magnitude lower than in the underlying ground water. In most field situations, ground-water contaminants will be present at concentrations that are several orders of magnitude lower than in the experiments. Furthermore, the source of contamination may be well below the water table. As a result, soil-gas concentrations may often be too low to detect. To illustrate this point, a simulation was conducted with the one-dimensional finite-difference model in which a continuous, dissolved source of TCE was located approximately 1-m below the water table. The simulated porous medium was Ottawa sand and all other variables were those used in the simulation of the mass-transfer experiment, presented in Chapter 2. Figure 5.1 shows the concentration profile that developed in this system after five years of diffusive transport. Concentrations in the unsaturated zone are five orders of magnitude lower than the source concentration.

The second implication of this work for soil-gas surveys is that concentration profiles in the unsaturated zone will seldom be straightforward. Even an *apparently* homogeneous system will include some heterogeneities and the different soil types will be characterized by different soil-moisture contents. Figure 3.7 illustrates that even two clean sands, which would probably not be distinguished in the field, can have distinctly different moisture profiles. Due to the strong dependence of the effective diffusion coefficient on gas-filled porosity, variations in soil-moisture content will produce large

spatial variations in the diffusion process. This may result in concentration profiles that are difficult to interpret.

The vertical extent of the capillary fringe will also influence soil-gas concentrations, as shown in Figures 3.7 and 3.8. In the experiments and simulations presented here, only sands were considered. In many cases, soils encountered in the field will be characterized by significantly more extensive capillary fringes [van Genuchten, 1978; Bumb et al., 1992]. Under these circumstances, the nature and extent of the capillary fringe must be carefully considered when extrapolating soil-gas data to underlying ground water. In addition to influencing the shape of steady-state concentration profiles, the capillary fringe will have a strong effect on the temporal characteristics of transport.

The fourth implication of this work for soil-gas monitoring is illustrated by data from the water-table drop experiment. It was shown that soil-gas concentrations throughout most of the unsaturated zone were temporarily elevated during a short-term water-table drop. In the deep part of the unsaturated zone, however, concentrations were governed by the position of the top of the tension-saturated zone. These concentrations decreased during the water-table drop and did not return to previous values after the water-table was raised to its original position. Conversely, it is probable that a rise of the water table would perturb soil-gas concentrations in an opposite manner. If the rise was due to *distant* recharge, low-concentration water from the capillary fringe would be incorporated into the saturated zone as it moved upward, effectively diluting the shallow ground water. This would result in lower soil-gas concentrations throughout most of the unsaturated zone. If the water table was raised due to *local* recharge, relatively clean infiltrating water could effectively cap a ground-water source. (LeBlanc et al. [1991] reported the apparent downward movement of a ground-water plume due, in part, to accretion of local recharge.) This masking effect could result in significantly lower soil-gas concentrations in the unsaturated zone [Rivett and Cherry, 1991]. In addition to the position of the water table, the position of the top of the tension-saturated zone would affect soil-gas concentrations. In the field, the position of the water-table is routinely

monitored, but the extent and nature of the capillary fringe and the effects of hysteresis are often not considered. Consequently, changes in soil-gas concentrations that result from water-table fluctuations may be misinterpreted.

5.3.2 *IN SITU* BIOREMEDIATION

The mass-transfer experiments and numerical simulations showed that for the conditions investigated, transport of TCE from ground water to the unsaturated zone was limited by aqueous-phase molecular diffusion. It can be assumed that, under similar conditions, exchange of gases between the saturated and unsaturated zones will be similarly limited. The relevance of this to *in situ* bioremediation is clear from the discussion in Chapter 1. As an example, the one-dimensional finite-difference model was used to simulate the transport of oxygen from the atmosphere to the saturated zone. The spatial discretization and soil-moisture profile used were identical to those used to simulate the mass-transfer experiment. The ground surface was simulated as a constant-concentration boundary. The water-table boundary was maintained at zero-concentration to simulate the rapid uptake of oxygen by microorganisms. The values used for free-water and free-gas diffusion coefficients, Henry's Constant, and the soil-water partition coefficient are given in Table 5.1. Transport over a 150-day period was simulated and the results indicated that steady-state conditions had been reached. The results are shown in Figure 5.2. Using a dissolved oxygen concentration of 10 mg/l at ground surface, calculations based on Fick's First Law (equation 2.1) show that for the conditions simulated, the steady-state flux of oxygen into ground water is $2.3 \text{ mg m}^{-2} \text{ d}^{-1}$. Assuming that three grams of oxygen are required to biodegrade one gram of hydrocarbon, the natural reaeration of ground water will only supply enough oxygen to sustain a hydrocarbon biodegradation rate of approximately $0.75 \text{ mg m}^{-2} \text{ d}^{-1}$. For a ground-water plume extending 100 m in length and 10 m in width, this corresponds to a total biodegradation rate of only 0.75 g d^{-1} . This is clearly an insignificant rate for most field cases.

5.3.3 NUMERICAL MODELING

Simulations from both the two-dimensional particle-tracking and one-dimensional finite-difference models showed that molecular diffusion was the dominant vertical dispersion process in the mass-transfer experiment. Therefore, numerical simulations that incorporate vertical mechanical dispersion may significantly overestimate mass exchange between ground water and the unsaturated zone.

It has been common in the literature to neglect the capillary fringe and assume that soil-gas concentrations just above the water table are in equilibrium with aqueous concentrations just below the water table (e.g., Borden and Bedient [1986], Barber et al. [1990]). Due to the complex nature of transport in the capillary fringe, this is not the case. While it is reasonable to assume equilibrium between the phases at any point in space, the sharp decreases in concentration between the water table and the top of the capillary fringe seen in the experimental data clearly show that the assumption of concentration equilibrium between ground water and soil gas above the capillary fringe is not valid.

A comparison of the results from the two-dimensional and one-dimensional numerical simulations of the mass-transfer experiment was shown in Figure 4.2. For this case, agreement between the two models was very good. The results of the example simulations shown in Figure 4.6, in which the effects of a fine-grained layer in the unsaturated zone were investigated, are shown again in Figure 5.3 along with results of one-dimensional simulations of the same systems. In this case, the one-dimensional model slightly overpredicts concentrations in the unsaturated zone. This can be attributed to the fact that mass is not allowed to diffuse laterally in the one-dimensional domain. However, the effects of the fine-grained layer are clear in both simulations. This suggests that for many cases, a simple, one-dimensional approximation of the system can provide valuable insights, at least in a qualitative sense.

5.4 REFERENCES

Barber, C., G. B. Davis, D. Briegel and J. K. Ward, Factors controlling the concentration of methane and other volatiles in groundwater and soil-gas around a waste site, **J. Contam. Hydrol.**, **5**, 155-169, 1990.

Bumb, A. C., C. L. Murphy, and L. G. Everett, A comparison of three functional forms for representing soil moisture characteristics, **Ground Water**, **30**, 177-185, 1992.

Borden, R. C., and P. B. Bedient, Transport of dissolved hydrocarbons influenced by oxygen-limited biodegradation, 1, Theoretical development, **Water Resour. Res.**, **22**, 1973-1982, 1986

LeBlanc, D. R., S. P. Garabedian, K. M. Hess, L. W. Gelhar, R. D. Quadri, K. G. Stollenwerk, and W. W. Wood, Large-scale natural gradient tracer test in sand and gravel, Cape Cod, Massachusetts, 1. Experimental design and observed tracer movement, **Water Resour. Res.**, **27**, 895-910, 1991.

Millington, R. J., Gas diffusion in porous media, **Science**, **130**, 100-102, 1959.

Rivett, M. O., and J. A. Cherry, The effectiveness of soil gas surveys in delineation of groundwater contamination: Controlled experiments at the Borden field site, in Proceedings, NWWA/API Conference on Petroleum Hydrocarbons and Organic Chemicals in Ground Water: Prevention, Detection, and Restoration, Houston, Texas, November 20-22, 1991.

Thibodeaux, L. J., Chemodynamics, John Wiley & Sons, 501 pp., New York, 1979.

van Genuchten, M. Th., Numerical solutions of the one-dimensional saturated-unsaturated flow equation, Research Report 78-WR-09, Water Resources Program, Department of Civil Engineering, Princeton University, Princeton, New Jersey, 1978.

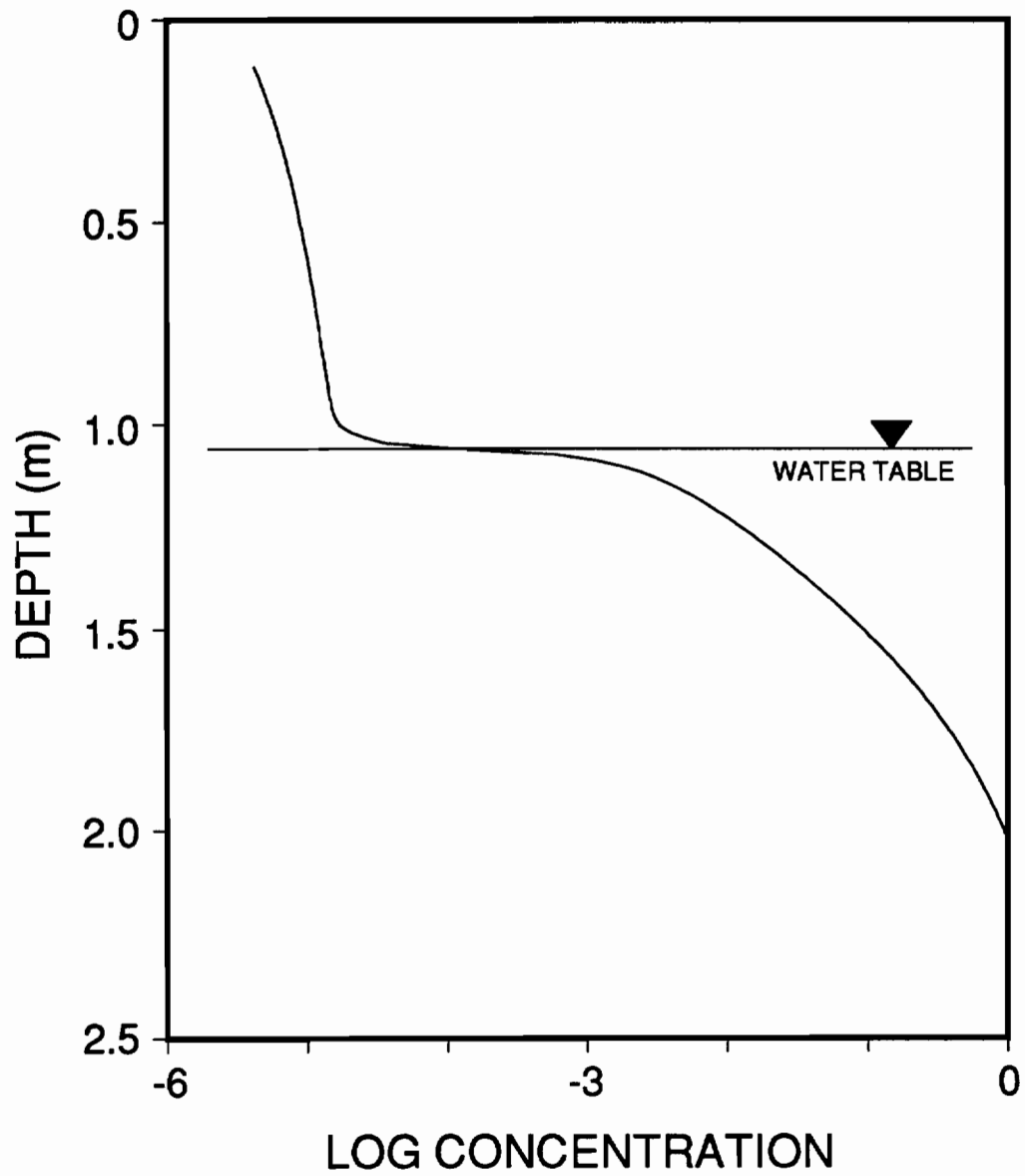


Figure 5.1. Results from the one-dimensional numerical simulation of transport from a dissolved TCE source located 1-m below the water table.

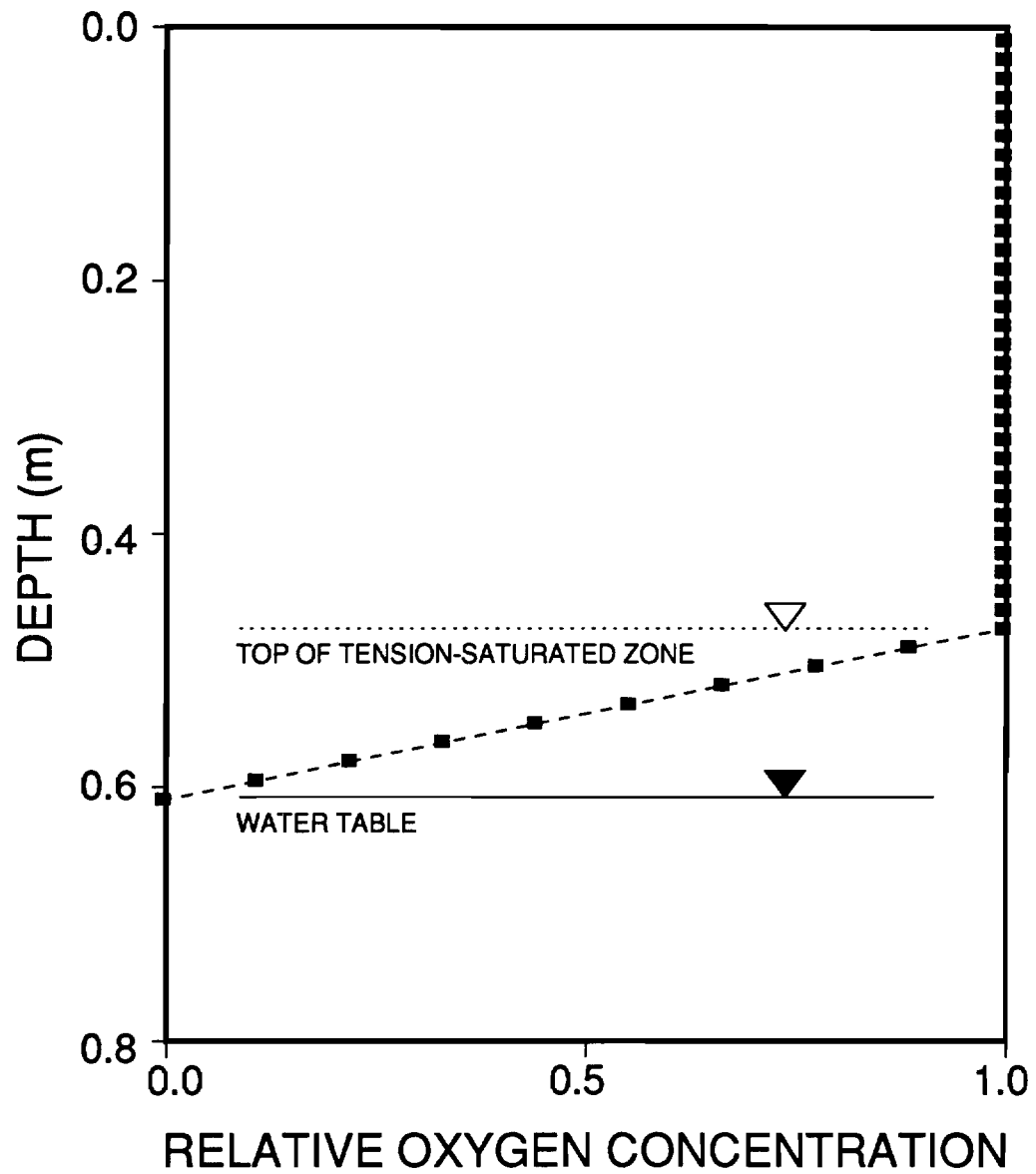


Figure 5.2. Steady-state profile of depth versus oxygen concentration from the one-dimensional numerical model.

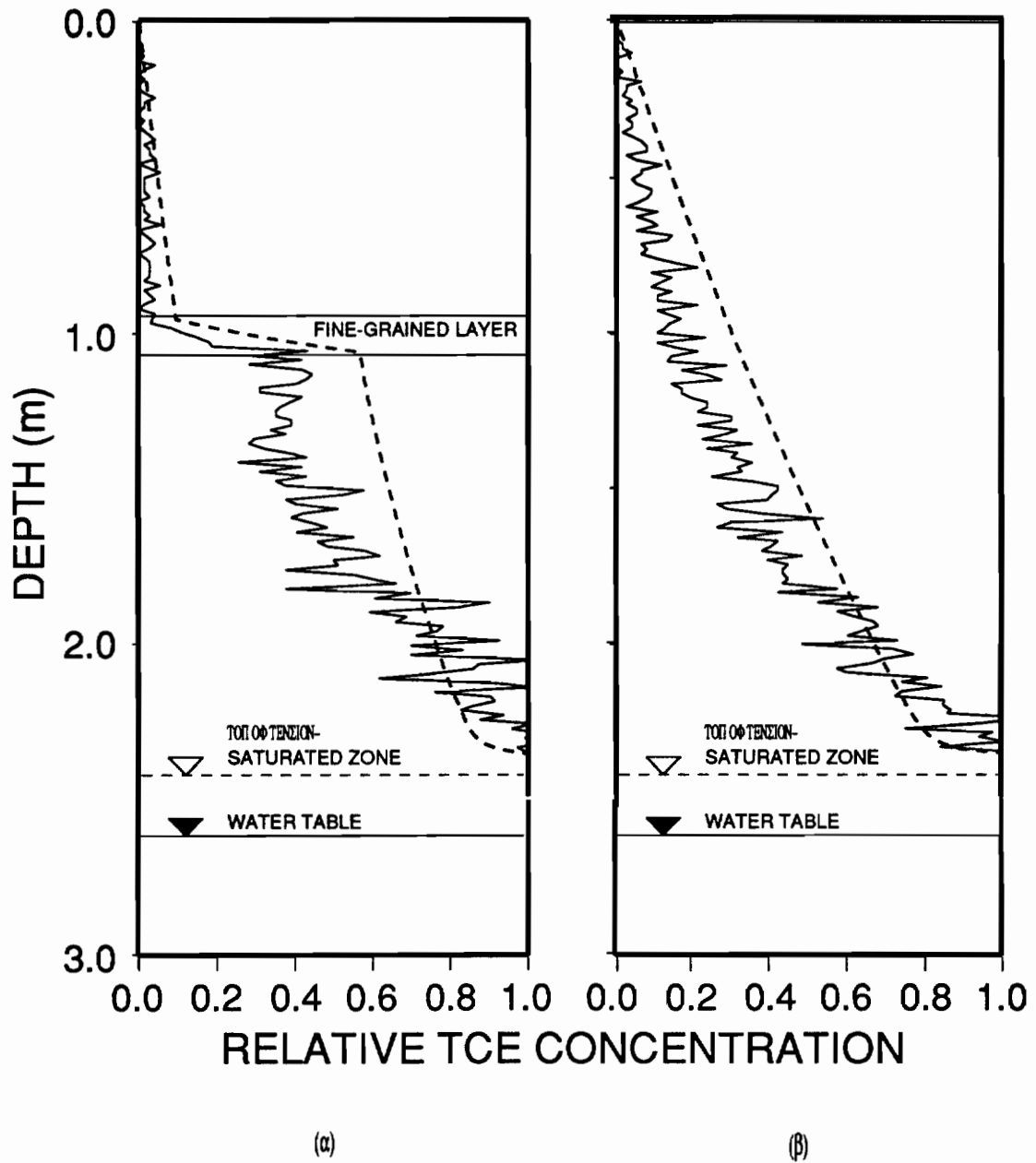


Figure 5.3. Simulation results from the one- and two-dimensional models for a domain a) with the fine-grained layer, and b) without the fine-grained layer. Results from the one-dimensional model are shown as dotted lines; results from the two-dimensional model are shown as solid lines.

TABLE 5.1. Numerical model input parameters for oxygen at 10 C.

PARAMETER	VALUE
FREE-WATER DIFFUSION COEFFICIENT (m ² /s)	1.5 x 10 ⁻⁹ ^a
FREE-GAS DIFFUSION COEFFICIENT (m ² /s)	1.9 x 10 ⁻⁵ ^a
HENRY'S CONSTANT (dimensionless)	25.4 ^a
SOIL-WATER PARTITION COEFFICIENT (dimensionless)	0

^a Thibodeaux, 1979

APPENDIX A

SELECTED EXPERIMENTAL DATA FROM THE MASS-TRANSFER EXPERIMENTS

This appendix contains experimental data from the mass-transfer experiments discussed in Chapter 2. The values given are concentrations from selected sampling ports and are reported relative to TCE-saturated air. Concentrations followed by an asterisk (*) are headspace concentrations resulting from 2-ml aqueous samples equilibrated in 5-ml vials and thus do not directly reflect original aqueous-phase concentrations. The reported times are relative to the beginning of the drainage experiment.

A.1 DRAINAGE EXPERIMENT

Bundle A
(x = 0.3 m)

DEPTH (m)	TIME (days)				
	25	30	35	49	53
0.28				1.93E-03	2.03E-03
0.34	2.59E-03	2.45E-03	3.55E-03	2.64E-03	2.74E-03
0.40	3.67E-03	3.53E-03	4.88E-03	3.62E-03	3.81E-03
0.43	8.21E-03	7.78E-03	1.12E-02	6.11E-03	6.27E-03
0.49	9.86E-02*	1.06E-01*	1.17E-01*	9.15E-02*	1.01E-01*
0.55	1.54E-01*	1.82E-01*	1.98E-01*	1.77E-01*	1.80E-01*
0.61	1.72E-01*	1.94E-01*	2.10E-01*	1.96E-01*	2.13E-01*
0.97	2.30E-01*	2.50E-01*	2.54E-01*	2.36E-01*	2.24E-01*

Bundle B
(x = 0.5 m)

DEPTH (m)	TIME (days)				
	25	30	35	49	53
0.28				1.69E-03	1.63E-03
0.34				2.19E-03	2.16E-03
0.40	3.15E-03	2.88E-03	4.14E-03	3.07E-03	3.00E-03
0.43	6.54E-03	5.78E-03	8.17E-03	5.07E-03	4.87E-03
0.49				8.22E-02*	7.75E-02*
0.55				1.57E-01*	1.81E-01*

Bundle C
(x = 0.7 m)

DEPTH (m)	TIME (days)				
	25	30	35	49	53
0.28				1.45E-03	1.32E-03
0.34				1.68E-03	1.58E-03
0.40	2.70E-03	2.64E-03	2.46E-03	2.40E-03	2.15E-03
0.43	3.96E-03	3.57E-03	4.86E-03	3.43E-03	3.25E-03
0.49			6.02E-02*	5.72E-02*	5.07E-02*
0.55			1.36E-01*	1.37E-01*	1.35E-01*
0.61			1.63E-01*	1.64E-01*	1.62E-01*
0.97			2.27E-01*	2.28E-01*	2.23E-01*

A.2 WATER-TABLE DROP EXPERIMENT

Bundle A
(x = 0.3 m)

DEPTH (m)	TIME (days)				
	95	98	99	100	102
0.10	4.95E-04	6.11E-04	7.32E-04		1.33E-03
0.16		9.32E-04	1.33E-03	2.30E-03	1.91E-03
0.22	1.09E-03	1.33E-03	1.89E-03		2.73E-03
0.28		1.72E-03	2.68E-03	3.83E-03	3.56E-03
0.34	1.87E-03	2.28E-03	3.37E-03		4.52E-03
0.40	2.66E-03	3.07E-03	4.25E-03	5.93E-03	5.43E-03
0.43	5.04E-03	3.80E-03	5.00E-03		5.75E-03
0.46	6.65E-03	5.29E-03	5.46E-03	6.87E-03	5.84E-03
0.49	1.04E-01*	2.37E-02	7.74E-03	8.32E-03	6.97E-03
0.55	1.93E-01*	1.96E-01*	8.46E-02*	1.86E-02	1.05E-02
0.61		1.95E-01*	2.00E-01*	1.37E-01*	1.12E-01*

Bundle B
(x = 0.5 m)

DEPTH (m)	TIME (days)				
	95	98	99	100	102
0.10	5.59E-04	6.11E-04	7.07E-04		1.40E-03
0.16		8.45E-04	1.16E-03	2.28E-03	1.73E-03
0.22	9.13E-04	1.14E-03	1.67E-03		2.29E-03
0.28		1.52E-03	2.32E-03	3.39E-03	2.93E-03
0.34	1.65E-03	2.08E-03	3.00E-03		3.80E-03
0.40	2.35E-03	2.69E-03	3.72E-03	5.28E-03	4.42E-03
0.43	3.89E-03	3.51E-03	4.63E-03		4.90E-03
0.46	7.61E-03	5.22E-03	5.14E-03	6.31E-03	5.28E-03
0.49	9.48E-02*	5.20E-02	9.72E-03	8.23E-03	6.46E-03
0.55	1.83E-01*	1.58E-01*	7.15E-02*	1.37E-02	8.99E-03
0.61		2.02E-01*	1.73E-01*	9.62E-02*	7.25E-02*

Bundle C
(x = 0.7 m)

DEPTH (m)	TIME (days)				
	95	98	99	100	102
0.10	5.67E-04	6.77E-04	7.40E-04		1.92E-03
0.16		7.15E-04	1.06E-03	3.44E-03	1.71E-03
0.22	8.70E-04	9.81E-04	1.52E-03		2.13E-03
0.28		1.33E-03	2.00E-03	3.24E-03	2.77E-03
0.34	1.25E-03	1.68E-03	2.56E-03		3.52E-03
0.40	1.81E-03	2.26E-03	3.16E-03	4.88E-03	4.01E-03
0.43	2.83E-03	3.02E-03	3.68E-03		4.51E-03
0.46	7.21E-03	3.84E-03	4.25E-03	6.02E-03	4.70E-03
0.49	5.45E-02*	1.96E-02	6.68E-03	7.43E-03	5.68E-03
0.55	1.60E-01*	1.17E-01*	3.55E-02*	1.35E-02	7.71E-03
0.61		1.85E-01*	1.52E-01*		

Bundle A
(x = 0.3 m)

DEPTH (m)	TIME (days)				
	105	106	107	109	113
0.10	8.76E-04	4.87E-04	4.08E-04	3.86E-04	5.40E-04
0.16	1.36E-03	8.51E-04	6.91E-04	6.83E-04	7.43E-04
0.22	1.94E-03	1.29E-03	1.13E-03	1.01E-03	1.11E-03
0.28	2.59E-03	1.68E-03	1.30E-03	1.34E-03	1.42E-03
0.34	3.26E-03	2.18E-03	1.71E-03	1.75E-03	1.88E-03
0.40	3.97E-03	2.58E-03	2.03E-03	2.15E-03	2.25E-03
0.43	4.32E-03	2.78E-03	2.17E-03	2.30E-03	2.52E-03
0.46	4.21E-03	2.81E-03	2.25E-03	2.36E-03	2.62E-03
0.49	5.09E-03	3.34E-03	2.58E-03	2.66E-03	2.78E-03
0.52		2.54E-03	3.18E-03	1.80E-03	5.16E-03
0.55	9.25E-03	2.85E-02*	3.75E-02*	2.98E-02*	5.07E-02*
0.61	1.04E-01*	1.02E-01*	1.43E-01*	1.30E-01*	1.70E-01*

Bundle B
(x = 0.5 m)

DEPTH (m)	TIME (days)				
	105	106	107	109	113
0.10	9.14E-04				4.91E-04
0.16	1.19E-03	7.39E-04	6.01E-04	5.11E-04	6.86E-04
0.22	1.55E-03	9.90E-04	7.87E-04	6.62E-04	8.59E-04
0.28	2.10E-03	1.32E-03	1.09E-03	1.03E-03	1.13E-03
0.34	2.60E-03	1.64E-03	1.29E-03	1.35E-03	1.39E-03
0.40	3.11E-03	1.99E-03	1.59E-03	1.67E-03	1.72E-03
0.43	3.33E-03	2.12E-03	1.66E-03	1.88E-03	1.85E-03
0.46	3.62E-03	2.28E-03	1.86E-03	1.95E-03	2.03E-03
0.49	4.26E-03	2.87E-03	2.31E-03	2.44E-03	2.58E-03
0.52		5.09E-03	3.14E-03		7.12E-03
0.55	5.99E-03	1.77E-02*	2.94E-02*	2.13E-02*	4.53E-02*
0.61	8.92E-02*	9.20E-02*	1.09E-01*	1.07E-01*	1.33E-01*

Bundle C
(x = 0.7 m)

DEPTH (m)	TIME (days)				
	105	106	107	109	113
0.10	1.08E-03	5.03E-04		5.01E-04	6.15E-04
0.16	1.06E-03	6.13E-04	4.90E-04	4.65E-04	5.93E-04
0.22	1.42E-03	8.85E-04	7.08E-04	6.65E-04	7.01E-04
0.28	1.81E-03	1.13E-03	9.70E-04	8.46E-04	9.02E-04
0.34	2.20E-03	1.36E-03	1.02E-03	1.04E-03	1.05E-03
0.40	2.58E-03	1.57E-03	1.20E-03	1.20E-03	1.25E-03
0.43	2.74E-03	1.72E-03	1.34E-03	1.77E-03	1.42E-03
0.46	2.94E-03	1.88E-03	1.49E-03	1.50E-03	1.51E-03
0.49	3.57E-03	2.56E-03	1.96E-03	2.02E-03	2.08E-03
0.52		2.75E-03	2.28E-03	2.57E-03	2.36E-03
0.55	4.33E-03	1.37E-02*	1.77E-02*	1.30E-02*	1.86E-02*
0.61	6.16E-02*	8.70E-02*	1.01E-01*	7.31E-02*	1.05E-01*

A.3 IMBIBITION EXPERIMENT

Bundle A
(x = 0.3 m)

DEPTH (m)	TIME (days)				
	133	150	163	171	175
0.10		1.30E-03			
0.16		1.07E-03	8.81E-04	1.03E-03	1.04E-03
0.22		1.31E-03	1.32E-03		
0.28		1.58E-03	1.76E-03	2.01E-03	1.96E-03
0.34	2.60E-03	2.12E-03	2.27E-03		2.51E-03
0.40	3.10E-03	2.62E-03	2.85E-03	3.24E-03	3.12E-03
0.43	3.40E-03	2.84E-03	3.13E-03	3.55E-03	3.37E-03
0.46	3.55E-03	3.07E-03	3.58E-03	3.95E-03	3.73E-03
0.49	4.12E-03	3.75E-03	4.03E-03	4.72E-03	4.25E-03
0.52	1.23E-02*	2.93E-02*	4.02E-02*	4.51E-02*	4.84E-02*
0.55	8.42E-02*	1.02E-01*	1.35E-01*	1.56E-01*	1.52E-01*
0.61	2.53E-01*	2.07E-01*	2.13E-01*	2.56E-01*	2.42E-01*
0.67				2.70E-01*	2.54E-01*

Bundle B
(x = 0.5 m)

DEPTH (m)	TIME (days)	
	150	163
0.16	9.13E-04	7.32E-04
0.22	1.06E-03	1.03E-03
0.28	1.27E-03	1.31E-03
0.34	1.61E-03	1.69E-03
0.40	2.10E-03	2.10E-03
0.43	2.28E-03	2.37E-03
0.46	2.63E-03	2.69E-03
0.49	3.76E-03	3.70E-03
0.52	2.14E-02*	
0.55	9.50E-02*	
0.61	1.86E-01*	

Bundle C
(x = 0.7 m)

DEPTH (m)	TIME (days)				
	133	150	163	171	175
0.16		1.06E-03		6.36E-04	
0.22		8.83E-04	8.00E-04		
0.28		1.02E-03	1.01E-03	1.10E-03	1.13E-03
0.34	1.50E-03	1.19E-03	1.27E-03		1.41E-03
0.40	1.73E-03	1.42E-03	1.55E-03	1.64E-03	1.74E-03
0.43	1.82E-03	1.70E-03	1.85E-03	2.03E-03	1.97E-03
0.46	1.97E-03	1.85E-03	2.03E-03	2.25E-03	2.19E-03
0.49	2.64E-03	2.57E-03	2.86E-03	3.39E-03	3.05E-03
0.52	7.17E-03*	2.01E-02*	2.32E-02*	2.78E-02*	3.01E-02*
0.55	4.40E-02*	6.86E-02*	7.88E-02*	9.05E-02*	9.21E-02*
0.61	1.61E-01*	1.93E-01*	1.92E-01*	1.95E-01*	2.29E-01*
0.67				2.26E-01*	2.73E-01*

APPENDIX B

ONE-DIMENSIONAL NUMERICAL-MODEL CODE

This appendix contains the Fortran code for the one-dimensional finite-difference diffusion-dispersion numerical model discussed in Chapter 2.

```

$DEBUG
$DECLARE
CCCCCCCCCCCCCCCCCCCCCCCCCCCCCCCCCCCCCCCCCCCCCCCCCCCCCCCCCCCC
C
C          EXPLICIT, FINITE-DIFFERENCE, ONE-DIMENSIONAL, TRANSIENT      C
C    DIFFUSION/DISPERSION MODEL WITH DIRICHLET BOUNDARY CONDITIONS      C
C          by K. A. Mc Carthy, November, 1990                            C
C          modified June, 1992                                           C
C                                                                           C
CCCCCCCCCCCCCCCCCCCCCCCCCCCCCCCCCCCCCCCCCCCCCCCCCCCCCCCCCCCC
C
C*****DECLARE VARIABLES
C
C          INTEGER DF, I, J, K, N, NZ, NZ1, NZ2, NZ3, TEND
C          REAL*8  A, C1(500), C2(500), CI(500), DAE(500), DELTAT, DELTAZ,
C          &DG, DISP, DGE(1000), DW, FAC1, FAC2, H, KD, NG(500), N1,
C          &NW(500), P, P2, R(500), RB, TIME, TMAX, TREPORT, Z, KK,
C          &d1check, d2check, deff, dwe, dve
C          CHARACTER*40 INFILE, IOFILE
C
C*****READ INPUT AND OUTPUT FILES
C
C          WRITE(*,1)
C          1    FORMAT (' ', ' NAME OF INPUT FILE:  ')
C          READ(*,3) INFILE
C          WRITE(*,2)
C          2    FORMAT (' ', ' NAME OF OUTPUT FILE: ')
C          READ(*,3) IOFILE
C          3    FORMAT (40A)
C          OPEN (15, FILE=INFILE, STATUS='OLD')
C          OPEN (16, FILE=IOFILE, STATUS='UNKNOWN')
C
C*****DEFINE VARIABLES
C
C          C1(I)      CONCENTRATION AT NODE I (previous iteration)
C          C2(I)      CONCENTRATION AT NODE I (current iteration)
C          CI(I)      INITIAL CONCENTRATION AT NODE I
C          DAE(I)     EFFECTIVE AQUEOUS-PHASE DIFFUSION COEFFICIENT AT NODE I
C          DGE(I)     EFFECTIVE GAS-PHASE DIFFUSION COEFFICIENT AT NODE I
C          DELTAT     TIME STEP

```

```

C   DELTAZ      NODAL SPACING
C   DF          DIRECTIONAL FLAG (+1 FOR NODE NUMBERS INCREASING
C               UPWARD, -1 FOR DOWNWARD)
C   DISP        SATURATED-ZONE DISPERSION COEFFICIENT
C               (dispersivity*velocity)
C   DG          MOLECULAR DIFFUSION COEFFICIENT IN FREE AIR
C   DW          MOLECULAR DIFFUSION COEFFICIENT IN FREE SOLUTION
C   KD          SOIL-WATER PARTITION COEFFICIENT
C   N1          Z COORDINATE FOR NODE 1
C   NG(I)       GAS-FILLED POROSITY AT NODE I
C   NW(I)       WATER-FILLED POROSITY AT NODE I
C   NZ          TOTAL # OF NODES
C   NZ1         # OF NODES IN ZONE 1
C   NZ2         # OF NODES IN ZONE 2
C   NZ3         # OF NODES IN ZONE 3
C   P           ZONE 1 POROSITY
C   P2          ZONE 2 POROSITY
C   R           "PSEUDO" RETARDATION FACTOR
C   RB          SOIL BULK DENSITY
C
C*****READ MODEL PARAMETERS AND COMPOUND-SPECIFIC VARIABLES
C
      READ (15, *) DELTAT, TMAX, TREPORT, DF, N1
      READ (15, *) DELTAZ, NZ1, NZ2, NZ3, H
      READ (15, *) DW, DG, DISP, KD, RB
      READ (15, *) P, P2
      WRITE (16, 4) DELTAT, TMAX, TREPORT, DF, N1
      WRITE (16, 5) DELTAZ, NZ1, NZ2, NZ3, H
      WRITE (16, 6) DW, DG, DISP, KD, RB
      WRITE (16, *) P, P2
4     FORMAT (3F12.4, I6, F8.2)
5     FORMAT (F12.4, 3I6, F12.4)
6     FORMAT (2E12.3, 3F12.4)
      NZ=NZ1+NZ2+NZ3
C
C*****INITIALIZE VARIABLES
C
      K=0
C
C*****READ SOIL-MOISTURE ARRAY & INITIAL CONCENTRATIONS

```

```

C*****FILL NG and *R* ARRAYS
C
      DO 100 I=1,NZ1
        READ (15,*) NW(I),CI(I)
        NG(I)=P-NW(I)
        R(I)=H*NG(I)+NW(I)+KD*RB
        C1(I)=CI(I)
100    CONTINUE
      DO 102 I=NZ1+1,NZ1+NZ2
        READ (15,*) NW(I),CI(I)
        NG(I)=P2-NW(I)
        R(I)=H*NG(I)+NW(I)+KD*RB
        C1(I)=CI(I)
102    CONTINUE
      IF (NZ.EQ.NZ1+NZ2) GO TO 106
      DO 104 I=NZ1+NZ2+1,NZ
        READ (15,*) NW(I),CI(I)
        NG(I)=P-NW(I)
        R(I)=H*NG(I)+NW(I)+KD*RB
        C1(I)=CI(I)
104    CONTINUE
C
106    C2(1)=C1(1)
        C2(NZ)=C1(NZ)
C
C*****ASSIGN VALUES TO EFFECTIVE DIFFUSION COEFFICIENT ARRAYS
C*****ZONE 1
      DO 142 I=1,NZ1
C*****D(free solution)*tortuosity=effective D
        DAE(I)=DW*(NW(I)**(7./3.)/P**2.)
C*****D(free solution)*dispersivity*velocity*THETAw =
        THETAw*effective Dw
C
        DAE(I)=(DAE(I)+DISP)*NW(I)
        DGE(I)=DG*(NG(I)**(10./3.)/P**2.)*H
        IF (I.GT.1) GO TO 140
        D1CHECK=DAE(I)+DGE(I)
        GO TO 142
140    D2CHECK=DAE(I)+DGE(I)
C*****CHECK FOR MILLINGTON'S FALSE MINIMUM
      IF (D2CHECK.LT.D1CHECK) THEN

```

```

        DAE(I) = DAE(1)
        DGE(I) = DGE(1)
        ENDIF
142     CONTINUE
C*****ZONE 2
        DO 145 I=NZ1+1,NZ1+NZ2
            DAE(I)=DW*(NW(I)**(10./3.)/P2**2.)
            DGE(I)=DG*(NG(I)**(10./3.)/P2**2.)*H
145     CONTINUE
        IF (NZ.EQ.NZ1+NZ2) GO TO 160
C*****ZONE 3
        DO 148 I=NZ1+NZ2+1,NZ
            DAE(I)=DW*(NW(I)**(10./3.)/P**2.)
            DGE(I)=DG*(NG(I)**(10./3.)/P**2.)*H
148     CONTINUE
C
C*****WRITE TO OUTPUT FILE
C
160    DO 200 I=1,NZ
        Z=N1+(DF*(I-1)*DELTAZ)
        dwe=DAE(I)/R(I)
        dve=DGE(I)/R(I)
        deff=dwe+dve
        WRITE (16,195) Z,NW(I),CI(I),R(I),DWE,DVE,deff
195    FORMAT (2F7.3,5E15.5)
200    CONTINUE
C
C*****COMPUTE CONCENTRATIONS THROUGH TIME
C
        DELTAT=DELTAT*3600.
        TMAX=TMAX*3600.
        TREPORT=TREPORT*3600.
        TEND=TMAX/DELTAT+0.5
        WRITE (*,*) TEND
        TIME=DELTAT
C
        DO 600 N=1,TEND
        DO 250 I=2,(NZ-1)
            FAC1=DGE(I)+DAE(I)
            FAC2=DGE(I+1)+DAE(I+1)

```

```

C
C*****CHECK STABILITY
C
      A=DELTAT*(FAC1+FAC2)/(DELTAZ*DELTAZ*R(I))
      IF (A.GT.1.0) GO TO 800
C
      C2(I)=C1(I)+DELTAT*(C1(I+1)*FAC2-C1(I)*(FAC1+FAC2)+C1(I-1)*
&FAC1)/(DELTAZ*DELTAZ*R(I))
      IF (C2(I).GT.10.**(-15.)) GO TO 250
      C2(I)=0.
250  CONTINUE
C
C*****UPDATE CONCENTRATIONS
C
      DO 300 J=2,NZ-1
      C1(J)=C2(J)
300  CONTINUE
C
C*****PRINT RESULTS
C
      K=K+1
      KK=INT(TREPORT/DELTAT+.5)
      IF (K.NE.KK) GO TO 595
      K=0
      TIME=TIME/3600.
      WRITE (16,325) TIME
      write (*,*) time
325  FORMAT (F10.2)
      DO 350 I=1,NZ
      Z=N1+(DF*(I-1)*DELTAZ)
      WRITE (16,650) C2(I)
350  CONTINUE
      TIME=TIME*3600.
595  TIME=TIME+DELTAT
600  CONTINUE
650  FORMAT (E15.5)
      GO TO 900
800  WRITE (16,805)
805  FORMAT (' ','CALCULATIONS ABORTED--SOLUTION IS UNSTABLE')
810  WRITE (16,*) A,FAC1,FAC2,DELTAT,I

```

900 STOP
END

APPENDIX C

SELECTED EXPERIMENTAL DATA FROM THE DIFFUSION EXPERIMENTS

This appendix contains experimental data from the diffusion experiments discussed in Chapter 3. The values given are time-series effluent concentrations from selected diffusion cells and are reported relative to the bottom-reservoir concentration of each cell.

MOISTURE CONTENT = 0.04 (volume/volume)

TIME (min)		TIME (min)	
0.0	0.00E+00	123.0	3.89E-01
4.0	0.00E+00	126.5	3.88E-01
7.5	2.86E-01	130.0	3.88E-01
11.0	3.35E-01	133.5	3.87E-01
14.5	3.51E-01	137.0	3.86E-01
18.0	3.59E-01	140.5	3.85E-01
22.0	3.63E-01	144.0	3.87E-01
25.5	3.65E-01	147.5	3.86E-01
29.0	3.68E-01	151.0	3.85E-01
32.5	3.69E-01	154.5	3.84E-01
37.0	3.70E-01	158.0	3.85E-01
40.5	3.72E-01	161.5	3.85E-01
44.0	3.74E-01	165.0	3.85E-01
47.5	3.76E-01	168.5	3.83E-01
51.0	3.78E-01	172.0	3.83E-01
54.5	3.78E-01	175.5	3.83E-01
59.0	3.80E-01	179.0	3.83E-01
62.5	3.81E-01	182.5	3.83E-01
66.0	3.82E-01	186.0	3.83E-01
69.5	3.84E-01	189.5	3.82E-01
73.0	3.84E-01	193.0	3.82E-01
76.5	3.86E-01	196.5	3.82E-01
81.0	3.86E-01	200.0	3.81E-01
84.5	3.95E-01	203.5	3.82E-01
88.0	3.97E-01	207.0	3.82E-01
91.5	3.95E-01	210.5	3.81E-01
95.0	3.94E-01	214.0	3.82E-01
98.5	3.93E-01	217.5	3.83E-01
102.0	3.90E-01	221.0	3.83E-01
105.5	3.89E-01	224.5	3.84E-01
119.5	3.88E-01	228.0	3.86E-01

MOISTURE CONTENT = 0.07 (volume/volume)

TIME (min)		TIME (min)	
1.0	0.00E+00	78.0	3.29E-01
4.5	1.47E-01	81.5	3.32E-01
8.0	2.56E-01	85.0	3.33E-01
11.5	2.94E-01	88.5	3.33E-01
15.0	3.08E-01	92.0	3.33E-01
18.5	3.13E-01	95.5	3.33E-01
22.0	3.16E-01	99.0	3.36E-01
25.5	3.19E-01	102.5	3.38E-01
29.0	3.20E-01	106.0	3.39E-01
32.5	3.22E-01	109.5	3.39E-01
36.0	3.23E-01	113.0	3.38E-01
39.5	3.24E-01	116.5	3.38E-01
43.0	3.25E-01	120.0	3.38E-01
46.5	3.26E-01	123.5	3.38E-01
50.0	3.26E-01	127.0	3.37E-01
53.5	3.27E-01	130.5	3.37E-01
57.0	3.27E-01	134.0	3.37E-01
60.5	3.27E-01	137.5	3.36E-01
64.0	3.28E-01	141.0	3.36E-01
67.5	3.27E-01	144.5	3.36E-01
71.0	3.28E-01	148.0	3.35E-01

MOISTURE CONTENT = 0.12 (volume/volume)

TIME (min)		TIME (min)	
0.0	0.00E+00	82.0	2.02E-01
3.0	5.42E-02	85.5	2.03E-01
6.5	1.43E-01	89.0	2.03E-01
10.0	1.81E-01	92.5	2.05E-01
13.5	1.95E-01	106.0	2.08E-01
17.0	2.00E-01	109.5	2.09E-01
20.5	2.03E-01	113.0	2.08E-01
24.0	2.03E-01	116.5	2.07E-01
27.5	2.04E-01	120.0	2.06E-01
31.0	2.05E-01	123.5	2.06E-01
34.5	2.05E-01	127.0	2.06E-01
40.0	2.04E-01	130.5	2.04E-01
43.5	2.04E-01	134.0	2.05E-01
47.0	2.04E-01	137.5	2.04E-01
50.5	2.04E-01	141.0	2.04E-01
54.0	2.05E-01	144.5	2.05E-01
57.5	2.04E-01	148.0	2.05E-01
61.0	2.03E-01	151.5	2.05E-01
64.5	2.03E-01	155.0	2.06E-01
68.0	2.03E-01	158.5	2.05E-01
71.5	2.03E-01	162.0	2.06E-01
75.0	2.02E-01	165.5	2.06E-01
78.5	2.02E-01		

MOISTURE CONTENT = 0.17 (volume/volume)

TIME (min)		TIME (min)	
0.0	0.00E+00	53.0	1.31E-01
3.0	6.87E-03	56.0	1.31E-01
6.0	6.01E-02	59.0	1.31E-01
9.0	9.33E-02	62.0	1.31E-01
12.0	1.12E-01	65.0	1.31E-01
15.0	1.19E-01	68.0	1.31E-01
20.0	1.23E-01	71.0	1.31E-01
23.0	1.26E-01	74.0	1.31E-01
26.0	1.27E-01	77.0	1.31E-01
29.0	1.27E-01	80.0	1.31E-01
32.0	1.28E-01	83.0	1.31E-01
35.0	1.28E-01	86.0	1.32E-01
38.0	1.29E-01	89.0	1.31E-01
41.0	1.30E-01	92.0	1.31E-01
44.0	1.30E-01	95.0	1.31E-01
47.0	1.31E-01	98.0	1.31E-01
50.0	1.30E-01		

MOISTURE CONTENT = 0.23 (volume/volume)

TIME (min)		TIME (min)	
2.0	1.21E-02	41.0	2.41E-02
5.0	1.33E-02	44.0	2.41E-02
8.0	1.66E-02	47.0	2.41E-02
11.0	1.89E-02	50.0	2.42E-02
14.0	2.07E-02	53.0	2.40E-02
17.0	2.18E-02	56.0	2.43E-02
20.0	2.25E-02	59.0	2.50E-02
23.0	2.30E-02	62.0	2.49E-02
26.0	2.34E-02	65.0	2.50E-02
29.0	2.36E-02	85.0	2.45E-02
32.0	2.38E-02	102.0	2.52E-02
35.0	2.40E-02	105.0	2.54E-02
38.0	2.40E-02	115.0	2.52E-02

MOISTURE CONTENT = 0.26 (volume/volume)

TIME (min)		TIME (min)	
39.0	4.27E-02	90.0	4.60E-02
42.0	4.31E-02	93.0	4.59E-02
45.0	4.49E-02	96.0	4.60E-02
48.0	4.50E-02	99.0	4.59E-02
51.0	4.52E-02	102.0	4.59E-02
54.0	4.55E-02	105.0	4.60E-02
57.0	4.60E-02	108.0	4.57E-02
60.0	4.60E-02	111.0	4.61E-02
63.0	4.60E-02	114.0	4.57E-02
66.0	4.60E-02	117.0	4.57E-02
69.0	4.60E-02	120.0	4.58E-02
72.0	4.61E-02	123.0	4.60E-02
75.0	4.60E-02	126.0	4.59E-02
78.0	4.62E-02	129.0	4.59E-02
81.0	4.60E-02	132.0	4.62E-02
84.0	4.60E-02	135.0	4.62E-02
87.0	4.61E-02	138.0	4.63E-02

MOISTURE CONTENT = 0.30 (volume/volume)

TIME (min)		TIME (min)	
40.0	3.47E-04	1165.0	1.47E-03
55.0	4.02E-04	1180.0	1.43E-03
119.0	5.68E-04	1195.0	1.42E-03
179.0	5.77E-04	1210.0	1.43E-03
239.0	6.71E-04	1225.0	1.45E-03
299.0	7.31E-04	1240.0	1.50E-03
359.0	7.76E-04	1255.0	1.50E-03
419.0	8.24E-04	1270.0	1.50E-03
479.0	8.65E-04	1285.0	1.46E-03
539.0	9.12E-04	1300.0	1.53E-03
599.0	9.77E-04	1315.0	1.54E-03
659.0	1.02E-03	1330.0	1.55E-03
719.0	1.06E-03	1345.0	1.55E-03
779.0	1.09E-03	1360.0	1.49E-03
839.0	1.12E-03	1375.0	1.47E-03
899.0	1.15E-03	1390.0	1.51E-03
959.0	1.21E-03	1409.0	1.52E-03
1024.0	1.34E-03	1424.0	1.53E-03
1084.0	1.29E-03	1439.0	1.57E-03
1120.0	1.42E-03	1454.0	1.55E-03
1136.0	1.44E-03	1469.0	1.53E-03
1150.0	1.44E-03	1484.0	1.52E-03

MOISTURE CONTENT = 0.31 (volume/volume)

TIME (days)		TIME (days)		TIME (days)	
0.35	2.15E-05	0.68	9.86E-05	1.39	6.50E-04
0.36	2.29E-05	0.69	1.03E-04	1.43	6.74E-04
0.37	2.34E-05	0.70	1.02E-04	1.48	6.85E-04
0.38	2.48E-05	0.71	1.07E-04	1.52	7.36E-04
0.39	2.63E-05	0.72	1.09E-04	1.56	8.97E-04
0.40	2.70E-05	0.73	1.12E-04	1.60	9.86E-04
0.41	2.86E-05	0.89	1.18E-04	1.64	1.07E-03
0.42	2.95E-05	0.90	1.19E-04	1.68	1.06E-03
0.43	3.12E-05	0.91	1.24E-04	1.73	1.02E-03
0.44	3.27E-05	0.92	1.29E-04	1.77	1.01E-03
0.45	3.38E-05	0.93	1.38E-04	2.77	9.99E-04
0.46	3.53E-05	0.94	1.40E-04	2.81	9.72E-04
0.47	4.48E-05	0.95	1.48E-04	2.83	9.90E-04
0.48	4.51E-05	0.96	1.55E-04	2.84	9.95E-04
0.49	4.83E-05	0.97	1.59E-04	2.85	1.02E-03
0.50	4.85E-05	0.98	1.59E-04	2.86	1.03E-03
0.51	5.13E-05	0.99	1.70E-04	2.87	1.04E-03
0.52	5.50E-05	1.00	1.72E-04	2.88	1.05E-03
0.53	5.57E-05	1.01	1.74E-04	2.90	1.06E-03
0.55	5.90E-05	1.02	1.77E-04	2.90	1.07E-03
0.56	6.07E-05	1.03	1.87E-04	2.90	1.07E-03
0.57	6.24E-05	1.05	1.92E-04	2.91	1.07E-03
0.58	6.54E-05	1.06	1.95E-04	2.92	1.09E-03
0.59	6.80E-05	1.07	2.00E-04	2.92	1.09E-03
0.60	6.95E-05	1.08	2.01E-04	2.92	1.09E-03
0.61	7.35E-05	1.09	2.09E-04	2.93	1.09E-03
0.62	7.72E-05	1.10	2.16E-04	2.93	1.09E-03
0.63	8.33E-05	1.18	2.81E-04	2.94	1.11E-03
0.64	8.74E-05	1.23	3.55E-04	2.94	1.18E-03
0.65	8.72E-05	1.27	3.58E-04	2.94	1.22E-03
0.66	9.37E-05	1.31	5.58E-04	3.00	1.24E-03
0.67	9.77E-05	1.35	6.27E-04	3.11	1.28E-03

MOISTURE CONTENT = 0.31 (volume/volume), Continued

TIME (days)		TIME (days)		TIME (days)	
3.12	1.30E-03	4.61	1.37E-03	6.26	1.25E-03
3.12	1.30E-03	4.69	1.36E-03	6.34	1.26E-03
3.12	1.28E-03	4.84	1.35E-03	6.42	1.26E-03
3.13	1.29E-03	4.92	1.41E-03	6.51	1.26E-03
3.13	1.28E-03	5.01	1.35E-03	6.59	1.24E-03
3.14	1.29E-03	5.09	1.33E-03	6.67	1.23E-03
3.14	1.30E-03	5.17	1.31E-03	6.76	1.22E-03
3.14	1.32E-03	5.26	1.29E-03	6.84	1.22E-03
3.15	1.34E-03	5.34	1.29E-03	6.92	1.25E-03
3.15	1.33E-03	5.42	1.29E-03	7.01	1.24E-03
3.82	1.49E-03	5.51	1.27E-03	7.09	1.24E-03
4.04	1.38E-03	5.59	1.26E-03	7.17	1.26E-03
4.04	1.33E-03	5.67	1.25E-03	7.26	1.27E-03
4.06	1.66E-03	5.76	1.24E-03	7.34	1.28E-03
4.19	1.40E-03	5.84	1.23E-03	7.42	1.29E-03
4.28	1.40E-03	5.92	1.27E-03	7.51	1.29E-03
4.36	1.37E-03	6.01	1.28E-03	7.59	1.29E-03
4.44	1.36E-03	6.09	1.27E-03	7.67	1.29E-03
4.53	1.38E-03	6.17	1.24E-03		

MOISTURE CONTENT = 0.32 (volume/volume)

TIME (days)		TIME (days)		TIME (days)	
0.00	0.00E+00	1.54	5.29E-04	3.52	9.75E-04
0.08	0.00E+00	1.58	5.44E-04	3.56	8.86E-04
0.17	0.00E+00	1.63	5.70E-04	3.60	9.83E-04
0.25	0.00E+00	1.67	6.12E-04	3.64	1.02E-03
0.33	0.00E+00	1.73	5.89E-04	3.68	9.95E-04
0.42	0.00E+00	1.77	5.69E-04	3.72	1.02E-03
0.46	0.00E+00	1.87	5.70E-04	3.77	1.04E-03
0.50	1.52E-05	1.96	5.74E-04	3.81	1.04E-03
0.54	2.04E-05	2.00	6.13E-04	3.85	1.04E-03
0.58	2.64E-05	2.04	5.84E-04	3.89	1.03E-03
0.63	3.71E-05	2.08	6.55E-04	3.94	1.03E-03
0.67	4.48E-05	2.12	6.54E-04	3.99	1.02E-03
0.71	5.61E-05	2.68	9.55E-04	4.03	1.04E-03
0.75	6.59E-05	2.72	9.45E-04	4.07	1.04E-03
0.79	7.71E-05	2.77	8.93E-04	4.11	1.02E-03
0.83	8.79E-05	2.81	9.01E-04	4.15	9.04E-04
0.88	1.01E-04	2.85	9.22E-04	4.19	9.35E-04
0.92	1.13E-04	2.89	9.08E-04	4.24	9.31E-04
0.96	1.41E-04	2.93	9.12E-04	4.28	9.36E-04
1.00	1.44E-04	2.97	9.22E-04	4.32	9.36E-04
1.04	1.72E-04	3.02	9.50E-04	4.36	9.31E-04
1.08	1.84E-04	3.06	9.29E-04	4.40	9.34E-04
1.13	1.99E-04	3.10	9.48E-04	4.44	9.28E-04
1.17	2.09E-04	3.14	8.36E-04	4.49	9.11E-04
1.21	2.80E-04	3.18	9.97E-04	4.53	9.02E-04
1.25	2.96E-04	3.22	9.96E-04	4.57	8.99E-04
1.29	3.14E-04	3.27	1.04E-03	4.61	8.98E-04
1.33	3.18E-04	3.31	1.03E-03	4.65	8.89E-04
1.38	3.70E-04	3.35	1.03E-03	4.69	8.95E-04
1.42	4.47E-04	3.39	1.08E-03	4.74	9.08E-04
1.46	4.83E-04	3.43	1.03E-03	4.78	9.13E-04
1.50	5.05E-04	3.47	1.07E-03	4.82	9.29E-04

MOISTURE CONTENT = 0.32 (volume/volume), Continued

TIME (days)		TIME (days)		TIME (days)	
4.86	9.11E-04	5.28	9.71E-04	5.70	9.27E-04
4.90	9.12E-04	5.32	8.39E-04	5.75	9.21E-04
4.94	9.04E-04	5.36	8.93E-04	5.79	9.42E-04
4.99	9.10E-04	5.40	9.03E-04	5.83	9.54E-04
5.03	9.18E-04	5.44	8.98E-04	5.87	9.38E-04
5.07	9.13E-04	5.49	8.86E-04	5.91	9.66E-04
5.11	9.33E-04	5.53	9.05E-04	5.95	9.35E-04
5.15	9.33E-04	5.57	9.10E-04	6.00	9.83E-04
5.19	9.71E-04	5.61	9.15E-04	6.04	9.60E-04
5.24	9.71E-04	5.66	9.09E-04		

 MOISTURE CONTENT = 0.34 (volume/volume)

TIME (days)		TIME (days)		TIME (days)	
0.00	0.00E+00	2.06	2.49E-04	3.46	2.94E-04
0.31	0.00E+00	2.11	2.56E-04	3.50	2.91E-04
0.60	0.00E+00	2.15	2.62E-04	3.54	2.91E-04
0.85	0.00E+00	2.19	2.69E-04	3.58	2.89E-04
0.89	2.84E-05	2.23	2.75E-04	3.63	2.86E-04
0.93	3.27E-05	2.27	2.76E-04	3.67	2.97E-04
0.98	3.87E-05	2.31	2.81E-04	3.71	3.06E-04
1.02	4.43E-05	2.36	2.86E-04	3.75	3.11E-04
1.06	5.23E-05	2.40	2.86E-04	3.79	3.13E-04
1.11	6.16E-05	2.44	2.88E-04	3.83	3.16E-04
1.15	7.61E-05	2.48	2.93E-04	3.88	3.18E-04
1.19	8.04E-05	2.52	2.96E-04	3.92	3.44E-04
1.23	8.90E-05	2.56	2.98E-04	3.96	3.69E-04
1.31	1.04E-04	2.65	3.05E-04	4.08	3.76E-04
1.36	1.15E-04	2.69	3.08E-04	4.17	3.69E-04
1.40	1.21E-04	2.73	3.11E-04	4.25	3.28E-04
1.44	1.40E-04	2.77	3.13E-04	4.33	3.21E-04
1.48	1.52E-04	2.86	3.14E-04	4.42	3.12E-04
1.52	1.62E-04	2.90	3.15E-04	4.50	3.18E-04
1.56	1.70E-04	2.96	3.42E-04	4.58	3.15E-04
1.61	1.80E-04	3.00	3.68E-04	4.67	3.14E-04
1.65	1.87E-04	3.04	3.71E-04	4.71	3.19E-04
1.69	1.98E-04	3.08	3.79E-04	4.75	3.21E-04
1.73	2.02E-04	3.13	3.88E-04	4.79	3.18E-04
1.77	2.07E-04	3.17	3.82E-04	4.83	3.19E-04
1.81	2.16E-04	3.21	3.63E-04	4.88	3.20E-04
1.86	2.22E-04	3.25	3.50E-04	4.93	3.21E-04
1.90	2.27E-04	3.29	3.42E-04	4.97	3.52E-04
1.94	2.31E-04	3.33	3.31E-04	5.03	3.90E-04
1.98	2.39E-04	3.38	3.21E-04	5.04	3.92E-04
2.02	2.42E-04	3.42	3.02E-04	5.05	3.95E-04

APPENDIX D

TWO-DIMENSIONAL NUMERICAL-MODEL CODE

This appendix contains the Fortran code for the two-dimensional particle-tracking advection-diffusion numerical model discussed in Chapter 4.

```
C
C yacpim.f
C
C JUNE 1992 -- version 1.20
C APRIL 1991 -- version 1.00
C
C TWO-DIMENSIONAL PARTICLE TRACKING CODE
C
C THIS CODE SIMULATES THE TRANSPORT OF AQUEOUS- AND VAPOR-PHASE
C "PARTICLES"
C PHYSICAL PROCESSES INCLUDED IN THE MODEL ARE:
C 1. ADVECTION IN THE HORIZONTAL DIRECTION
C    -- CODE IS CURRENTLY LIMITED TO HORIZONTAL, UNIFORM
C    VELOCITIES IN THE AQUEOUS PHASE ONLY
C 2. DIFFUSION IN THE AQUEOUS AND GAS PHASES,
C    TRANSITION REGION BETWEEN THE SATURATED AND UNSATURATED ZONES.
C
C RICK JOHNSON
C KATHY MCCARTHY
C DON BUCHHOLZ
C
C
C    PROGRAM YACPIM
C    include 'yacpim.inc'
C    DOUBLE PRECISION  BENCHSTART, BENCHEND
C    DOUBLE PRECISION  DAY, MCFVEL, YLINE
C    DOUBLE PRECISION  XDISTW
C    DOUBLE PRECISION  R_GAS, R_WAT
C    INTEGER  I, ICYCLE, IT, J, JL, JU
C    INTEGER  OUTX, OUTY
C    INTEGER  KPRINT, LOGSKIP, SRC_COUNT
C    INTEGER  OLDNTPART, PID
C    REAL  R
C    INTEGER  GETPID
C    DOUBLE PRECISION  NORMRAND, DCLOCK
C    REAL  RAND
C    INTRINSIC  RAND
C    EXTERNAL  GETPID, NORMRAND, DCLOCK
```

```

* *****
* *****
* ***** Initial I/O Chores (one-time jobs): *****
* ***** 1. make file names from command line args *****
* ***** 2. open Fortran logical units *****
* ***** 3. read main input file (*.in) *****
* *****
* *****
      CALL MAKE_FILE_NAMES
*   Open Fortran logical units.
*   -- do not open SRC_UNIT until it is determined to be
*   necessary.
      OPEN( IN_UNIT, FILE=IN_FILNAM, STATUS='OLD')
      OPEN( LOG_UNIT, FILE=LOG_FILNAM, STATUS='NEW')
      OPEN( GRD_UNIT, FILE=GRD_FILNAM, STATUS='NEW')
      OPEN( BND_UNIT, FILE=BND_FILNAM, STATUS='NEW')
*
*   Read input file (unit=IN_UNIT).
*
      CALL READ_INPUT
C
C Calculate retardation coefficients for the residual-moisture and
C ground-water zones.
C
      H=1.0/KH
      R_GAS = 1.0/(THETA_W + THETA_G*H + RHO_B*KP)
      R_WAT = 1.0/(THETA_T + RHO_B * KP)
C
C Calculate the advective displacement distances for the
C ground-water zone
C
      XDISTW = DT * VW * R_WAT * THETA_T
      MCFVEL = - CF / XDISTW

```

```

* *****
* *****
* ***** Initialize for DISPERS. *****
* *****
* *****
      CALL WFPINIT( WFP_FILNAM, WFP_UNIT, LOG_UNIT, STDERR,
*                   EPS, DY, YTRANS, YWATER)
      CALL DCINIT
C Check time step
      IF ( MIN(DX,DY) .LE. SQRT(2.0*DIFCOGR*DTTINY) ) GOTO 9200
      IF ( MIN(DX,DY) .LE. SQRT(2.0*DIFCOWR*DT) ) GOTO 9200
      IF ( XMAX .LE. XDISTW ) GOTO 9200
C Calculate the number of bins needed to count the particles for
C generating a concentration field. Check that the number of
C bins doesn't exceed allocated storage.
C
      NBINX = (XMAX/DX) + 0.5
      NBINY = (YMAX/DY) + 0.5
      IF ( NBINX .GT. MXBINX .OR. NBINY .GT. MXBINY ) GOTO 9300
      OBXBIN = NBINX + 1
      OBYBIN = NBINY + 1
*
* Seed the random number generator. The PID is as
* random a seed as can be obtained on the RS/6000.
*
      PID = GETPID()
      CALL SRAND( PID)
*
* Skip number to print line at 0.5% of each ICYCLE.
*
      LOGSKIP = MAX(10,NSTEPS/200)

```

```

* *****
* ***** Additional I/O Chores (one-time jobs) *****
* ***** -- many of these require constants that *****
* ***** were just calculated. *****
* *****
*
* Some source types require an input file.
* This is determined after NBINY has been
* calculated for NSOURCE=1.
*
* IF ( NSOURCE .EQ. 1 ) CALL READ_SRC_FILE
*
* Generate ACE grid and boundary files.
*
* CALL MK_GRD_FILE( GRD_UNIT, NBINX,NBINY, DX,DY, IN_FILNAM)
* CLOSE( GRD_UNIT)
* CALL MK_BND_FILE( BND_UNIT, NBINX,NBINY, IN_FILNAM)
* CLOSE( BND_UNIT)
* *****
* echo calculated variable to 'run.log' file
* *****
* WRITE(LOG_UNIT,*)
* WRITE(LOG_UNIT,*) ' PID = ', PID, ' first NORMRAND() = ',
+ NORMRAND()
* WRITE(LOG_UNIT,*) ' NBINX,NBINY',NBINX,NBINY
* WRITE(LOG_UNIT,*) ' OBXBIN,OBYBIN',OBXBIN,OBYBIN
* WRITE(LOG_UNIT,*) ' XDISTW = ', XDISTW
* *****
* ***** START OF CYCLES USED TO INCREASE NUMBER OF PARTICLES *****
* *****
*
* To generate a statistically significant number of particles in the
* least amount of time, multiple simulations are conducted and the
* results superposed.
*
* DO 1000 ICYCLE=1,NCYCLE
*
* Reset to zero:
* number of particles, print time, summation block
* Open file to store the results of this cycle.

```

```

*      Call PRN_ACE_CONC with iteration count of zero; it will write
*      a header and the initial concentration profile.
*      Record the cycle # and the filename in log and FLUSH it.
*
      NTPART=0
      KPRINT = 0
      DO 10 J=0,MXBINY+1
        DO 10 I=0,MXBINX+1
10          SUM(I,J) = 0
      CALL MK_TMP_NAME( TMP1_FILNAM, BASENAME, PID, ICYCLE)
      OPEN( TMP1_UNIT, FILE=TMP1_FILNAM, STATUS='UNKNOWN')
      CALL PRN_ACE_CONC( TMP1_UNIT, 0)
      WRITE( LOG_UNIT, 9901) ICYCLE, TMP1_FILNAM
      CALL FLUSH( LOG_UNIT)
* *****
* ***      BEGIN TIME-STEPPING      ***
* *****
*
*      At each cycle:
*      -- reset 'lost particle' counters
*
      BENCHSTART = DCLOCK()
      DO 500 IT=1,NSTEPS
        IF ( MOD(IT,LOGSKIP) .EQ. 0 ) THEN
          OUTX=0
          OUTY=0
          DO 15 I=1,NBINY
15            OUTX = OUTX + SUM(OBXBIN, I)
          DO 17 I=1,NBINX
17            OUTY = OUTY + SUM(I, OBYBIN)
          WRITE( LOG_UNIT, 9500) IT, IT*DT, NTPART, NR_MAX, OUTX, OUTY
          CALL FLUSH( LOG_UNIT)
        ENDIF
        SRC_COUNT = 0
        KPRINT = KPRINT + 1
*
*      ADVECT/DISPERSE OLD PARTICLES:
*      -----
*
*      The advection distance will depend on the particle position
*      !! NOTE !! Model only supports horizontal flow in the

```

```

*           completely saturated zone.
*
*           Dispersion is in a separate subroutine.  The subroutine
*           applies some boundary conditions.
*
*           The count is from the top of the array to the bottom
*           in order that the algorithm used to keep track of the
*           particles moved out of the system works correctly.
*           Note also the any particle with *both* x and y coordinates
*           greater than their respective maximums will be counted
*           as a particle that had  $x > x_{max}$ , but  $y \leq y_{max}$ .
*
DO 20 I = NTPART, 1, -1
    IF ( PARTY(I) .LE. YWATER)
+       PARTX(I) = PARTX(I) + XDISTW
CALL DISPERS( PARTX(I), PARTY(I))
    CALL CHK_BOUNDS(I)
*
*           For Dirichlet BC, keep count of particles
*           in the source region.  If too many, delete.
*
    IF ( NSOURCE .EQ. 10 ) THEN
        IF ( PARTX(I) .LT. SRCRIGHT .AND.
+           PARTY(I) .GE. SRCBOTTOM .AND.
+           PARTY(I) .LT. SRCTOP .AND.
+           PARTX(I) .GE. SRCLEFT ) THEN
            IF ( SRC_COUNT .GE. NPART ) THEN
                PARTX(I) = PARTX(NTPART)
                PARTY(I) = PARTY(NTPART)
                NTPART = NTPART - 1
            ELSE
                SRC_COUNT = SRC_COUNT + 1
            ENDIF
        ENDIF
    ENDIF
20 CONTINUE
*
*           CREATE/ADVECT/DISPERSE NEW PARTICLES:
*           -----
*           Check if source is active and "create" new particles as

```

```

*      necessary.
*      Update the NTPART counter to reflect the change.
*
*      For first time step, ignore tests for X>XMAX and Y>YMAX.
*
*      IF ( IT .LE. NSRCSTEP ) THEN
*
*      Constant Concentration (NSOURCE=10)
*
*      IF ( NSOURCE .EQ. 10 ) THEN
*          OLDNTPART = NTPART
*          NTPART = NTPART + MAX( 0, NPART-SRC_COUNT)
*          IF ( NTPART .GT. MXPARTS )
+             GOTO 9100
*          DO 100 I = NTPART, OLDNTPART+1, -1
*              PARTX(I) = SRCLEFT + RAND()*SRCWIDTH
*              PARTY(I) = SRCBOTTOM + RAND()*SRCHEIGHT
100          CONTINUE
*
*      Use Array from *.src file. (NSOURCE=1)
*
*      The SRC input file gives the relative input fluxes
*      for each source bin.
*      The relative fluxes are then normalized such that the
*      sum of all the fluxes is 1. Each number in the SRC
*      array is the sum of all normalized fluxes upto
*      and including that bin. We obtain a random number
*      R such that 0.0 < R < 1.0. Then find J such that
*      SRC(J-1) < R <= SRC(J). J is the destination bin
*      for the particle. Then assign the particle a random
*      position in the bin.
*
*      ELSE IF ( NSOURCE .EQ. 1 ) THEN
*          OLDNTPART = NTPART
*          NTPART = NTPART + NPART
*          IF ( NTPART .GT. MXPARTS ) GOTO 9100
*          DO 200 I=NTPART,OLDNTPART+1,-1
*              R = RAND()
*          JL = 0
*          JU = SRC_NBIN

```

```

190         IF ( JU-JL .GT. 1 ) THEN
           J = (JU+JL)/2
           IF ( R .GT. SRC(J) ) THEN
             JL = J
           ELSE
             JU = J
           ENDIF
           GOTO 190
        ENDIF
        PARTY(I) = (JL + RAND()) * SRC_DY
        IF ( PARTY(I) .GT. YWATER ) THEN
          PARTX(I) = 0.0D0
          CALL DISPERS( PARTX(I), PARTY(I))
          CALL CHK_BOUNDS(I)
        ELSE
          PARTX(I) = XDISTW * RAND()
        ENDIF
200        CONTINUE
*
*         Default is to use Original Source (NSOURCE = 0)
*         The newly created particles will have diffused some distance
*         in the x-direction.  The x-coordinate of the new particles
*         is uniformly distributed over a band that is one time step's
*         advection width.  The y-coordinate is distributed uniformly
*         in the saturated zone.
        ELSE
          write( stderr, 9090)
          write( log_unit, 9090)
          stop
        ENDIF
*
*
        END IF
        IF ( KPRINT .GE. TREPORT ) THEN
          CALL PRN_ACE_CONC( TMP1_UNIT, IT)
          KPRINT = 0
        ENDIF
500        CONTINUE
        BENCHEND = DCLOCK()
        WRITE(LOG_UNIT,9510) ICYCLE,BENCHSTART,BENCHEND,

```

```
+                               BENCHEND-BENCHSTART  
WRITE(*,9510) ICYCLE,BENCHSTART,BENCHEND,  
+                               BENCHEND-BENCHSTART
```

```

* *****
* ***           END TIME-STEPPING           ***
* *****
      IF ( KPRINT .GT. 1 ) THEN
        CALL PRN_ACE_CONC( TMP1_UNIT, IT)
      ENDIF
      CLOSE( TMP1_UNIT)
* For superposition of results:
* IF ( ICYCLE .EQ. 1 ) THEN
*   CALL RENAME_FILE( TMP1_FILNAM, CNC_FILNAM)
* ELSE
*   CALL MK_TMP_NAME( TMP2_FILNAM, 'cnc.TMP2-', PID, ICYCLE)
*   CALL RENAME_FILE( CNC_FILNAM, TMP2_FILNAM)
*   REWIND( TMP1_UNIT)
*   OPEN( TMP2_UNIT, FILE=TMP2_FILNAM, STATUS='OLD')
*   OPEN( CNC_UNIT, FILE=CNC_FILNAM, STATUS='NEW')
*   CALL CNC_OLIDATE( TMP1_UNIT, TMP2_UNIT, CNC_UNIT,
* +                   NBINX*NBINY, LOG_UNIT)
*   CLOSE( TMP1_UNIT)
*   CLOSE( TMP2_UNIT)
*   CLOSE( CNC_UNIT)
*   CALL DELETE_FILE( TMP1_FILNAM)
*   CALL DELETE_FILE( TMP2_FILNAM)
* ENDIF
1000 CONTINUE
* *****
* ****   END OF CYCLES USED TO INCREASE NUMBER OF PARTICLES   ****
* *****
* jump to files closed and exit
      GOTO 10000
C *****
C  FORMAT STRINGS
C *****
9500 FORMAT( ' IT, DAY, NTPART, NRMAX, OUTX, OUTY', 2X, I6, F10.5, I10, F9.4, 2I10)
9510 FORMAT( 1X, 'BENCH( ', I2, ' ): start=', E13.5, ', end=', E13.5,
+ ', diff=', E15.5)
9090 FORMAT( ' ERROR -- bad NSOURCE value: original (0) was removed'/
+          5X, 'check input file')
9901 FORMAT( '/# ICYCLE = ', I4, '    TMP_FILE:', A50)

```

```

C *****
C  ERROR MESSAGES AND EXITS
C  *****
C  -----
C  too many particles
C  -----
9100 WRITE( STDERR, 9101) IT,NTPART,MXPARTS
      WRITE( LOG_UNIT, 9101) IT,NTPART,MXPARTS
9101 FORMAT( ' Too many particles: '//
+ T5, 'IT: ', I5, '   (iteration count) '//
+ T5, 'NTPART: ', I12, '   (total number of particles) '//
+ T5, 'MXPARTS: ', I12, '   (maximum allowed) '//
+ )
      GOTO 10000
C  -----
C  grid too fine //  time step too large
C  -----
9200 WRITE( LOG_UNIT, 9201) DX,DY,DT,DTTINY
      WRITE( STDERR, 9201) DX,DY,DT,DTTINY
      WRITE( LOG_UNIT, 9202)
      WRITE( STDERR, 9202)
      IF ( MIN(DX,DY) .LE. SQRT(2.0*DIFCOWR*DT) ) THEN
      WRITE( LOG_UNIT, 9203) MIN(DX,DY), SQRT(2.0*DIFCOWR*DT)
      WRITE( STDERR, 9203) MIN(DX,DY), SQRT(2.0*DIFCOWR*DT)
      ELSE
      WRITE( LOG_UNIT, 9204) MIN(DX,DY), SQRT(2.0*DIFCOWR*DT)
      WRITE( STDERR, 9204) MIN(DX,DY), SQRT(2.0*DIFCOWR*DT)
      ENDIF
      WRITE( LOG_UNIT, 9205)
      WRITE( STDERR, 9205)
      IF ( MIN(DX,DY) .LE. SQRT(2.0*DIFCOGR*DTTINY) ) THEN
      WRITE( LOG_UNIT, 9203) MIN(DX,DY), SQRT(2.0*DIFCOGR*DTTINY)
      WRITE( STDERR, 9203) MIN(DX,DY), SQRT(2.0*DIFCOGR*DTTINY)
      ELSE
      WRITE( LOG_UNIT, 9204) MIN(DX,DY), SQRT(2.0*DIFCOGR*DTTINY)
      WRITE( STDERR, 9204) MIN(DX,DY), SQRT(2.0*DIFCOGR*DTTINY)
      ENDIF
      WRITE( LOG_UNIT, 9206) DIFCOWR*DT/(MIN(DX,DY))**2,
+           DIFCOGR*DT/(MIN(DX,DY))**2
      WRITE( STDERR, 9206) DIFCOWR*DT/(MIN(DX,DY))**2,

```

```

IF ( PARTX(I) .GT. XMAX ) THEN
  IBINY = MIN( OBYBIN, INT(PARTY(I)/DY))
  SUM(OBXBIN,IBINY) = SUM(OBXBIN,IBINY) + 1
  PARTX(I) = PARTX(NTPART)
  PARTY(I) = PARTY(NTPART)
  NTPART = NTPART - 1

```

```
ENDIF
```

```

IF ( PARTY(I) .GT. YMAX ) THEN
  IBINX = MIN( OBXBIN, INT(PARTX(I)/DX))
  SUM(IBINX,OBYBIN) = SUM(IBINX,OBYBIN) + 1
  PARTX(I) = PARTX(NTPART)
  PARTY(I) = PARTY(NTPART)
  NTPART = NTPART - 1

```

```
ENDIF
```

```
END
```

```

* =====
* ===== DCLOCK() =====
* =====

```

```

DOUBLE PRECISION FUNCTION DCLOCK()
  INTEGER MCLOCK
  EXTERNAL MCLOCK
  DCLOCK = MCLOCK() / 100.0
  RETURN
END

```

```

* =====
* ===== DCINIT =====
* ===== -- initializes constants used for dispersion calculations =====
* =====
* ===== Preparation: =====
* ===== 1. The following variables must be set prior to =====
* ===== calling this routine: =====
* ===== BT, KH, KP, RHOB, THETAG, THETAT, THETA =====
* ===== DIFCOG, DIFCOW =====
* =====
SUBROUTINE DCINIT
  include 'yacpim.inc'
  DOUBLE PRECISION R,R_GAS,R_WAT,TTR,TTS
  DOUBLE PRECISION WFPOR
  EXTERNAL WFPOR
  DOUBLE PRECISION DGH_THT2,DW_THT2,INV_2EPS,
+ DSTARS,DSTARR,
+ RHOBKP,SQRT2DWT,Y_REFL_XMAX
  COMMON /DCONS2/ DGH_THT2,DW_THT2,INV_2EPS,
+ DSTARS,DSTARR,
+ RHOBKP,SQRT2DWT,Y_REFL_XMAX
  SAVE /DCONS2/
*
* "Retardation" factors for residual and saturated zones:
*
  H=1.0/KH
  R_GAS = 1.0 / (THETA + H*THETAG + RHOB*KP)
  R_WAT = 1.0 / (THETA + RHOB * KP)
*
* Tortuosity values * THETA for the residual and saturated zones:
*
  TTR = THETAG**3.333/THETA**2.0
  TTS = THETA**3.333/THETA**2.0
*
* Un"retarded" and "retarded" effective diffusion coefficients:
*
  DSTARR = DIFCOG * TTR * H + DIFCOW * THETA**3.333/THETA**2.0
  DSTARS = DIFCOW * TTS
  DIFCOGR = R_GAS * DSTARR
  DIFCOWR = R_WAT * DSTARR

```

```

*
*   'Average' diffusional length for full time step (DT)
*   in the fully saturated zone:
*
*   SQRT2DWT = SQRT(2.0 * DIFCOWR * DT)
*
*   Y coordinate of reflective boundary at XMAX:
*
*   Y_REFL_XMAX = BW - CF / 2.0D0
*
*   combine constants to used in DSTAR
*
*   DGH_THT2 = DIFCOG * H / (THETAT*THETAT)
*   DW_THT2 = DIFCOW / (THETAT*THETAT)
*   RHOBKP = RHOB * KP
*   INV_2EPS = 0.5 / EPS
* *****
*   echo calculated variables to 'run.log' file
* *****
*   WRITE( LOG_UNIT, 1020) 'H',H
*   WRITE( LOG_UNIT, 1010) 'R_GAS',R_GAS,'R_WAT',R_WAT
*   WRITE( LOG_UNIT, 1010) 'TTR',TTR,'TTS',TTS
*   WRITE( LOG_UNIT, 1010) 'DSTARR',DSTARR,'DSTARS',DSTARS
*   WRITE( LOG_UNIT, 1010) 'DIFCOGR',DIFCOGR,'DIFCOWR',DIFCOWR
*   WRITE( LOG_UNIT, 1020) 'SQRT2DWT',SQRT2DWT
*   WRITE( LOG_UNIT, 1010) 'DGH_THT2',DGH_THT2,'DW_THT2',DW_THT2
*   WRITE( LOG_UNIT, 1020) 'RHOBKP',RHOBKP
*   WRITE( LOG_UNIT, 1020) 'INV_2EPS',INV_2EPS
1010 FORMAT( 'calc: ',A10,' = ',E12.6,T40,A10,' = ',E12.6)
1020 FORMAT( 'calc: ',A10,' = ',E12.6)
*   RETURN
*   END

```

```

* =====
* ===== DISPERS =====
* ===== -- applies diffusive/dispersive component of particle =====
* ===== step =====
* ===== The algorithm is: =====
* ===== IF ( Y > YDT ) THEN =====
* ===== DO J=1,NDTINY =====
* ===== Move particle a DTTINY step =====
* ===== CONTINUE =====
* ===== ELSE =====
* ===== Move particle a normal (DT) step =====
* ===== ENDIF =====
* ===== Moving a particle from its old coordinates (X_old,Y_old) =====
* ===== to its news coordinates (X_new, Y_new) is done by: =====
* ===== X_new = X_old + Vx*dt + Z*SQRT(2*Deff*dt) =====
* ===== Y_new = Y_old + R*(dDeff/dy)*dt + Z*SQRT(2*Deff*dt) =====
* =====
* ===== where Vx is the velocity in the x-direction (Vy is 0), =====
* ===== Deff is the effective diffusion coefficnet, and dt is =====
* ===== the time step. =====
* ===== The (dDeff/dy) term is a "psuedo-velocity" which is =====
* ===== included to account for the change in Deff in the =====
* ===== y-direction. There is no corresponding x-component =====
* ===== because (dDeff/dx)=0. =====
* ===== THIS MODULE DOES NOT ADD THE TRUE ADVECTIVE TERM (Vx)!!! =====
* ===== Preparation: =====
* ===== 1. DCINIT must be called (once) prior to this =====
* ===== routine so that constants are initialized. =====
* ===== Arguments: =====
* ===== X -- starting x-coordinate of particle =====
* ===== Y -- starting y-coordinate of particle =====
* =====
SUBROUTINE DISPERS( X, Y)
DOUBLE PRECISION X,Y
include 'yacpim.inc'
INTEGER I,J
DOUBLE PRECISION PSUVEL, R, SQDDTT, WFP, Y1, Y2
DOUBLE PRECISION DSTAR, NORMRAND, WFPOR
EXTERNAL DSTAR, NORMRAND, WFPOR
DOUBLE PRECISION DGH_THT2, DW_THT2, INV_2EPS,

```

```

+           DSTARS, DSTARR,
+           RHOBKP, SQRT2DWT, Y_REFL_XMAX
COMMON /DCONS2/ DGH_THT2, DW_THT2, INV_2EPS,
+           DSTARS, DSTARR,
+           RHOBKP, SQRT2DWT, Y_REFL_XMAX
SAVE /DCONS2/
IF ( Y .GE. YDT) THEN
*
*   Proceed with a multiple (NDTINY) steps of size (DTTINY).
*
DO 290 J=1, NDTINY
  Y1 = Y - EPS
  Y2 = Y + EPS
  PSUVEL = INV_2EPS * (DSTAR(Y2) - DSTAR(Y1))
  WFP = WFPOR(Y)
  R = 1.0 / (WFP + H*(THETAT-WFP) + RHOBKP)
  SQDDTT = SQRT( 2.0D0 * R * DSTAR(Y) * DTTINY)
  X = X + NORMRAND()*SQDDTT
  Y = Y + R*PSUVEL*DTTINY + NORMRAND()*SQDDTT
*
*   Boundary conditions:
*   1. The bottom is reflective
*   2. Halfway up the capillary fringe there are reflective
*      boundaries that extend to the top of the domain.
*   3. Other boundaries are open.
100  X = ABS(X)
     Y = ABS(Y)
     IF ( Y .GT. Y_REFL_XMAX .AND. X .GT. XMAX )
+       X = 2.0 * XMAX - X
290  CONTINUE
ELSE
*
*   Use the normal time step (DT).
*   YDT is in the saturated region, therefore
*       DIF = DIFCOWR
*       SQDIFDT = SQRT(2.0 * DIFCOWR * DT)
*   this quantity is calculated once only in the DCINIT
*   subroutine.
*
X = X + NORMRAND() * SQRT2DWT

```

```
Y = Y + NORMRAND() * SQRT2DWT
  X = ABS(X)
  Y = ABS(Y)
  IF ( Y .GT. Y_REFL_XMAX .AND. X .GT. XMAX )
+   X = 2.0 * XMAX - X
  ENDIF
RETURN
END
```

```

* =====
* =====  NORMRAND  =====
* =====  Function returns random numbers from a normally  =====
* =====  distributed deviate with zero mean and unit variance.  =====
* =====  It uses the system supplied random number generator  =====
* =====  RAND() as a source of uniform deviates.  The uniform  =====
* =====  deviates are transformed to a normal deviate by the  =====
* =====  Box-Muller method.  =====
* =====
* =====
      DOUBLE PRECISION FUNCTION NORMRAND()
      DOUBLE PRECISION  V1,V2,R,FAC,GSET
      INTEGER ISET
      DOUBLE PRECISION NR_MAX
      COMMON /NRCOMM/ NR_MAX
      REAL  RAND
      INTRINSIC RAND
      SAVE ISET,GSET,/NRCOMM/
      DATA ISET/0/
      IF (ISET .EQ. 0) THEN
1      V1 = 2.0 * RAND() - 1.0
      V2 = 2.0 * RAND() - 1.0
      R = V1**2 + V2**2
      IF(R .GE. 1.0) GOTO 1
      FAC = SQRT(-2.0 * LOG(R) / R)
      GSET = V1 * FAC
      NORMRAND = V2 * FAC
      nr_max = max( nr_max, abs(gset), abs(normrand))
      ISET = 1
      ELSE
      NORMRAND = GSET
      ISET = 0
      ENDIF
      RETURN
      END

```

```

* *****
*   yacpio.f
*   -- v1.20
*   This module provides the routines used for reading/writing
*   data to/from the particle tracking code.
* *****
C #####
C #####                                     #####
C #####                INPUT ROUTINES      #####
C #####                                     #####
C #####
*   READ_INPUT
*   -- used to read data from "*.in" file
*   Preparation:
*     1. IN_UNIT must be OPEN'd
*     2. LOG_UNIT must be OPEN'd
* =====
      SUBROUTINE READ_INPUT
      include 'yacpim.inc'
      WRITE( LOG_UNIT, *) 'Reading Input File ...'
*   The following is the expected format of the input file:
*
*     NSTEPS      = total number of time steps
*
*     TREPORT     = write to output file every "TREPORTth" time step
*
*     NCYCLE      = number of times to repeat simulation
*
*     DT          = length of time step (DAYS)
*
*     NDTINY      = number of small time steps to replace a single step
*                  of DT in the transition & unsaturated zones
*
*     YDT         = y-coordinate for switching to smaller time step (M)
*
*     NSOURCE     = source type flag
*                   0 -> original source; introduce NPART particles into
*                   domain, distributed evenly across the saturated
*                   region, with a linear decrease in probability upward
*                   through the capillary fringe.

```

```
*      1 -> constant flux source; introduce NPART particles per
*          time step, but use source array file (*.src) for
*          distribution pattern
*      10 -> constant concentration source; set the region bounded
*          by SRCLEFT,SRCTOP,SRCRIGHT,SRCBOTTOM to contain NPART
*          particles at the end of every time step
*
*      NPART      = source strength
*
*      NSRCSTEP= number of time steps to add particles from source
*          negative number -> all time steps
*
*      SRCLEFT,SRCTOP,SRCRIGHT,SRCBOTTOM = left, top, right, and bottom
*          coordinates of a fixed concentration source bin.
*
*      XMAX      = the largest x-coordinate in system (M)
*
*      YMAX      = the largest y-coordinate in system (M)
*
*      BW        = thickness of saturated zone (M)
*          Note: This is everywhere that the saturation is 100%,
*          including the capillary fringe.
*
*      CF        = thickness of capillary fringe (M)
*
*      BT        = thickness of the transition zone (M)
*
*      DX        = horizontal bin size for output reporting (M)
*
*      DY        = vertical bin size for output reporting (M)
*
*      VW        = velocity of groundwater (M/DAY)
*
*      DIFCOW     = free-solution diffusion coefficient (M**2/DAY)
*
*      DIFCOG     = free-air diffusion coefficient (M**2/DAY)
*
*      THETAT     = total porosity
*
*      THETAW     = residual water content
```

```
*
*   RHOB  = bulk density (g/mL = kg/L)
*
*   KP    = soil/water partition coefficient (mL/g)
*
*   KH    = water/air partition coefficient (dimensionless)
*
*
*   READ( IN_UNIT, *) NSTEPS
*   READ( IN_UNIT, *) TREPORT
*   READ( IN_UNIT, *) NCYCLE
*   READ( IN_UNIT, *) DT
*   READ( IN_UNIT, *) NDTINY
*   READ( IN_UNIT, *) YDT
*   READ( IN_UNIT, *) NSOURCE
*   READ( IN_UNIT, *) NPART
*   READ( IN_UNIT, *) NSRCSTEP
*   READ( IN_UNIT, *) SRCLEFT, SRCTOP, SRCRIGHT, SRCBOTTOM
*   READ( IN_UNIT, *) XMAX
*   READ( IN_UNIT, *) YMAX
*   READ( IN_UNIT, *) BW
*   READ( IN_UNIT, *) CF
*   READ( IN_UNIT, *) BT
*   READ( IN_UNIT, *) DX
*   READ( IN_UNIT, *) DY
*   READ( IN_UNIT, *) VW
*   READ( IN_UNIT, *) DIFCOW
*   READ( IN_UNIT, *) DIFCOG
*   READ( IN_UNIT, *) THETAT
*   READ( IN_UNIT, *) THETAW
*   READ( IN_UNIT, *) RHOB
*   READ( IN_UNIT, *) KP
*   READ( IN_UNIT, *) KH
*
*
*   echo to log file
*
*
*   WRITE( LOG_UNIT, *) 'NSTEPS =', NSTEPS
*   WRITE( LOG_UNIT, *) 'TREPORT =', TREPORT
*   WRITE( LOG_UNIT, *) 'NCYCLE =', NCYCLE
*   WRITE( LOG_UNIT, *) 'DT =', DT
*   WRITE( LOG_UNIT, *) 'NDTINY =', NDTINY
```

```

WRITE( LOG_UNIT, *) 'YDT =', YDT
WRITE( LOG_UNIT, *) 'NSOURCE =', NSOURCE
WRITE( LOG_UNIT, *) 'NPART =', NPART
WRITE( LOG_UNIT, *) 'NSRCSTEP =', NSRCSTEP
IF ( NSRCSTEP .LT. 0 ) THEN
  NSRCSTEP = NSTEPS
  WRITE( LOG_UNIT, *) '    adjusted to NSRCSTEP =',NSRCSTEP
ENDIF
WRITE( LOG_UNIT, *) 'SRCLEFT,SRCTOP =', SRCLEFT,SRCTOP
WRITE( LOG_UNIT, *) '    SRCRIGHT,SRCBOTTOM =', SRCRIGHT,SRCBOTTOM
WRITE( LOG_UNIT, *) 'XMAX =', XMAX
WRITE( LOG_UNIT, *) 'YMAX =', YMAX
WRITE( LOG_UNIT, *) 'BW =', BW
WRITE( LOG_UNIT, *) 'CF =', CF
WRITE( LOG_UNIT, *) 'BT =', BT
WRITE( LOG_UNIT, *) 'DX =', DX
WRITE( LOG_UNIT, *) 'DY =', DY
WRITE( LOG_UNIT, *) 'VW =', VW
WRITE( LOG_UNIT, *) 'DIFCOW =', DIFCOW
WRITE( LOG_UNIT, *) 'DIFCOG =', DIFCOG
WRITE( LOG_UNIT, *) 'THETAT =', THETAT
WRITE( LOG_UNIT, *) 'THETAW =', THETAW
WRITE( LOG_UNIT, *) 'RHOB =', RHOB
WRITE( LOG_UNIT, *) 'KP =', KP
WRITE( LOG_UNIT, *) 'KH =', KH
* *****
*   Calculate constants
*   Echo to LOG_UNIT
* *****
C
C   Lengths/coordinates.
C
  BG      = YMAX - BT - BW
  YTRANS = BW + BT
  YWATER = BW
  YCF     = BW - CF
  WRITE( LOG_UNIT, 1500) 'BG',BG
  WRITE( LOG_UNIT, 1500) 'YTRANS',YTRANS
  WRITE( LOG_UNIT, 1500) 'YWATER',YWATER
  WRITE( LOG_UNIT, 1500) 'YCF',YCF

```

```

      IF (
+       XMAX .LE. 0.0D0 .OR.
+       YMAX .LE. 0.0D0 .OR.
+       BW .LE. 0.0D0 .OR.
+       BT .LE. 0.0D0 .OR.
+       BG .LE. 0.0D0 .OR.
+       CF .LE. 0.0D0 .OR.
+       YCF .LE. 0.0D0 .OR.
+       YTRANS .GT. YMAX
+ ) THEN
          WRITE( STDERR, 1550) 'XMAX,YMAX,BW,BT,BG,CF,YCF,YTRANS'
          WRITE( LOG_UNIT, 1550) 'XMAX,YMAX,BW,BT,BG,CF,YCF,YTRANS'
          STOP
      ENDIF
C
C   Gas-phase porosity in residual-moisture zone.
C
      THETAG = THETAT - THETAW
      WRITE( LOG_UNIT, 1500) 'THETAG',THETAG
      IF (
+       THETAT .GT. 1.0D0 .OR.
+       THETAW .GT. 1.0D0 .OR.
+       THETAG .GT. 1.0D0 .OR.
+       THETAT .LT. 0.0D0 .OR.
+       THETAW .LT. 0.0D0 .OR.
+       THETAG .LT. 0.0D0
+ ) THEN
          WRITE( STDERR, 1550) 'THETAT,THETAW,THETAG'
          WRITE( LOG_UNIT, 1550) 'THETAT,THETAW,THETAG'
          STOP
      ENDIF
C
C   Short time step.
C
      DTTINY = DT/NDTINY
      WRITE( LOG_UNIT, 1500) 'DTTINY',DTTINY
      IF ( DT .LE. 0.0D0 .OR. DTTINY .LE. 0.0D0 ) THEN
          WRITE( STDERR, 1550) 'DT,DTTINY'
          WRITE( LOG_UNIT, 1550) 'DT,DTTINY'
          STOP
      
```

```

        ENDIF
C
C   Source height/width.
        SRCHEIGHT = SRCRIGHT - SRCLEFT
        SRCWIDTH  = SRCTOP - SRCBOTTOM

        WRITE( LOG_UNIT, 1500) 'SRCHEIGHT',SRCHEIGHT
        WRITE( LOG_UNIT, 1500) 'SRCWIDTH',SRCWIDTH
        IF ( NSOURCE .EQ. 10 .AND.
+ (SRCRIGHT .LE. SRCLEFT .OR. SRCTOP .LE. SRCBOTTOM)
+ ) THEN
            WRITE( STDERR, 1550) 'SRCLEFT,SRCTOP,SRCRIGHT,SRCBOTTOM'
            WRITE( LOG_UNIT, 1550) 'SRCLEFT,SRCTOP,SRCRIGHT,SRCBOTTOM'
            STOP
        ENDIF
        WRITE( LOG_UNIT, *) 'Finished reading input file ...'
        RETURN
1500 FORMAT('calc: ',A10,' = ',F10.6)
1550 FORMAT(1X,'ERROR -- read or calculated bad value in list:'//
+ T5,A60/)
        END
* =====
* READ_SRC_FILE
* -- used to read data from "*.src" file
* Preparation:
*   1. LOG_UNIT must be OPEN'd
*   2. SRC_FILNAM must be built
* =====
        SUBROUTINE READ_SRC_FILE
        include 'yacpim.inc'
        INTEGER I
        REAL BINFLUX, SUMFLUX
        DOUBLE PRECISION YY
        WRITE( LOG_UNIT,*)' Reading Source File ...'
        OPEN( SRC_UNIT, FILE=SRC_FILNAM, STATUS='OLD')
        IF ( NSOURCE .EQ. 1 ) THEN
*
*   The source term is to be constant-flux with respect
*   to time, but vary with respect to y.
*   Read the file containing information on number of

```

```

*      particles to emit into system at x=0.
*
*      An integer "concentration" for each bin's center at x=0
*      MUST be provided. . .use zero's as needed.
*
*      Check for too many points
*
      READ( SRC_UNIT, *) SRC_NBIN, SRC_DY
      IF ( SRC_NBIN .GT. MXBINY ) THEN
        WRITE( STDERR, 1000) SRC_NBIN,MXBINY
        WRITE( LOG_UNIT, 1000) SRC_NBIN,MXBINY
        STOP
1000      FORMAT( /1X,'ERROR -- reading source array'/
+          T6,'SRC_NBIN =',I5,'      MXBINY =',I5/)
      ELSE
*          -- check number of source bins.
*          -- read data
*          -- normalize the total flux to a value of 1
*          -- print the results to the log file
*
          SUMFLUX = 0.0
          DO 5 I=1,SRC_NBIN
            READ( SRC_UNIT,*) SRC(I)
            SUMFLUX = SUMFLUX + SRC(I)
5          CONTINUE
          BINFLUX = 0.0
          DO 25 I=1,SRC_NBIN
            BINFLUX = BINFLUX + SRC(I)
          YY = I*SRC_DY
            WRITE( LOG_UNIT,1010) I,YY,SRC(I),BINFLUX/SUMFLUX
          SRC(I) = BINFLUX/SUMFLUX
1010      FORMAT('I,YY,input,SRC(I)',I4,F11.4,1X,F13.5,1X,F12.9)
          25 CONTINUE
          ENDIF
      ELSE
*      Error in value for NSOURCE.
*
          WRITE( STDERR, 1050) NSOURCE
          WRITE( LOG_UNIT, 1050) NSOURCE
1050      FORMAT(/1X,'READ_SRC_FILE: bad source type - NSOURCE =',I6/)

```

```
STOP  
ENDIF  
CLOSE (SRC_UNIT)  
RETURN  
END
```

```

C #####
C #####
C #####          OUTPUT ROUTINES          #####
C #####          #####
C #####          #####
C #####          #####
* ===== MK_BND_FILE                      =====
* ===== -- creates ACE boundary file     =====
* =====
* ===== Arguments:                       =====
* =====   UNIT -- Fortran unit number for making file.  =====
* =====   NX  -- number of nodes in x-direction         =====
* =====   NY  -- number of nodes in y-direction         =====
* =====   FILENAME -- character string for line 1 of file =====
* =====
      SUBROUTINE MK_BND_FILE( UNIT,NX,NY,FILENAME)
      INTEGER UNIT,NX,NY
      CHARACTER*(*) FILENAME
      INTEGER I
*
      WRITE( UNIT, 1000) FILENAME
1000  FORMAT( 'grid from YACPIM input: ',A50)
      WRITE( UNIT, 1010)
1010  FORMAT( 1X,'1')
      DO 100  I=1,NX
100    WRITE( UNIT, 1500) I
      DO 110  I=2,NY-1
110    WRITE( UNIT, 1500) I*NX
      DO 120  I=NX,1,-1
120    WRITE( UNIT, 1500) NX*(NY-1) + I
      DO 130  I=NY-1,2,-1
130    WRITE( UNIT, 1500) NX*(I-1) + 1
1500  FORMAT(1X,I5)
      RETURN
      END
* =====
* MK_GRD_FILE
* -- creates an ACE-compatible grid file so results can be viewed
* with ACE/vis.
* Arguments:
*   UNIT -- Fortran unit number for making file.

```

```

*   NX -- number of nodes in x-direction
*   NY -- number of nodes in y-direction
*   DX -- node spacing for the x-direction
*   DY -- node spacing for the y-direction
*   FILENAME -- character string to put at top of file
* =====
SUBROUTINE MK_GRD_FILE( UNIT,NX,NY,DX,DY,FILENAME)
  INTEGER UNIT,NX,NY
  DOUBLE PRECISION DX,DY
  CHARACTER*(*) FILENAME
  INTEGER I,J,N,N1,N2,N3,NELEMS,NNODES
  DOUBLE PRECISION XOFF,YOFF,X,Y
  DOUBLE PRECISION WFPOR
  EXTERNAL WFPOR
  XOFF = DX/2.0D0
  YOFF = DY/2.0D0
  NNODES = NX*NY
  NELEMS = (NX-1)*(NY-1)*2
  WRITE( UNIT, 1000) FILENAME
1000 FORMAT( 'grid from YACPIM input: ',A50)
  WRITE( UNIT, 1010) NELEMS, NNODES
1010 FORMAT( 2I8)
  N = 1
  DO 150 I=1,NY
    DO 100 J=1,NX
      X = XOFF+(J-1)*DX
      Y = YOFF+(I-1)*DY
      WRITE( UNIT, 1100) N, X, Y, WFPOR(Y)
      N = N + 1
100    CONTINUE
150  CONTINUE
1100 FORMAT(1X,I5,1X,F9.5,1X,F9.5,1X,F7.5)
  N = 0
  DO 250 I=1,NY-1
    DO 200 J=1,NX-1
      N = N + 1
      N1 = (I-1) * NX + J
      N2 = I * NX + J+1
      N3 = I * NX + J
      WRITE( UNIT, 1200) N,3,N1,N2,N3
    
```

```
      N = N + 1
      N1 = (I-1) * NX + J
      N2 = (I-1) * NX + J+1
      N3 = I * NX + J+1
      WRITE( UNIT, 1200) N, 3, N1, N2, N3
200    CONTINUE
250    CONTINUE
1200  FORMAT(1X, I5, I3, 1X, I5, 1X, I5, 1X, I5)
      RETURN
      END
```

```

* =====
* ===== PRN_ACE_CONC =====
* ===== -- outputs results ACE/vis format =====
* =====
* ===== Arguments: =====
* =====     UNIT = unit number of output file =====
* =====     ITER = iteration count =====
* =====
* ===== Note: The first call must be with IT=0 =====
* =====
      SUBROUTINE PRN_ACE_CONC (UNIT, ITER)
      INTEGER UNIT, ITER
      INCLUDE 'yacpim.inc'
      REAL XB(MXBINX),YB(MXBINY)
      REAL TIME
      INTEGER I,IX,IY,NPRINT
      LOGICAL INIT
      DATA INIT /.FALSE./
      SAVE INIT,NPRINT,XB,YB
*
* calculate x,y coordinates of the bins' centers and the number of
* time steps that will be found in each concentration file.
*
      IF ( .NOT. INIT ) THEN
      DO 3 I=1,NBINX
        XB(I) = DX * (I-1) + DX / 2.0
      3 CONTINUE
      DO 4 I=1,NBINY
        YB(I) = DY * (I-1) + DY / 2.0
      4 CONTINUE
      NPRINT = NSTEPS/TREPORT + 1
      IF ( MOD( NSTEPS, TREPORT) .GE. 1 ) NPRINT = NPRINT + 1
      INIT = .TRUE.
      ENDIF
* Reset the counters for each bin in the simulated domain.
* DO NOT reset the bins that count particles that have left
* the domain:
*     SUM( 0, iy)          SUM( OBXBIN, iy)
*     SUM( ix, 0)          SUM( ix, OBYBIN)
      DO 20 IY = 1,NBINY

```

```

        DO 10 IX = 1,NBINX
            SUM(IX,IY) = 0
10     CONTINUE
20 CONTINUE
*
* Count the particles in each bin.
*
        DO 50 I = 1, NTPART
            IX = PARTX(I) / DX + 1
            IY = PARTY(I) / DY + 1
            SUM(IX,IY) = SUM(IX,IY) + 1
50 CONTINUE
*
* If ITER=0, write file header before outputting data.
*
        IF ( ITER .EQ. 0 ) THEN
            WRITE( UNIT, *) NPRINT
            DO 80 I=1,NBINX*NBINY
80         WRITE( UNIT, 4000) I
            ENDIF
*
* Write time and data.
*
        TIME = DT * MAX(0,ITER-1)
        WRITE( UNIT, *) TIME
        I = 0
        DO 220 IY = 1, NBINY
            DO 200 IX = 1, NBINX
                I = I + 1
                WRITE( UNIT, 5020) I, SUM(IX,IY)
200     CONTINUE
220 CONTINUE
        CALL FLUSH( UNIT)
        RETURN
4000 FORMAT( 1X,I5,' 1')
5000 FORMAT( ' TIME =',F10.5,'      ITER =',I6,'      ICYCLE=',I4)
5020 FORMAT( 1X,I5,1X,I8)
        END

```

```

C #####
C #####
C #####   GENERIC AND SYSTEM DEPENDENT UTILITIES   #####
C #####
C #####
* =====
* =====   CNC_OLIDATE   =====
* =====   -- combines two ACE/ch3dsal (*.cnc) files into a   =====
* =====   single file.   =====
* =====
* =====   Arguments:   =====
* =====   UNIT1 -- unit number of 1st input file   =====
* =====   UNIT2 -- unit number of 2nd input file   =====
* =====   DESTUNIT -- unit number of resultant file   =====
* =====   NNODES -- number of nodes   =====
* =====   LOGUNIT -- unit number for error messages, if   =====
* =====   LOGUNIT<0 then no messages will be sent.   =====
* =====
* =====   Uses system-dependent logical unit 0 for STDERR.   =====
* =====
* =====
SUBROUTINE CNC_OLIDATE( UNIT1,UNIT2,DESTUNIT,NNODES,LOGUNIT)
  INTEGER UNIT1,UNIT2,DESTUNIT,LOGUNIT
  INTEGER NNODES
  INTEGER STDERR
  PARAMETER(STDERR=0)
  INTEGER I,N,NT1,NT2,N1,N2,C1,C2,LINE
  REAL T1,T2
  CHARACTER*256 NAME
  INTEGER IGETLEN
  EXTERNAL IGETLEN
  LINE=1
*
*   read/write header
*
  READ( UNIT1, *) NT1
  READ( UNIT2, *) NT2
  WRITE(DESTUNIT, *) NT1
  IF ( NT1 .NE. NT2 ) GOTO 9000
  LINE = LINE + 1

```

```

DO 40 I=1,NNODES
  READ( UNIT1, *)
  READ( UNIT2, *)
  WRITE(DESTUNIT, 1010) I
  LINE = LINE + 1
40 CONTINUE
1010 FORMAT( 1X,I5,' 1')
*
* loop through number of time steps
*
DO 100 N=1,NT1
  READ( UNIT1, *) T1
  READ( UNIT2, *) T2
  WRITE(DESTUNIT, *) T1
  IF ( T1 .NE. T2 ) GOTO 9000
  LINE = LINE + 1
  DO 90 I=1,NNODES
    READ( UNIT1, *) N1, C1
    READ( UNIT2, *) N2, C2
    WRITE(DESTUNIT,1050) N1, C1+C2
    IF ( N1 .NE. N2 ) GOTO 9000
    LINE = LINE + 1
  90 CONTINUE
100 CONTINUE
1050 FORMAT(1X,I5,1X,I8)
  RETURN
*
* error message and STOP
*
9000 WRITE(STDERR,9001) LINE
  IF (LOGUNIT.GE.0) WRITE(STDERR,9001) LINE
9001 FORMAT('ERROR -- CONSOLIDATE: data mismatch on line =',I7)
  INQUIRE( UNIT1, NAME=NAME)
  WRITE(STDERR,9002) NAME(1:IGETLEN(NAME))
  IF (LOGUNIT.GE.0) WRITE(STDERR,9002) NAME(1:IGETLEN(NAME))
9002 FORMAT(T4,'file1: ',A65)
  INQUIRE( UNIT2, NAME=NAME)
  WRITE(STDERR,9003) NAME(1:IGETLEN(NAME))
  IF (LOGUNIT.GE.0) WRITE(STDERR,9003) NAME(1:IGETLEN(NAME))
9003 FORMAT(T4,'file2: ',A65)

```

```
INQUIRE( DESTUNIT, NAME=NAME)
WRITE(STDERR,9004) NAME(1:IGETLEN(NAME))
IF (LOGUNIT.GE.0) WRITE(STDERR,9004) NAME(1:IGETLEN(NAME))
9004 FORMAT(T4,'dest: ',A65/ )
STOP
END
```

```

* =====
* =====
* ===== FLUSH =====
* ===== -- flush i/o buffers =====
* ===== -- system dependent =====
* =====
* ===== Arguments: =====
* ===== IUNIT -- unit number of file to be flushed =====
* =====
* ===== RS/6000 notes: =====
* ===== OPEN(iunit, file=name(1:igetlen(name)), status='old') =====
* ===== The first i/o operation following FLUSH() to =====
* ===== IUNIT should be a WRITE operation, in order that =====
* ===== the file pointer be positioned at end of file. =====
* =====
* ===== CRAY notes: =====
* ===== OPEN( iunit, file=name(1:igetlen(name)), =====
* ===== position='append') =====
* =====
* =====
SUBROUTINE FLUSH( IUNIT)
  INTEGER IUNIT
  CHARACTER*256 NAME
  INTEGER IGETLEN
  EXTERNAL IGETLEN
  INQUIRE( IUNIT, NAME=NAME)
  CLOSE( IUNIT)
  OPEN( IUNIT, FILE=NAME(1:IGETLEN(NAME)), STATUS='OLD')
  RETURN
END

```

```
* =====
* ===== IGETLEN =====
* ===== -- function returns position of last non-blank =====
* ===== in a CHARACTER array =====
* =====
* ===== Arguments: =====
* ===== STR = character array =====
* =====
* =====
      INTEGER FUNCTION IGETLEN( STR)
      CHARACTER*(*) STR
      INTEGER I
      IGETLEN = 0
      DO 100 I = LEN(STR), 1, -1
      IF ( STR(I:I) .NE. ' ' ) THEN
          IGETLEN = I
          RETURN
      ENDIF
100 CONTINUE
      RETURN
      END
```

```

* =====
* ===== MAKE_FILE_NAMES =====
* ----- -- This routine gets the command line argument and -----
* ----- builds filenames from it.  If there is no -----
* -----
* -----
* ----- Note:  uses system dependent GETARG() routine -----
* =====

SUBROUTINE MAKE_FILE_NAMES
  include 'yacpim.inc'
  INTEGER  ARGLEN
  INTEGER  IGETLEN
  EXTERNAL IGETLEN
  CALL GETARG( 1, BASENAME)
  IF ( BASENAME .EQ. ' ' ) BASENAME = 'yacpim'
  basename = basename(1:igetlen(basename)) // '.'
  ARGLEN = IGETLEN(BASENAME)
  IN_FILNAM = BASENAME(1:ARGLEN) // 'in'
  LOG_FILNAM = BASENAME(1:ARGLEN) // 'log'
  SRC_FILNAM = BASENAME(1:ARGLEN) // 'src'
  WFP_FILNAM = BASENAME(1:ARGLEN) // 'wfp'
  GRD_FILNAM = BASENAME(1:ARGLEN) // 'grd'
  CNC_FILNAM = BASENAME(1:ARGLEN) // 'cnc'
  BND_FILNAM = BASENAME(1:ARGLEN) // 'bnd'
END

```

```

* =====
* ===== MK_TMP_NAME =====
* ===== -- builds a filename of the form YACTMP.i1.i2 =====
* =====
* ===== Arguments: =====
* =====     NAME = destination for the resultant name =====
* =====     BASE = base string to build upon =====
* =====     I1  = first integer =====
* =====     I2  = second integer =====
* =====
* =====
SUBROUTINE MK_TMP_NAME( NAME, BASE, I1, I2)
CHARACTER*(*) NAME, BASE
INTEGER I1, I2
INTEGER I, J, N
CHARACTER*50 NSTR
INTEGER IGETLEN
EXTERNAL IGETLEN
NAME = BASE(1:IGETLEN(BASE)) // '.'
N = IGETLEN(NAME)
I = ABS(I1)
WRITE( NSTR, '(I10)') I
DO 10 J=1, 10
  IF ( NSTR(J:J) .NE. ' ' ) THEN
    NAME(N:N) = NSTR(J:J)
    N = N + 1
  ENDIF
10 CONTINUE
NAME(N:N) = '.'
N = N + 1
I = ABS(I2)
WRITE( NSTR, '(I10)') I
DO 20 J=1, 10
  IF ( NSTR(J:J) .NE. ' ' ) THEN
    NAME(N:N) = NSTR(J:J)
    N = N + 1
  ENDIF
20 CONTINUE
RETURN
END

```

VITA

The author was born in Myrtle Point, Oregon, in 1955, and was raised in Coquille, Oregon.

After spending eight years as a secretary, the author began attending classes at Portland State University and eventually obtained a B. S. in Civil Engineering.

Upon graduation, the author was employed by the Water Resources Division of the U. S. Geological Survey in Portland, Oregon. After one summer of full-time employment, she so desperately missed the good life that she applied for and was granted a Cooperative Student appointment. She then entered the Master's program at Portland State University to pursue a degree in Civil Engineering while continuing her employment on a part-time basis. While supplementing her Portland State curriculum with courses at the Oregon Graduate Institute (OGI), she applied for and was accepted into the Ph.D. program at OGI where she eventually was granted her degree.

The author continues to be employed, as a hydrologist, by the U. S. Geological Survey.